PhD

PROGRAM IN TRANSLATIONAL AND MOLECULAR MEDICINE

DIMET

UNIVERSITY OF MILANO-BICOCCA
SCHOOL OF MEDICINE AND SCHOOL OF SCIENCE

The role of the liver serine protease TMPRSS6 in iron homeostasis

Coordinator: Prof. Andrea Biondi
Tutor: Prof. Giuliana Ferrari
Co-Tutor: Dr. Laura Silvestri

Dr. Marco Rausa

Matr. No. 077978

XXVII CYCLE
ACADEMIC YEAR
2013-2014

A mamma e papà

che mi hanno sempre sostenuto e incoraggiato

INDEX

CHAPTER 1

Introduction

1. Hepcidin, the master regulator of systemic iron homeostasis

Iron is essential for multiple cell processes but it is also potentially deleterious because of its ability to generate free radicals. Since an active excretory mechanism does not exist in the organism, iron uptake from the diet and iron release from the stores have to be strictly regulated to maintain the correct iron balance. This important function is performed by the liver hormone hepcidin, the master regulator of systemic iron homeostasis.

Hepcidin was first recognized as a component of the innate immunity and named LEAP-1 (liver expressed antimicrobial peptide-1) due to its defensin-like structure. It is a protein encoded by the *HAMP* gene

which maps to chromosome 19q13 and it is translated in a 84 amino acid propeptide characterized by a N-terminal targeting signal for the secretory pathway and a consensus cleavage sites for the subtilisin-like pro convertase furin [1]. The mature form of the protein derived from furin cleavage is a 25 amino acid hairpin structure with four intramolecular disulfide bonds [2,3,4] and has low antimicrobial activity [2,5]. Hepcidin is released in the systemic circulation upon iron or inflammatory stimuli and it binds to ferroportin with its N-terminus, triggering the internalization, polyubiquitination and lysosomal degradation of the target protein [6,7]. Ferroportin is the only known mammalian iron exporter and is essential for iron release in the blood stream where iron is transported bound to its carrier protein transferrin (Tf). Reduction of ferroportin on the cell membrane is fundamental to control iron release from the stores (macrophages or hepatocytes) or the absorption from the diet (duodenal enterocytes) (Figure 1). Dietetic iron is absorbed in the duodenum and involves the reduction of $Fe3^{+}$ by the duodenal cytochrome b (Dcytb) and the subsequent transport of the bivalent ion across the apical membrane of enterocytes by divalent metal transporter 1 (DMT1) [8]. Dietary heme can directly be absorbed through a still unknown mechanism and it is metabolized in enterocytes by heme-oxygenase 1 (HOX1) to liberate $Fe2^{+}$[9]. Then iron can be managed by enterocytes and eventually exported across the basolateral membrane into the bloodstream via ferroportin [10,11]. The release by enterocytes is also mediated by the ferroxidase hephaestin which catalyzes iron re-oxidation to $Fe3^{+}$ (in the other tissues this reaction occurs through ceruloplasmin): the only oxidation state which permits the binding of Tf. The iron content of Tf

is less than 0.1% of total body iron, but is highly dynamic in order to sustain erythropoiesis: indeed Tf-iron is mainly delivered to the bone marrow for the production of red blood cells (RBCs) and only a low amount is used for myoglobin synthesis. Iron recycling is due to reticuloendothelial macrophages which clear senescent RBCs which metabolize haemoglobin and heme to export $Fe2^{+}$ in the blood stream through ferroportin [12].

The important function of hepcidin in regulating body iron homeostasis has been identified by studies on animal models. *Hamp* knock-out mice are characterized by severe iron overload because of unrestricted iron absorption from the gut [13] and iron release from the stores. On the contrary transgenic mice with high *Hamp* levels [13] or injected with hepcidin [14], and patients with Hamp-producing adenomas [15], develop iron restricted mycrocytic anemia. The main regulation of hepcidin occurs at the transcriptional level and it is the result of a balance between its inhibition and activation. Hepcidin expression is stimulated by iron and inflammation in order to limit iron availability, while it is downregulated by iron deficiency, anemia and hypoxia in order to increase the availability of the metal for erythropoiesis [16,17]. Inactivation of genes involved in hepcidin regulation leads to pathological conditions characterized by iron overload (Hemochromatosis) or iron deficiency (Anemia). Hemochromatosis is a heterogeneous disorder characterized by inappropriate low hepcidin, caused by mutations in the genes that code for HFE (*HFE*), hemojuvelin (*HFE2 or HJV*), transferrin receptor 2 (*TFR2*), hepcidin itself (*HAMP*). In these cases hemochromatosis has recessive autosomal transmission.

Hemochromatosis is also caused by mutations in the gene encoding ferroportin (*SLC40A1*). In this case the disease has autosomal dominant transmission and the phenotype depends on the functional alteration of the protein which can affect ferroportin membrane localization, its ability to export iron or the binding with hepcidin. On the other side mutations in *TMPRSS6,* the gene that encodes for the hepatic transmembrane serine protease matriptase-2, cause iron refractory iron deficiency anemia (IRIDA) due to inappropriately high hepcidin levels.

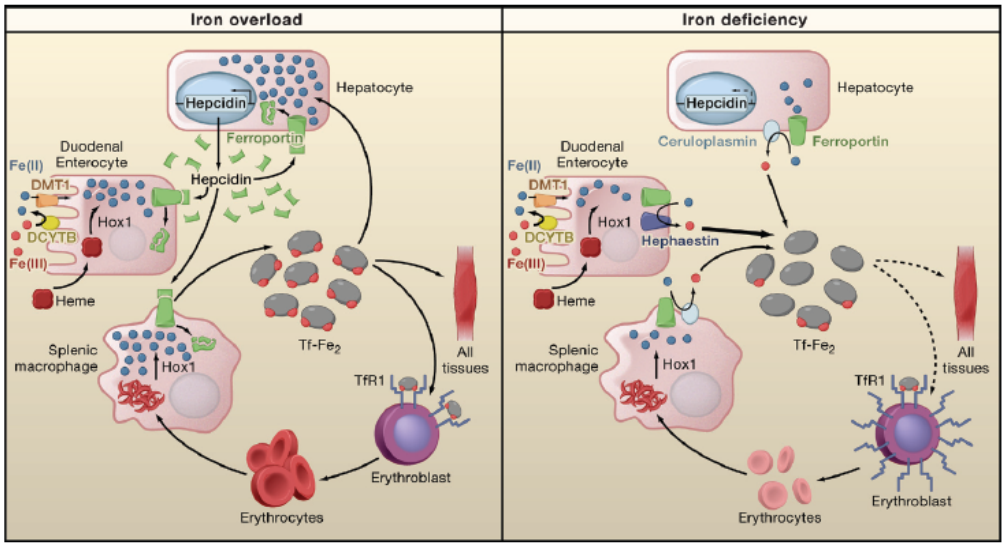

Figure 1. Hepcidin regulation [12].
When serum iron increases, *HAMP* is upregulated and hepcidin is released in the blood stream to avoid excessive iron intake from enterocytes and iron release from macrophages through its binding and degradation of ferroportin. When serum iron is low, hepcidin transcription is repressed and ferroportin is stabilized to the cell surface, thus increasing iron release into the blood stream.

2. Iron dependent activation of hepcidin

It is known that *HAMP* transcription is induced by iron in the liver as a negative feedback mechanism that maintains iron homeostasis. However, which kind of iron is involved in this regulation is still under investigation. *In vitro* studies performed on isolated murine hepatocytes demonstrated that *Hamp* expression is increased by iron loaded Tf (holoTf) [18,19]. However *Hamp* regulation in response to chronic iron loading (when holoTF saturation is maintained high for several days) is directly related to liver iron stores [20]. In the currently accepted model iron-dependent hepcidin activation in the liver occurs via two different mechanisms. The first related to the iron increase in the iron stores that would activate the Bone Morphogenic Proteins (BMPs)- Hemojuvelin (HJV)- Sons of Mother Against Decapentaplegic (SMAD) pathway; the second related to circulating iron bound to Tf would activate hepcidin through the interaction of Tf with transferrin receptor 1 and 2 (TFR1 and TFR2), with the hemochromatosis protein HFE as an intermediary (Figure 2).

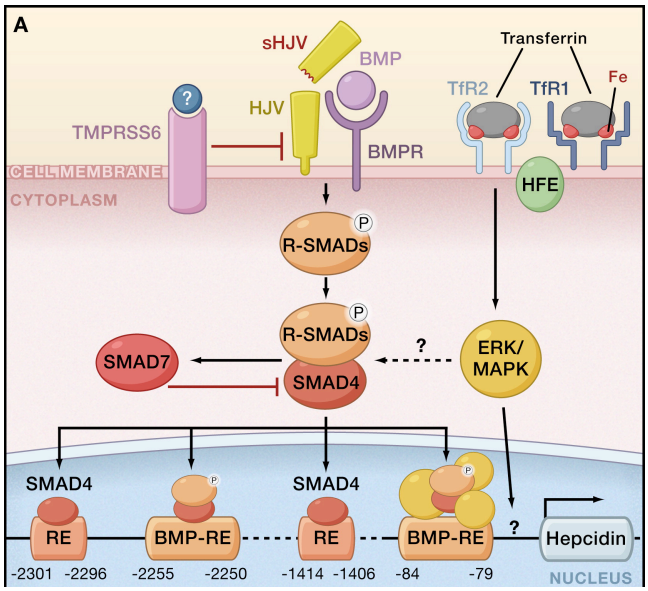

Figure 2. Iron mediated hepcidin activation [12].
HAMP transcription is promoted by two different mechanisms induced either by iron stores (BMPs mediated) or by circulating iron (holoTf mediated).

2.1 The BMP-SMAD pathway induction by iron stores

The central molecules involved in the iron-stores mediated *HAMP* activation are the BMPs, the BMP receptors (BMPRs) and their co-receptor hemojuvelin. In response to accumulation in iron stores, BMPs bind to BMPR and to the membrane-bound isoform of the GPI-anchored protein HJV (m-HJV) [21], inducing phosphorylation of cytoplasmic SMAD1, SMAD5 and SMAD8. Phosphorylated SMAD proteins interact with SMAD4 and the complex translocates to the nucleus where it activates *HAMP* transcription upon binding with the two BMP–responsive elements (the proximal BMP-RE1 and the distal BMP-RE2) [22,23,24] (Figure 2). Although several BMPs act as

BMPRs ligands *in vitro*, Bmp6 only mediates this function *in vivo* [25].

In vitro BMP6 and HJV are able to bind both BMPR type-I (ALK2, ALK3 and ALK6) and BMPR type-II (ACTRIIA, BMPRII and ACTRIIB), however ALK2, ALK3, ACTRIIA and BMPRII only are expressed in human liver [26]. Liver specific inactivation of *Alk2* or *Alk3* in mice leads to iron overload due to hepcidin deficiency [22,27]. Moreover Alk3 is important for the basal BMP signalling activation and hepcidin gene expression, while both Alk2 and Alk3 are important for iron mediated hepcidin upregulation [27]. Differently from BMP-type I receptors, BMPR type-II have redundant role in regulating hepcidin expression. Indeed inactivation of either ACTRIIA or BMPRII does not affect hepcidin synthesis, while deficiency of both type-II receptors decreases *HAMP* transcription *in vitro* and causes iron overload *in vivo* [28].

BMP-SMAD signalling activates other target genes than hepcidin, as *ID1, SMAD7* AND *ATOH8* through SMAD binding elements on their promoters [29-31]. These three genes have been shown to modulate hepcidin expression. ID1 promotes *TMPRSS6* activation [32], SMAD7 is an inhibitor of the BMP-SMAD signalling and thus both act through a negative feedback mechanism to downregulate hepcidin [33]. ATOH8 acts as transcription factor on hepcidin promoter as positive feedback of Bmp6-mediated *Hamp* upregulation [34].

2.1.1 BMP6, the activator of hepcidin

BMP proteins are members of the transforming growth factor-beta (TGF-beta) superfamily and are involved in a variety of cellular and

systemic functions, having a crucial role in embryonic development and postnatal life [35]. They have also a role in iron metabolism by binding to BMPRs in the presence of the coreceptor HJV and promoting hepcidin expression [21]. Several BMPs (BMP2, BMP4 and BMP6) may function as BMPRs ligands *in vitro* in hepatoma cell lines but *in vivo* this role is played by BMP6 only. Indeed *Bmp6*$^{-/-}$ mice have low hepcidin levels and severe iron overload, thus indicating that BMP6-mediated hepcidin activation is not redundant and that BMP6 has a key role in response to iron increase [25]. *BMP6* is positively regulated by iron at transcriptional level [31], but the mechanism leading to this induction has not been clarified yet, although it has been proposed that liver ferritin could function as signalling molecule to address *BMP6* upregulation in response to increase iron [36].

In mice *Bmp6* deficiency causes rapid and massive accumulation of iron in the liver, heart and pancreas. Despite the severe iron overload, which should increase BMP-SMAD signalling, *Bmp6*$^{-/-}$ mice show low phosphorylated SMADs levels indicating that the pathway is not activated. Although mice with inactivation of *Bmp6* show an impairment in the BMP-SMAD pathway, they still retain the capacity to induce hepcidin in response to inflammatory stimuli [37]. Nevertheless liver specific deletion of *Smad4* strongly down-regulates IL6-mediated *Hamp* activation [22], thus suggesting that BMP-SMAD signalling is implicated in inflammation mediated hepcidin upregulation, but its induction is not BMP6 dependent. BMP6 regulation is liver-specific since no other tissue modulates *Bmp6* in response to iron [38]. The liver is composed by several cell types:

parenchymal cells (hepatocytes) and non-parenchymal cells which include Kupffer cells (resident macrophages), stellate cells and sinusoidal endothelial cells (LSECs). Recently it has been reported that non parenchymal cells express high Bmp6 levels compared to hepatocytes suggesting they may have a role in hepcidin regulation [39,40]. However, which cells respond to iron increase and which are the mechanisms that lead to *Bmp6* expression is still unknown.

2.1.2 The BMP coreceptor hemojuvelin

HJV, also called Repulsive Guidance Molecule type c (RGMc), is a glycosilphosphatidylinositol (GPI)-anchor protein, member of the RGM family that includes also RGMa and RGMb [41,42]. Unlike RGMa and RGMb, HJV is expressed mainly in the liver, heart and skeletal muscle [43,44]. HJV, as the other RGMs, is characterized by multiple domains including a N-terminal signal peptide, a RGD integrin-binding motif, a Gly-Asp-Pro-His sequence (GDPH), a partial von Willebrand type D (vWD) domain and a C-terminal glycosilphosphatidylinositol (GPI)-anchor domain [45] (Figure 3). The protein undergoes a partial autoproteolytic cleavage at the bond Asp-Pro (D172-P173) of the GDPH motif in the late secretory pathway [46] to produce a heterodimer that is exposed on the cell surface. This two chains isoform is composed by a C-terminal fragment of about 33 kDa [47], joint by disulfide bonds [48] to a N-terminal fragment reported to be of about 15-20 kDa [44,46,47,49,50]. However, *in vitro*, HJV is present on the cell surface both as heterodimeric and full-length isoform (single chain) [44,48], while it has been demonstrated by *in vivo* studies that RGMa is exposed on the

cell surface as disulfide-bonded heterodimer only [41,51] and RGMb as single chain only [42,52].

Figure 3. Hemojuvelin structure
HJV is a GPI anchored protein and it is composed by a signal peptide (SP), a glycine rich domain (GRR), a RGD motif and a partial von Willebrand type D domain (vWD). In the latter domain the autoproteolytic process occurs at the GDPH sequence to generate the N-terminal and C-terminal parts that form heterodimeric HJV. The sequence RNRR is the furin cleavage site (FCS) important for the release of s-HJV.

Single chain HJV has been detected in the extracellular cell fluid of cultured cells and in blood [44,53]. Like the other RGMs, HJV is able to interact with the membrane protein neogenin, originally identified as receptor of RGMa [51]. Neogenin preferentially binds heterodimeric HJV, while BMP-2 interacts with single-chain HJV [54]. This interaction between RGMs and neogenin has been recently exploited to generate the crystallographic structure of RGMb which shares 48% homology with HJV [55] (Figure 4).

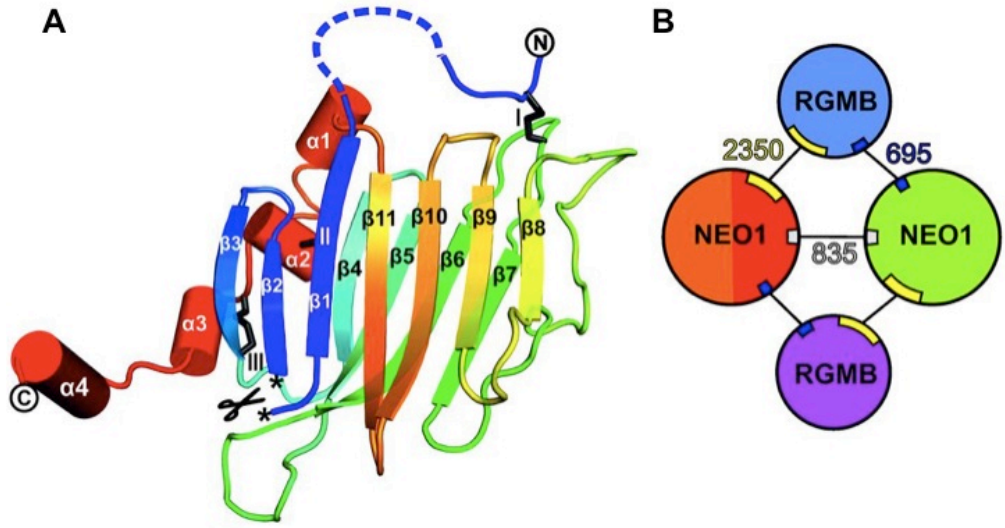

Figure 4. Crystallography structure of RGMb-Neogenin complex [55]
A) RGMb Tertiary structure
B) Schematic representation of Neogenin-RGMb complex

HJV and the other RGMs function as BMP coreceptors that bind to BMP and BMP receptors to enhance SMADs phosphorylation in response to BMP signals [56]. However, compared to RGMa and RGMb, HJV preferentially binds to BMP5, BMP6 and BMP7 [57]. HJV is essential for BMP6-mediated *HAMP* activation since inactivation of *Hjv* in mice causes severe liver iron overload due to low hepcidin levels, although *Bmp6* is upregulated [58].

Inactivation of *HJV* in humans causes type II Juvenile Hemochromatosis (JH), a severe, early onset iron overload indistinguishable from hemochromatosis caused by inactivation of the hepcidin gene. This disease affects both genders equally and is characterized by a rapid and severe course due to massive hepatocellular iron deposition as well as iron deposition in endocrine glands associated with virtually undetectable hepcidin levels. If left

untreated, hemochromatosis leads to irreversible hypogonadism, refractory heart failure and even death in the second to third decades of life [59]. Among the different causal mutations in *HJV*, the most frequent is the missense variant G320V [45]. The pathological mechanism associated to some HJV mutations has been elucidated by studying their processing and functionality as BMP coreceptor. HJV needs a proper processing and folding to be correctly exposed on the cell surface and to act as co-activator of hepcidin expression, since only the heterodimeric isoform is able to activate *HAMP* [60]. Mutations that interfere with the autoproteolytic cleavage of HJV prevent its localization on plasma membrane and determine protein misfunction [47]. Moreover, also the integrity of the N-terminal part of the protein is essential for its activity. Most of the mutants at the N-terminus are, in fact, delayed in plasma membrane export and are unable to activate the *HAMP* promoter in a luciferase assay [60], probably due to their inability to bind BMPs [54]. Mice lacking *Hjv* recapitulate the phenotype observed in humans: they are characterized by iron overload and low splenic iron content due to ferroportin stabilization on enterocytes and macrophages, associated with very low hepcidin [61] despite high BMP6 levels [58]. Furthermore iron mediated *Hamp* induction is blunted in $Hjv^{-/-}$ hepatocytes [21].

HJV has been detected in human and rodent serum [62-64] also as a soluble form (s-HJV) of about 42 kDa. This soluble isoform is generated by furin cleavage at the consensus sequence RNRR at residues 332-335 (Figure 3). The cleavage mainly occurs in the endoplasmic reticulum (ER) since HJV mutants and the artificial

variant blocked in the ER and unable to reach the cell surface still release s-HJV [65].

Although membrane-bound HJV acts as BMP coreceptor, s-HJV antagonizes the BMP-SMAD pathway (Figure 2) acting as a decoy molecule. It is able to interfere with and to block BMP2 and BMP4 mediated signaling both *in vitro* and *in vivo* [18,66], presumably by binding and sequestering BMP ligands from interaction with BMP type I and type II receptors [57,66,67]. Although exogenous s-HJV inhibits BMP-SMAD signaling, the source, the amount and the physiologic role of this isoform *in vivo* have not been clarified yet. It has been hypothesized that skeletal muscle and heart could have a role in releasing s-HJV to suppress hepcidin during iron deficiency or hypoxia [46,62]. However total $Hjv^{-/-}$ mice and liver specific $Hjv^{-/-}$ mice show the same phenotype and in addition specific inactivation of *Hjv* in skeletal muscle does not alter hepcidin expression neither under basal condition nor after dietary iron changes [64,68]. Some evidences suggest that the release of s-HJV is increased in iron deficiency or hypoxia [65,69]. All these evidences demonstrated that HJV has a central role in the positive and negative regulation of the BMP-SMAD pathway: the soluble form inhibits the signaling, probably by competing with the membrane isoform for the binding to BMPs and BMPRs.

2.2 Hepcidin activation by circulating iron

The pathway that senses circulating iron (i.e. holoTf) is still partially uncharacterized. It has been hypothesized that the signaling is

regulated by TFR2, a protein homologous to TFR1 that co-operate with HFE, an atypical MHC class I protein, able to bind both TFRs. When circulating iron is low, HFE and TFR1 form a stable complex on the plasma membrane; on the contrary when Tf saturation increases, holoTf binds to TFR1, displacing HFE which interacts with TFR2, activating *HAMP* [70,71]. Indeed Tfr2 is stabilized on the cell surface by holoTf [72].

Patients with hemochromatosis due to TFR2 mutation are unable to respond to oral iron administration whereas hemochromatotic patients with mutation in HFE are still able to do it [73]. This would indicate TFR2 as the circulating iron sensor candidate (Figure 2). Moreover in transfected cells HFE and TFR2 may form a multi-protein complex with HJV [74].

The pathway of HFE-TFR2 remains to be fully elucidated, but it probably interferes with the BMP-HJV-SMAD system as shown in mice. Increased liver iron induces *Bmp6* in mice and *Hamp* activation; however, acute iron administration, that leads just only to holoTf increase, induces the SMADs signalling cascade without increasing *Bmp6* expression. The activation of the SMAD pathway may be mediated by the ERK-MAPK signalling [75,76] which may both increase SMADs phosphorylation, and also induces furin transcription, the proconvertase involved in the maturation of hepcidin and BMPs [77] generating a positive feedback for hepcidin expression. However, *in vivo*, the Erk1/2 signaling pathway in the liver is not activated by iron [78]. The hepatic form of TFR2, together with HFE, is mainly involved in *HAMP* regulation while the erythroid form of TFR2 seems to be involved in a different function (another

role has been recently identified for TFR2 in the erythoid compartment). TFR2 and the erythropoietin receptor (EPOR) are synchronously coexpressed during the differentiation of erythroid progenitors. TFR2 associates with EPOR in the endoplasmic reticulum and is required for the efficient transport of EPOR to the cell surface. Erythroid progenitors from *Tfr2*$^{-/-}$ mice show a decreased sensitivity to erythropoietin (Epo) and increased circulating Epo levels. In human erythroid progenitors, *TFR2* knockdown delays the terminal differentiation. These results demonstrate that TFR2 exhibits a non-hepatic function as a component of the EPOR complex and is required for efficient erythropoiesis [79].

2.2.1 Transferrin receptor 2 (TFR2)

TFR2 is considered the key molecule of the Tf sensing pathway. It is a type II transmembrane protein with 45% identity and 66% similarity with TFR1 in the extracellular domain. As TFR1, also TFR2 is able to bind holoTf, although with a 25-fold lower affinity [80,81]. *TFR2* maps on chromosome 7q22 in close proximity to erythropoietin (EPO).

TFR2 is specifically expressed in the liver, spleen, lung, muscle and the erythroid compartment [79,80,81,82]. TFR2 is localized in particular membrane structures called lipid rafts [75] and its expression on the cell surface is higher in iron-replete conditions since the protein is stabilized by the binding to holoTf [72]. Its expression is up-regulated during development and it is not modulated by iron. [83]

Mutations in *TFR2* are responsible of type III hemochromatosis, a rare disorder characterized by mild to intermediate iron-overload [84,85]

with an earlier onset as compared to *HFE* hemochromatosis. Although some individuals present signs of the disease in the second decade of life, others may manifest as adults with fatigue and arthralgia and/or organ involvement including cirrhosis, diabetes mellitus and arthropathy [86].

Several TFR2 mutations have been described [85,87,88], including insertions that cause frameshift and premature stop codon, missense mutations and in rare cases deletions. The first identified and most common mutation in *TFR2* is the nonsense mutation Y250X that generate a stop codon at amino acid 250 [84].

Tfr2 mutant mice exhibit a phenotype similar to type III hemochromatosis patients with low levels of *Hamp* mRNA in the liver, indicating that TFR2 acts upstream *HAMP* [89,90].

3. Inflammation dependent hepcidin activation

Hepcidin activation in inflammation or infection is a recognized defence mechanism against pathogens that proceeds through iron restriction, because iron is fundamental for bacterial growth. The activation of hepcidin by inflammation is mainly due to the cytokine IL-6 [91]. This cytokine binds to IL-6 receptor and promotes JAK2 signalling and further Signal Transducer and Activator of Transcription 3 (STAT3) phosphorylation, which in turn translocates to the nucleus and induces hepcidin [92] (Figure 5). The integrity of the BMP-SMAD pathway is essential to promote *HAMP* expression by inflammation. In fact, liver specific deletion of SMAD4 strongly down-regulates IL6-mediated *HAMP* activation [22] indicating that a

BMP-responsive element in hepcidin promoter is required to regulate the IL-6 dependent hepcidin expression [23]. This indicates a crosstalk between the two pathways (iron and inflammation-dependent) that induces *HAMP*. It has been proposed that this crosstalk occurs through activin B, another member of the TGF-beta superfamily that binds to type-I BMPR and activates hepcidin transcription inducing SMAD 1/5/8 phosphorylation [93]. On the contrary inactivation of the STAT3 responsive element on hepcidin promoter does not alter the BMP-mediated *HAMP* transcription [24].

Cytokines other than IL-6 might activate hepcidin, since *Il-6* deficient mice still responds to lipopolisaccharide (LPS) treatment [94]. IL-1 alpha and IL-1 beta induce hepcidin expression in primary mouse hepatocytes [94] and IL-22 seems an additional *HAMP* activator. It causes IL-6 independent hepcidin upregulation *in vitro* in human hepatoma cell lines [95]. Moreover IL-6 stimulates hepcidin production in macrophages to decrease their own membrane ferroportin with an autocrine effect, thus inhibiting iron release [96]. Since macrophages have a fundamental role in recycling iron for erythropoiesis, in chronic conditions the defence mechanism that limits iron availability to pathogens may cause anemia of chronic disorders or anemia of inflammation as a side effect, both characterized by iron-restricted erythropoiesis.

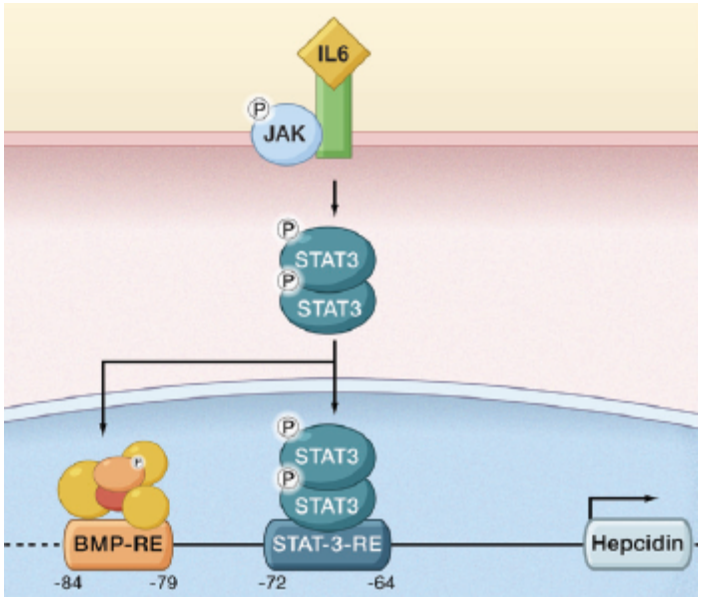

Figure 5. IL-6 mediated *HAMP* upregulation [12].
During inflammation IL-6 binds its receptor promoting JAK2 signalling and STAT3 phosphorylation. Phosphorylated STAT3 translocates to the nucleus and activates hepcidin expression.

4. Inhibition of hepcidin production

4.1. Inhibition of hepcidin by iron deficiency, hypoxia and erythropoiesis expansion

Hepcidin is suppressed in condition of hypoxia and iron deficiency, in order to stabilize ferroportin and to allow absorption of dietary iron and recycling of the stored one. The molecular mechanisms that regulate hepcidin downregulation are still partially understood [12], however they should be functionally related. Indeed iron deficiency induces a hypoxic condition stabilizing the Hypoxia-Inducible Factor-1 alpha (Hif-1 alpha) [97].

An essential inhibitor is the serine protease TMPRSS6 (also called Matriptase-2), encoded by the *TMPRSS6* gene on chromosome 22q12. TMPRSS6 is the only *HAMP* inhibitor whose role has been clearly demonstrated. *In vitro*, TMPRSS6 cleaves m-HJV thus reducing the BMP-SMAD dependent hepcidin expression [98]. Little is known about TMPRSS6 regulation. Recently a functional Hypoxia-Responsive Elements (HRE) has been identified on *TMPRSS6* promoter region that mediates *TMPRSS6* upregulation under hypoxic conditions *in vitro* [99,100], thus providing evidence of a new link between hypoxia and iron homeostasis and revealing a new regulative element for the suppression of *HAMP* transcription.

Another player that could participate to the regulation of hepcidin is the proconvertase furin. It is transcriptionally activated by iron deficiency and hypoxia through the canonical hypoxic pathway mediated by HIF-1alpha which binds to the HREs on the *Fur* promoter. Furin, as described above, cleaves HJV to generate s-HJV, which acts as decoy molecule in the BMP-SMAD pathway. In condition of iron overload *Furin* is downregulated, whereas it is upregulated in iron deficiency or hypoxia condition [65]. However, nowadays the role of furin *in vivo* is unclear since this proconvertase is important also for hepcidin maturation, a function that seems in contrast with the production of a BMP-SMAD decoy molecule that is supposed to inhibit hepcidin.

Hypoxia can also directly inhibit *HAMP* expression because a functional HRE has been identified on *HAMP* promoter [97], although this has been questioned [101,102].

In case of severe anemia, extra-iron is required for hemoglobin

synthesis, thus it is necessary to suppress hepcidin to increase circulating iron. The mechanism underlying erythropoiesis-mediated hepcidin downregulation is not fully clarified yet. It has been proposed that multiple signals cooperate in hepcidin suppression, such as hypoxia and increased erythropoietin [103]. In general a direct role has been ascribed to a bone marrow derived factor (erythroid factor) able to inhibit *HAMP* in response to the erythropoietic expansion.

Several erythroid mediators have been proposed, such as the growth differentiation factor 15 (GDF15) [104] and the twisted gastrulation 1 (TWSG1) [105], released by an expanded erythroid marrow, which could interfere with the BMP-SMAD pathway [105]. However, *Gdf15*$^{-/-}$ mice are able to suppress hepcidin as the wild type animals after bleeding and erythropoiesis expansion [106], thus suggesting that GDF15 is not involved in hepcidin suppression in conditions of stress erythropoiesis.

Platelet Derived Growth Factor (PDGF-BB) has also been proposed as a hypoxia-induced inhibitor of hepcidin transcription: its action is exerted through C/EBPα, CREB and CREB/H signalling pathways. PDGF-BB is indeed a target of HIF [107].

The most recent molecule proposed as the erythroid regulator is a tumor necrosis factor (TNF) α-like protein, Fam132b, called erythroferrone (ERFE). It is expressed in bone marrow, fetal liver, skeletal muscle and its expression is higher in intermediate erythroblasts. *Fam132b* is induced after erythropoietic stimulation, but not by hypoxia related or inflammatory stimuli. Moreover ERFE is a stress erythropoiesis regulator and it is not involved in baseline erythropoiesis. It is released by erythroblasts in response to EPO via

the JAK2/STAT-5 pathway, and directly acts on hepatocytes for hepcidin downregulation. The mechanism is still unclear, but it seems to act downstream and not to cross-talk to the BMP/SMAD signalling, since in mice treated with ERFE, *Id1* (a BMP-SMAD target gene) is not downregulated [108].

4.1.2 The liver serine-protease TMPRSS6

TMPRSS6 is a type II transmembrane serine protease and shares high structural enzymatic similarities with the serine protease matriptase-1. Its structure comprises a short N-terminal cytoplasmic tail followed by a Sea urchin sperm protein Enteropeptidase and Agrin (SEA) domain, a stem region containing two Complement factor C1r/C1s, an Urchin embryonic growth factor and a Bone morphogenetic protein 1 (CUB) domains, three Low-Density Lipoprotein Receptor (LDLR) class A repeats and a C-terminal trypsin like serine protease domain [109,110] (Figure 6). It is synthesized as a single chain inactive zymogen, which undergoes an autocatalytic cleavage at the arginine residue in the consensus sequence RIVGG between the prodomain and the catalytic domain [111]. After autoactivation it remains membrane-bound through a single disulphide bond that links the pro- and catalytic domain [112]. *In vitro*, in an overexpression system, TMPRSS6 activation is followed by the release of the serine-protease domain (about 25 kDa) in the culture media of transfected cells [98]. The regulation of *TMPRSS6* expression and activity is only partially known and besides the hypoxia-mediated regulation (see above), an iron-mediated modulation has been proposed. Indeed, the activation of the BMP6-SMAD pathway promotes *TMPRSS6* expression through

the upregulation of *ID1*; this would be a negative feedback loop to avoid excessive hepcidin activation by iron and to maintain a tight homeostatic balance of systemic iron levels [32].

TMPRSS6 is expressed mainly by the liver. Although *in vitro* the serine protease domain of TMPRSS6 hydrolyzes different synthetic substrates such as type I collagen, fibronectin and fibrinogen [109], its physiological substrate is HJV [98]. TMPRSS6 acts as a *HAMP* negative modulator by downregulating the BMP-SMAD pathway through cleavage of m-HJV on the cell surface and releasing of a characteristic pattern of soluble fragments *in vitro* [98]. Recently, one HJV cleavage site of TMPRSS6 has been proposed at ariginine (R) 288 [113] and it has been proposed that neogenin co-operate with the cleavage activity to facilitate HJV removal from the cell surface [114]. The formal proof that HJV is the TMPRSS6 substrate *in vivo* is still lacking and recently it has been questioned: it has been observed that Hjv protein levels are not increased in liver membrane fraction of *Tmprss6* deficient mice and that they even decrease compared to controls [50,115]. However, *Hjv* is still functioning in *Tmprss6*$^{-/-}$ animals since inactivation of *Hjv* in *Tmprss6*$^{-/-}$ mice reverted the IRIDA phenotype and caused a severe iron overload with very low hepcidin levels, a phenotype comparable to *Hjv*$^{-/-}$ animals, clearly indicating that TMPRSS6 acts upstream HJV [116], in agreement with HJV being the serine protease substrate.

TMPRSS6 deficiency leads to inappropriately high *HAMP* expression, lower plasma iron levels and causes a genetic disease defined as iron-refractory iron deficiency anemia (IRIDA). Patients with IRIDA suffer from anemia and are unresponsive to oral and partially

refractory to parenteral iron therapy [117]. Indeed IRIDA is characterized by congenital hypochromic microcytic anemia, low mean corpuscular erythrocyte volume, low transferrin saturation and normal/high serum ferritin.

IRIDA is caused by mutations in *TMPRSS6* both in humans [117] and in mice [118,119]. Up to now 63 different mutations have been reported in humans, spread along the entire gene sequence; some of them are missense mutations, some frameshifts and premature STOP codon insertions, affecting not only the protease catalytic domain, but also other domains likely impairing the autoactivation process [111,117,120,121,122,123,124,125,126,127,128,129,130].

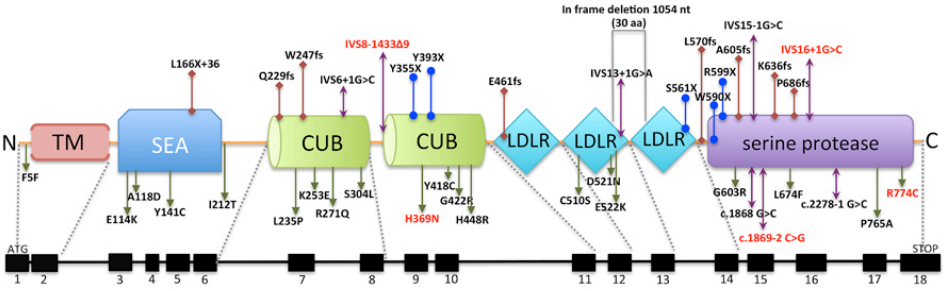

Figure 6. Mutations causing IRIDA affect different TMPRSS6 domains [131]. TMPRSS6 comprises a N-terminal Transmembrane Domain (TM), a Sea urchin sperm protein Enteropeptidase and Agrin domain (SEA), two Complement factor C1r/C1s Urchin embryonic growth factor and Bone morphogenetic protein 1 (CUB) domains, three Low-Density Lipoprotein Receptor (LDLR) class A repeats and a C-Terminal trypsin like serine protease domain.

In vitro studies have shown that almost all causal mutations induce a reduction in the cleavage activity of the protease on m-HJV and therefore the inability to inhibit the HJV-mediated *HAMP* activation at the same rate of the wild-type protein in a luciferase-based assay

[111,122,123,124,129,132]. IRIDA mice models are the *Tmprss6*$^{-/-}$ mice [119], which do not produce the serine protease, and the *Mask* mice [118]. The latter animal models have been generated by chemical mutagenesis that results in a missense mutation that eliminates a splice acceptor site in the gene, producing an abnormal splicing product that should encode for a Tmprss6 that lacks the serine protease domain. Both models show the same phenotype of iron deficiency with high hepcidin. Crossing these mice models with hemochromatosis mice provided important insights into the hierarchy of the proteins that are involved in *Hamp* regulation. Double knockout mice for *Tmprss6* and *Bmp6* are severely iron loaded as *Bmp6*$^{-/-}$, suggesting that TMPRSS6 activity needs an active BMP-SMAD pathway to perform its inhibitory activity. Indeed inactivation of *Bmp6* in *Tmprss6*$^{-/-}$ mice causes downregulation of BMP-SMAD pathway and, as a consequence, a decrease in hepcidin levels. Low hepcidin levels stabilize ferroportin and increase iron release from the enterocytes and from the stores reverting the IRIDA phenotype [133]. As discussed above the double *Hjv-Tmprss6* deficient mice behave as the *Hjv* deficient animals indicating that Tmprss6 acts upstream to the activation of BMP-SMAD signalling [116]. On the contrary the *Tmprss6-Hfe* double knockout mice have an IRIDA-like phenotype indicating that TMPRSS6 acts downstream HFE [134].

Aim of the Thesis

The expression of hepcidin is tightly regulated through a balance between inhibitory and activation signals. The aim of this work was to better investigate the relationships between the inhibitor serine protease TMPRSS6 and the proteins involved in promoting hepcidin expression as HJV, BMP6 and TFR2.

The inhibitory activity of TMPRSS6 on BMP-SMAD signaling occurs through the cleavage of the coreceptor HJV. Although one cleavage site was previously reported [113], the release of 3 discrete fragments *in vitro* in HeLa cells cotransfected with HJV and TMPRSS6 [98] suggested the presence of other cleavage sites. To better characterize the interaction between the serine protease and HJV and to investigate the existence of other TMPRSS6 cleavage sites we performed a broad mutagenesis of HJV Arginines residues. (**Chapter 2: Identification of TMPRSS6 cleavage sites of hemojuvelin.** Rausa M. et al, Journal of Cellular and Molecular Medicine, 2014).

The BMP coreceptor HJV interacts with BMPs to promote hepcidin expression and only BMP6 can play this role *in vivo* [25]. It is known that *BMP6* is positively regulated by iron at transcriptional level [31], nevertheless which liver cells respond to iron increase and which are the mechanisms upregulating *Bmp6* remains unclear. We optimized and exploited a method to isolate the hepatic cell populations [135] from mice fed iron deficient, iron replete or iron loaded diet to study chronic and stable conditions. We also took advantage of two different disease mice models, whose hepcidin expression is not correlated to liver iron: *Tmprss6*$^{-/-}$ mice and *Hjv*$^{-/-}$ mice. (**Chapter 3: *Bmp6***

expression in murine liver non parenchymal cells: a mechanism to control their high iron exporter activity and protect hepatocytes from iron overload? Rausa M. et al., *under revision*)

TFR2 co-operates with HFE to activate hepcidin [71] although mechanisms remain unclear. *Hfe* is genetically upstream *Tmprss6* in the pathway of hepcidin regulation and a role for HFE has been proposed in regulation of TMPRSS6 [134]. Since TFR2 and HFE act together in promoting hepcidin expression, we aimed at investigating whether Tmprss6 is implicated in the modulation of the Tfr2-dependent hepcidin expression. To this aim we generated two different double knock-out models, the total *Tfr2*$^{-/-}$-*Tmprss6*$^{-/-}$ and the liver-specific *Tfr2* knock-out (*Tfr2*^{LCKO}) -*Tmprss6*$^{-/-}$ mice and analyzed the BMP-SMAD signaling. (**Chapter 4: The erythroid function of transferring receptor 2 revealed by Tmprss6 inactivation in different models of transferring receptor 2 knockout mice.** Nai A. et al., Haematologica, 2013).

References

1. Valore EV, Ganz T (2008) Posttranslational processing of hepcidin in human hepatocytes is mediated by the prohormone convertase furin. Blood cells, molecules & diseases 40: 132-138.
2. Park CH, Valore EV, Waring AJ, Ganz T (2001) Hepcidin, a urinary antimicrobial peptide synthesized in the liver. The Journal of biological chemistry 276: 7806-7810.
3. Pigeon C, Ilyin G, Courselaud B, Leroyer P, Turlin B, et al. (2001) A new mouse liver-specific gene, encoding a protein homologous to human antimicrobial peptide hepcidin, is overexpressed during iron overload. The Journal of biological chemistry 276: 7811-7819.
4. Jordan JB, Poppe L, Haniu M, Arvedson T, Syed R, et al. (2009) Hepcidin revisited, disulfide connectivity, dynamics, and structure. The Journal of biological chemistry 284: 24155-24167.
5. Krause A, Neitz S, Magert HJ, Schulz A, Forssmann WG, et al. (2000) LEAP-1, a novel highly disulfide-bonded human peptide, exhibits antimicrobial activity. FEBS letters 480: 147-150.
6. Nemeth E, Tuttle MS, Powelson J, Vaughn MB, Donovan A, et al. (2004) Hepcidin regulates cellular iron efflux by binding to ferroportin and inducing its internalization. Science 306: 2090-2093.
7. Qiao B, Sugianto P, Fung E, Del-Castillo-Rueda A, Moran-Jimenez MJ, et al. (2012) Hepcidin-induced endocytosis of ferroportin is dependent on ferroportin ubiquitination. Cell metabolism 15: 918-924.
8. Andrews NC (1999) The iron transporter DMT1. The international journal of biochemistry & cell biology 31: 991-994.
9. Ferris CD, Jaffrey SR, Sawa A, Takahashi M, Brady SD, et al. (1999) Haem oxygenase-1 prevents cell death by regulating cellular iron. Nature cell biology 1: 152-157.
10. McKie AT, Marciani P, Rolfs A, Brennan K, Wehr K, et al. (2000) A novel duodenal iron-regulated transporter, IREG1, implicated in the basolateral transfer of iron to the circulation. Molecular cell 5: 299-309.
11. Donovan A, Brownlie A, Zhou Y, Shepard J, Pratt SJ, et al. (2000) Positional cloning of zebrafish ferroportin1 identifies a conserved vertebrate iron exporter. Nature 403: 776-781.
12. Hentze MW, Muckenthaler MU, Galy B, Camaschella C (2010) Two to tango: regulation of Mammalian iron metabolism. Cell 142: 24-38.
13. Nicholas KM, Wentworth P, Jr., Harwig CW, Wentworth AD, Shafton A, et al. (2002) A cofactor approach to copper-dependent catalytic antibodies. Proceedings of the National Academy of Sciences of the United States of America 99: 2648-2653.
14. Rivera S, Nemeth E, Gabayan V, Lopez MA, Farshidi D, et al. (2005) Synthetic hepcidin causes rapid dose-dependent hypoferremia and is concentrated in ferroportin-containing organs. Blood 106: 2196-2199.
15. Weinstein DA, Roy CN, Fleming MD, Loda MF, Wolfsdorf JI, et al. (2002) Inappropriate expression of hepcidin is associated with iron refractory

anemia: implications for the anemia of chronic disease. Blood 100: 3776-3781.
16. Babitt JL, Lin HY (2010) Molecular mechanisms of hepcidin regulation: implications for the anemia of CKD. American journal of kidney diseases : the official journal of the National Kidney Foundation 55: 726-741.
17. Ganz T (2013) Systemic iron homeostasis. Physiological reviews 93: 1721-1741.
18. Lin L, Valore EV, Nemeth E, Goodnough JB, Gabayan V, et al. (2007) Iron transferrin regulates hepcidin synthesis in primary hepatocyte culture through hemojuvelin and BMP2/4. Blood 110: 2182-2189.
19. Ramey G, Deschemin JC, Vaulont S (2009) Cross-talk between the mitogen activated protein kinase and bone morphogenetic protein/hemojuvelin pathways is required for the induction of hepcidin by holotransferrin in primary mouse hepatocytes. Haematologica 94: 765-772.
20. Ramos E, Kautz L, Rodriguez R, Hansen M, Gabayan V, et al. (2011) Evidence for distinct pathways of hepcidin regulation by acute and chronic iron loading in mice. Hepatology 53: 1333-1341.
21. Babitt JL, Huang FW, Wrighting DM, Xia Y, Sidis Y, et al. (2006) Bone morphogenetic protein signaling by hemojuvelin regulates hepcidin expression. Nature genetics 38: 531-539.
22. Wang RH, Li C, Xu X, Zheng Y, Xiao C, et al. (2005) A role of SMAD4 in iron metabolism through the positive regulation of hepcidin expression. Cell metabolism 2: 399-409.
23. Verga Falzacappa MV, Casanovas G, Hentze MW, Muckenthaler MU (2008) A bone morphogenetic protein (BMP)-responsive element in the hepcidin promoter controls HFE2-mediated hepatic hepcidin expression and its response to IL-6 in cultured cells. Journal of molecular medicine 86: 531-540.
24. Casanovas G, Mleczko-Sanecka K, Altamura S, Hentze MW, Muckenthaler MU (2009) Bone morphogenetic protein (BMP)-responsive elements located in the proximal and distal hepcidin promoter are critical for its response to HJV/BMP/SMAD. Journal of molecular medicine 87: 471-480.
25. Andriopoulos B, Jr., Corradini E, Xia Y, Faasse SA, Chen S, et al. (2009) BMP6 is a key endogenous regulator of hepcidin expression and iron metabolism. Nature genetics 41: 482-487.
26. Xia Y, Babitt JL, Sidis Y, Chung RT, Lin HY (2008) Hemojuvelin regulates hepcidin expression via a selective subset of BMP ligands and receptors independently of neogenin. Blood 111: 5195-5204.
27. Steinbicker AU, Bartnikas TB, Lohmeyer LK, Leyton P, Mayeur C, et al. (2011) Perturbation of hepcidin expression by BMP type I receptor deletion induces iron overload in mice. Blood 118: 4224-4230.
28. Mayeur C, Leyton PA, Kolodziej SA, Yu B, Bloch KD (2014) BMP type II receptors have redundant roles in the regulation of hepatic hepcidin gene expression and iron metabolism. Blood 124: 2116-2123.
29. Nagarajan RP, Zhang J, Li W, Chen Y (1999) Regulation of Smad7 promoter by direct association with Smad3 and Smad4. The Journal of biological chemistry 274: 33412-33418.
30. Korchynskyi O, ten Dijke P (2002) Identification and functional characterization of distinct critically important bone morphogenetic protein-specific

response elements in the Id1 promoter. The Journal of biological chemistry 277: 4883-4891.
31. Kautz L, Meynard D, Monnier A, Darnaud V, Bouvet R, et al. (2008) Iron regulates phosphorylation of Smad1/5/8 and gene expression of Bmp6, Smad7, Id1, and Atoh8 in the mouse liver. Blood 112: 1503-1509.
32. Meynard D, Vaja V, Sun CC, Corradini E, Chen S, et al. (2011) Regulation of TMPRSS6 by BMP6 and iron in human cells and mice. Blood 118: 747-756.
33. Valdimarsdottir G, Goumans MJ, Itoh F, Itoh S, Heldin CH, et al. (2006) Smad7 and protein phosphatase 1alpha are critical determinants in the duration of TGF-beta/ALK1 signaling in endothelial cells. BMC cell biology 7: 16.
34. Patel N, Varghese J, Masaratana P, Latunde-Dada GO, Jacob M, et al. (2014) The transcription factor ATOH8 is regulated by erythropoietic activity and regulates HAMP transcription and cellular pSMAD1,5,8 levels. British journal of haematology 164: 586-596.
35. Shi Y, Massague J (2003) Mechanisms of TGF-beta signaling from cell membrane to the nucleus. Cell 113: 685-700.
36. Feng Q, Migas MC, Waheed A, Britton RS, Fleming RE (2012) Ferritin upregulates hepatic expression of bone morphogenetic protein 6 and hepcidin in mice. American journal of physiology Gastrointestinal and liver physiology 302: G1397-1404.
37. Meynard D, Kautz L, Darnaud V, Canonne-Hergaux F, Coppin H, et al. (2009) Lack of the bone morphogenetic protein BMP6 induces massive iron overload. Nature genetics 41: 478-481.
38. Kautz L, Besson-Fournier C, Meynard D, Latour C, Roth MP, et al. (2011) Iron overload induces BMP6 expression in the liver but not in the duodenum. Haematologica 96: 199-203.
39. Zhang AS, Anderson SA, Wang J, Yang F, DeMaster K, et al. (2011) Suppression of hepatic hepcidin expression in response to acute iron deprivation is associated with an increase of matriptase-2 protein. Blood 117: 1687-1699.
40. Enns CA, Ahmed R, Wang J, Ueno A, Worthen C, et al. (2013) Increased iron loading induces Bmp6 expression in the non-parenchymal cells of the liver independent of the BMP-signaling pathway. PloS one 8: e60534.
41. Monnier PP, Sierra A, Macchi P, Deitinghoff L, Andersen JS, et al. (2002) RGM is a repulsive guidance molecule for retinal axons. Nature 419: 392-395.
42. Samad TA, Srinivasan A, Karchewski LA, Jeong SJ, Campagna JA, et al. (2004) DRAGON: a member of the repulsive guidance molecule-related family of neuronal- and muscle-expressed membrane proteins is regulated by DRG11 and has neuronal adhesive properties. The Journal of neuroscience : the official journal of the Society for Neuroscience 24: 2027-2036.
43. Kuninger D, Kuzmickas R, Peng B, Pintar JE, Rotwein P (2004) Gene discovery by microarray: identification of novel genes induced during growth factor-mediated muscle cell survival and differentiation. Genomics 84: 876-889.
44. Kuninger D, Kuns-Hashimoto R, Kuzmickas R, Rotwein P (2006) Complex biosynthesis of the muscle-enriched iron regulator RGMc. Journal of cell science 119: 3273-3283.

45. Papanikolaou G, Samuels ME, Ludwig EH, MacDonald ML, Franchini PL, et al. (2004) Mutations in HFE2 cause iron overload in chromosome 1q-linked juvenile hemochromatosis. Nature genetics 36: 77-82.
46. Zhang AS, West AP, Jr., Wyman AE, Bjorkman PJ, Enns CA (2005) Interaction of hemojuvelin with neogenin results in iron accumulation in human embryonic kidney 293 cells. The Journal of biological chemistry 280: 33885-33894.
47. Silvestri L, Pagani A, Fazi C, Gerardi G, Levi S, et al. (2007) Defective targeting of hemojuvelin to plasma membrane is a common pathogenetic mechanism in juvenile hemochromatosis. Blood 109: 4503-4510.
48. Nili M, David L, Elferich J, Shinde U, Rotwein P (2013) Proteomic analysis and molecular modelling characterize the iron-regulatory protein haemojuvelin/repulsive guidance molecule c. The Biochemical journal 452: 87-95.
49. Zhang AS, Yang F, Meyer K, Hernandez C, Chapman-Arvedson T, et al. (2008) Neogenin-mediated hemojuvelin shedding occurs after hemojuvelin traffics to the plasma membrane. The Journal of biological chemistry 283: 17494-17502.
50. Frydlova J, Fujikura Y, Vokurka M, Necas E, Krijt J (2013) Decreased hemojuvelin protein levels in mask mice lacking matriptase-2-dependent proteolytic activity. Physiological research / Academia Scientiarum Bohemoslovaca 62: 405-411.
51. Matsunaga E, Chedotal A (2004) Repulsive guidance molecule/neogenin: a novel ligand-receptor system playing multiple roles in neural development. Development, growth & differentiation 46: 481-486.
52. Samad TA, Rebbapragada A, Bell E, Zhang Y, Sidis Y, et al. (2005) DRAGON, a bone morphogenetic protein co-receptor. The Journal of biological chemistry 280: 14122-14129.
53. Kuninger D, Kuns-Hashimoto R, Nili M, Rotwein P (2008) Pro-protein convertases control the maturation and processing of the iron-regulatory protein, RGMc/hemojuvelin. BMC biochemistry 9: 9.
54. Kuns-Hashimoto R, Kuninger D, Nili M, Rotwein P (2008) Selective binding of RGMc/hemojuvelin, a key protein in systemic iron metabolism, to BMP-2 and neogenin. American journal of physiology Cell physiology 294: C994-C1003.
55. Bell CH, Healey E, van Erp S, Bishop B, Tang C, et al. (2013) Structure of the repulsive guidance molecule (RGM)-neogenin signaling hub. Science 341: 77-80.
56. Babitt JL, Zhang Y, Samad TA, Xia Y, Tang J, et al. (2005) Repulsive guidance molecule (RGMa), a DRAGON homologue, is a bone morphogenetic protein co-receptor. The Journal of biological chemistry 280: 29820-29827.
57. Wu Q, Sun CC, Lin HY, Babitt JL (2012) Repulsive guidance molecule (RGM) family proteins exhibit differential binding kinetics for bone morphogenetic proteins (BMPs). PloS one 7: e46307.
58. Zhang AS, Gao J, Koeberl DD, Enns CA (2010) The role of hepatocyte hemojuvelin in the regulation of bone morphogenic protein-6 and hepcidin expression in vivo. The Journal of biological chemistry 285: 16416-16423.

59. Lanzara C, Roetto A, Daraio F, Rivard S, Ficarella R, et al. (2004) Spectrum of hemojuvelin gene mutations in 1q-linked juvenile hemochromatosis. Blood 103: 4317-4321.
60. Pagani A, Silvestri L, Nai A, Camaschella C (2008) Hemojuvelin N-terminal mutants reach the plasma membrane but do not activate the hepcidin response. Haematologica 93: 1466-1472.
61. Niederkofler V, Salie R, Arber S (2005) Hemojuvelin is essential for dietary iron sensing, and its mutation leads to severe iron overload. The Journal of clinical investigation 115: 2180-2186.
62. Lin L, Goldberg YP, Ganz T (2005) Competitive regulation of hepcidin mRNA by soluble and cell-associated hemojuvelin. Blood 106: 2884-2889.
63. Zhang AS, Anderson SA, Meyers KR, Hernandez C, Eisenstein RS, et al. (2007) Evidence that inhibition of hemojuvelin shedding in response to iron is mediated through neogenin. The Journal of biological chemistry 282: 12547-12556.
64. Chen W, Huang FW, de Renshaw TB, Andrews NC (2011) Skeletal muscle hemojuvelin is dispensable for systemic iron homeostasis. Blood 117: 6319-6325.
65. Silvestri L, Pagani A, Camaschella C (2008) Furin-mediated release of soluble hemojuvelin: a new link between hypoxia and iron homeostasis. Blood 111: 924-931.
66. Babitt JL, Huang FW, Xia Y, Sidis Y, Andrews NC, et al. (2007) Modulation of bone morphogenetic protein signaling in vivo regulates systemic iron balance. The Journal of clinical investigation 117: 1933-1939.
67. Nili M, Shinde U, Rotwein P (2010) Soluble repulsive guidance molecule c/hemojuvelin is a broad spectrum bone morphogenetic protein (BMP) antagonist and inhibits both BMP2- and BMP6-mediated signaling and gene expression. The Journal of biological chemistry 285: 24783-24792.
68. Gkouvatsos K, Wagner J, Papanikolaou G, Sebastiani G, Pantopoulos K (2011) Conditional disruption of mouse HFE2 gene: maintenance of systemic iron homeostasis requires hepatic but not skeletal muscle hemojuvelin. Hepatology 54: 1800-1807.
69. Chen W, Sun CC, Chen S, Meynard D, Babitt JL, et al. (2013) A novel validated enzyme-linked immunosorbent assay to quantify soluble hemojuvelin in mouse serum. Haematologica 98: 296-304.
70. Goswami T, Andrews NC (2006) Hereditary hemochromatosis protein, HFE, interaction with transferrin receptor 2 suggests a molecular mechanism for mammalian iron sensing. The Journal of biological chemistry 281: 28494-28498.
71. Gao J, Chen J, Kramer M, Tsukamoto H, Zhang AS, et al. (2009) Interaction of the hereditary hemochromatosis protein HFE with transferrin receptor 2 is required for transferrin-induced hepcidin expression. Cell metabolism 9: 217-227.
72. Johnson MB, Chen J, Murchison N, Green FA, Enns CA (2007) Transferrin receptor 2: evidence for ligand-induced stabilization and redirection to a recycling pathway. Molecular biology of the cell 18: 743-754.
73. Girelli D, Trombini P, Busti F, Campostrini N, Sandri M, et al. (2011) A time course of hepcidin response to iron challenge in patients with HFE and TFR2 hemochromatosis. Haematologica 96: 500-506.

74. D'Alessio F, Hentze MW, Muckenthaler MU (2012) The hemochromatosis proteins HFE, TfR2, and HJV form a membrane-associated protein complex for hepcidin regulation. Journal of hepatology 57: 1052-1060.
75. Calzolari A, Raggi C, Deaglio S, Sposi NM, Stafsnes M, et al. (2006) TfR2 localizes in lipid raft domains and is released in exosomes to activate signal transduction along the MAPK pathway. Journal of cell science 119: 4486-4498.
76. Wallace DF, Summerville L, Crampton EM, Frazer DM, Anderson GJ, et al. (2009) Combined deletion of Hfe and transferrin receptor 2 in mice leads to marked dysregulation of hepcidin and iron overload. Hepatology 50: 1992-2000.
77. Poli M, Luscieti S, Gandini V, Maccarinelli F, Finazzi D, et al. (2010) Transferrin receptor 2 and HFE regulate furin expression via mitogen-activated protein kinase/extracellular signal-regulated kinase (MAPK/Erk) signaling. Implications for transferrin-dependent hepcidin regulation. Haematologica 95: 1832-1840.
78. Corradini E, Rozier M, Meynard D, Odhiambo A, Lin HY, et al. (2011) Iron regulation of hepcidin despite attenuated Smad1,5,8 signaling in mice without transferrin receptor 2 or Hfe. Gastroenterology 141: 1907-1914.
79. Forejtnikova H, Vieillevoye M, Zermati Y, Lambert M, Pellegrino RM, et al. (2010) Transferrin receptor 2 is a component of the erythropoietin receptor complex and is required for efficient erythropoiesis. Blood 116: 5357-5367.
80. Fleming RE, Migas MC, Holden CC, Waheed A, Britton RS, et al. (2000) Transferrin receptor 2: continued expression in mouse liver in the face of iron overload and in hereditary hemochromatosis. Proceedings of the National Academy of Sciences of the United States of America 97: 2214-2219.
81. Kawabata H, Yang R, Hirama T, Vuong PT, Kawano S, et al. (1999) Molecular cloning of transferrin receptor 2. A new member of the transferrin receptor-like family. The Journal of biological chemistry 274: 20826-20832.
82. Kawabata H, Germain RS, Ikezoe T, Tong X, Green EM, et al. (2001) Regulation of expression of murine transferrin receptor 2. Blood 98: 1949-1954.
83. Kawabata H, Nakamaki T, Ikonomi P, Smith RD, Germain RS, et al. (2001) Expression of transferrin receptor 2 in normal and neoplastic hematopoietic cells. Blood 98: 2714-2719.
84. Camaschella C, Roetto A, Cali A, De Gobbi M, Garozzo G, et al. (2000) The gene TFR2 is mutated in a new type of haemochromatosis mapping to 7q22. Nature genetics 25: 14-15.
85. Roetto A, Daraio F, Alberti F, Porporato P, Cali A, et al. (2002) Hemochromatosis due to mutations in transferrin receptor 2. Blood cells, molecules & diseases 29: 465-470.
86. Girelli D, Bozzini C, Roetto A, Alberti F, Daraio F, et al. (2002) Clinical and pathologic findings in hemochromatosis type 3 due to a novel mutation in transferrin receptor 2 gene. Gastroenterology 122: 1295-1302.
87. Biasiotto G, Camaschella C, Forni GL, Polotti A, Zecchina G, et al. (2008) New TFR2 mutations in young Italian patients with hemochromatosis. Haematologica 93: 309-310.

88. Roetto A, Totaro A, Piperno A, Piga A, Longo F, et al. (2001) New mutations inactivating transferrin receptor 2 in hemochromatosis type 3. Blood 97: 2555-2560.
89. Kawabata H, Fleming RE, Gui D, Moon SY, Saitoh T, et al. (2005) Expression of hepcidin is down-regulated in TfR2 mutant mice manifesting a phenotype of hereditary hemochromatosis. Blood 105: 376-381.
90. Roetto A, Di Cunto F, Pellegrino RM, Hirsch E, Azzolino O, et al. (2010) Comparison of 3 Tfr2-deficient murine models suggests distinct functions for Tfr2-alpha and Tfr2-beta isoforms in different tissues. Blood 115: 3382-3389.
91. Nemeth E, Rivera S, Gabayan V, Keller C, Taudorf S, et al. (2004) IL-6 mediates hypoferremia of inflammation by inducing the synthesis of the iron regulatory hormone hepcidin. The Journal of clinical investigation 113: 1271-1276.
92. Verga Falzacappa MV, Vujic Spasic M, Kessler R, Stolte J, Hentze MW, et al. (2007) STAT3 mediates hepatic hepcidin expression and its inflammatory stimulation. Blood 109: 353-358.
93. Besson-Fournier C, Latour C, Kautz L, Bertrand J, Ganz T, et al. (2012) Induction of activin B by inflammatory stimuli up-regulates expression of the iron-regulatory peptide hepcidin through Smad1/5/8 signaling. Blood 120: 431-439.
94. Lee P, Peng H, Gelbart T, Wang L, Beutler E (2005) Regulation of hepcidin transcription by interleukin-1 and interleukin-6. Proceedings of the National Academy of Sciences of the United States of America 102: 1906-1910.
95. Armitage AE, Eddowes LA, Gileadi U, Cole S, Spottiswoode N, et al. (2011) Hepcidin regulation by innate immune and infectious stimuli. Blood 118: 4129-4139.
96. Theurl I, Theurl M, Seifert M, Mair S, Nairz M, et al. (2008) Autocrine formation of hepcidin induces iron retention in human monocytes. Blood 111: 2392-2399.
97. Peyssonnaux C, Zinkernagel AS, Schuepbach RA, Rankin E, Vaulont S, et al. (2007) Regulation of iron homeostasis by the hypoxia-inducible transcription factors (HIFs). The Journal of clinical investigation 117: 1926-1932.
98. Silvestri L, Pagani A, Nai A, De Domenico I, Kaplan J, et al. (2008) The serine protease matriptase-2 (TMPRSS6) inhibits hepcidin activation by cleaving membrane hemojuvelin. Cell metabolism 8: 502-511.
99. Lakhal S, Schodel J, Townsend AR, Pugh CW, Ratcliffe PJ, et al. (2011) Regulation of type II transmembrane serine proteinase TMPRSS6 by hypoxia-inducible factors: new link between hypoxia signaling and iron homeostasis. The Journal of biological chemistry 286: 4090-4097.
100. Maurer E, Gutschow M, Stirnberg M (2012) Matriptase-2 (TMPRSS6) is directly up-regulated by hypoxia inducible factor-1: identification of a hypoxia-responsive element in the TMPRSS6 promoter region. Biological chemistry 393: 535-540.
101. Volke M, Gale DP, Maegdefrau U, Schley G, Klanke B, et al. (2009) Evidence for a lack of a direct transcriptional suppression of the iron regulatory peptide hepcidin by hypoxia-inducible factors. PloS one 4: e7875.

102. Liu Q, Davidoff O, Niss K, Haase VH (2012) Hypoxia-inducible factor regulates hepcidin via erythropoietin-induced erythropoiesis. The Journal of clinical investigation 122: 4635-4644.
103. Yoon D, Pastore YD, Divoky V, Liu E, Mlodnicka AE, et al. (2006) Hypoxia-inducible factor-1 deficiency results in dysregulated erythropoiesis signaling and iron homeostasis in mouse development. The Journal of biological chemistry 281: 25703-25711.
104. Tanno T, Bhanu NV, Oneal PA, Goh SH, Staker P, et al. (2007) High levels of GDF15 in thalassemia suppress expression of the iron regulatory protein hepcidin. Nature medicine 13: 1096-1101.
105. Tanno T, Porayette P, Sripichai O, Noh SJ, Byrnes C, et al. (2009) Identification of TWSG1 as a second novel erythroid regulator of hepcidin expression in murine and human cells. Blood 114: 181-186.
106. Casanovas G, Vujic Spasic M, Casu C, Rivella S, Strelau J, et al. (2013) The murine growth differentiation factor 15 is not essential for systemic iron homeostasis in phlebotomized mice. Haematologica 98: 444-447.
107. Sonnweber T, Nachbaur D, Schroll A, Nairz M, Seifert M, et al. (2014) Hypoxia induced downregulation of hepcidin is mediated by platelet derived growth factor BB. Gut 63: 1951-1959.
108. Kautz L, Jung G, Valore EV, Rivella S, Nemeth E, et al. (2014) Identification of erythroferrone as an erythroid regulator of iron metabolism. Nature genetics 46: 678-684.
109. Velasco G, Cal S, Quesada V, Sanchez LM, Lopez-Otin C (2002) Matriptase-2, a membrane-bound mosaic serine proteinase predominantly expressed in human liver and showing degrading activity against extracellular matrix proteins. The Journal of biological chemistry 277: 37637-37646.
110. Ramsay AJ, Reid JC, Velasco G, Quigley JP, Hooper JD (2008) The type II transmembrane serine protease matriptase-2--identification, structural features, enzymology, expression pattern and potential roles. Frontiers in bioscience : a journal and virtual library 13: 569-579.
111. Ramsay AJ, Quesada V, Sanchez M, Garabaya C, Sarda MP, et al. (2009) Matriptase-2 mutations in iron-refractory iron deficiency anemia patients provide new insights into protease activation mechanisms. Human molecular genetics 18: 3673-3683.
112. Ramsay AJ, Hooper JD, Folgueras AR, Velasco G, Lopez-Otin C (2009) Matriptase-2 (TMPRSS6): a proteolytic regulator of iron homeostasis. Haematologica 94: 840-849.
113. Maxson JE, Chen J, Enns CA, Zhang AS (2010) Matriptase-2- and proprotein convertase-cleaved forms of hemojuvelin have different roles in the down-regulation of hepcidin expression. The Journal of biological chemistry 285: 39021-39028.
114. Enns CA, Ahmed R, Zhang AS (2012) Neogenin interacts with matriptase-2 to facilitate hemojuvelin cleavage. The Journal of biological chemistry 287: 35104-35117.
115. Krijt J, Fujikura Y, Ramsay AJ, Velasco G, Necas E (2011) Liver hemojuvelin protein levels in mice deficient in matriptase-2 (Tmprss6). Blood cells, molecules & diseases 47: 133-137.

116. Finberg KE, Whittlesey RL, Fleming MD, Andrews NC (2010) Down-regulation of Bmp/Smad signaling by Tmprss6 is required for maintenance of systemic iron homeostasis. Blood 115: 3817-3826.
117. Finberg KE, Heeney MM, Campagna DR, Aydinok Y, Pearson HA, et al. (2008) Mutations in TMPRSS6 cause iron-refractory iron deficiency anemia (IRIDA). Nature genetics 40: 569-571.
118. Du X, She E, Gelbart T, Truksa J, Lee P, et al. (2008) The serine protease TMPRSS6 is required to sense iron deficiency. Science 320: 1088-1092.
119. Folgueras AR, de Lara FM, Pendas AM, Garabaya C, Rodriguez F, et al. (2008) Membrane-bound serine protease matriptase-2 (Tmprss6) is an essential regulator of iron homeostasis. Blood 112: 2539-2545.
120. Guillem F, Lawson S, Kannengiesser C, Westerman M, Beaumont C, et al. (2008) Two nonsense mutations in the TMPRSS6 gene in a patient with microcytic anemia and iron deficiency. Blood 112: 2089-2091.
121. Melis MA, Cau M, Congiu R, Sole G, Barella S, et al. (2008) A mutation in the TMPRSS6 gene, encoding a transmembrane serine protease that suppresses hepcidin production, in familial iron deficiency anemia refractory to oral iron. Haematologica 93: 1473-1479.
122. Silvestri L, Guillem F, Pagani A, Nai A, Oudin C, et al. (2009) Molecular mechanisms of the defective hepcidin inhibition in TMPRSS6 mutations associated with iron-refractory iron deficiency anemia. Blood 113: 5605-5608.
123. De Falco L, Totaro F, Nai A, Pagani A, Girelli D, et al. (2010) Novel TMPRSS6 mutations associated with iron-refractory iron deficiency anemia (IRIDA). Human mutation 31: E1390-1405.
124. Altamura S, D'Alessio F, Selle B, Muckenthaler MU (2010) A novel TMPRSS6 mutation that prevents protease auto-activation causes IRIDA. The Biochemical journal 431: 363-371.
125. Sato T, Iyama S, Murase K, Kamihara Y, Ono K, et al. (2011) Novel missense mutation in the TMPRSS6 gene in a Japanese female with iron-refractory iron deficiency anemia. International journal of hematology 94: 101-103.
126. Choi HS, Yang HR, Song SH, Seo JY, Lee KO, et al. (2012) A novel mutation Gly603Arg of TMPRSS6 in a Korean female with iron-refractory iron deficiency anemia. Pediatric blood & cancer 58: 640-642.
127. Guillem F, Kannengiesser C, Oudin C, Lenoir A, Matak P, et al. (2012) Inactive matriptase-2 mutants found in IRIDA patients still repress hepcidin in a transfection assay despite having lost their serine protease activity. Human mutation 33: 1388-1396.
128. Pellegrino RM, Coutinho M, D'Ascola D, Lopes AM, Palmieri A, et al. (2012) Two novel mutations in the tmprss6 gene associated with iron-refractory iron-deficiency anaemia (irida) and partial expression in the heterozygous form. British journal of haematology 158: 668-672.
129. De Falco L, Silvestri L, Kannengiesser C, Moran E, Oudin C, et al. (2014) Functional and clinical impact of novel tmprss6 variants in iron-refractory iron-deficiency anemia patients and genotype-phenotype studies. Human mutation 35: 1321-1329.
130. Kodama K, Noguchi A, Adachi H, Hebiguchi M, Yano M, et al. (2014) Novel mutation in the TMPRSS6 gene with iron-refractory iron deficiency

anemia. Pediatrics international : official journal of the Japan Pediatric Society 56: e41-44.
131. Wang CY, Meynard D, Lin HY (2014) The role of TMPRSS6/matriptase-2 in iron regulation and anemia. Frontiers in pharmacology 5: 114.
132. Silvestri L, Rausa M, Pagani A, Nai A, Camaschella C (2013) How to assess causality of TMPRSS6 mutations? Human mutation 34: 1043-1045.
133. Lenoir A, Deschemin JC, Kautz L, Ramsay AJ, Roth MP, et al. (2011) Iron-deficiency anemia from matriptase-2 inactivation is dependent on the presence of functional Bmp6. Blood 117: 647-650.
134. Finberg KE, Whittlesey RL, Andrews NC (2011) Tmprss6 is a genetic modifier of the Hfe-hemochromatosis phenotype in mice. Blood 117: 4590-4599.
135. Liu W, Hou Y, Chen H, Wei H, Lin W, et al. (2011) Sample preparation method for isolation of single-cell types from mouse liver for proteomic studies. Proteomics 11: 3556-3564.

CHAPTER 2

Identification of TMPRSS6 cleavage sites of hemojuvelin

Marco Rausa[1,2], Michela Ghitti[1], Alessia Pagani[1,2], Antonella Nai[2], Alessandro Campanella[1,2], Giovanna Musco[1], Clara Camaschella[1,2] and Laura Silvestri[1,2]

[1] Division of Genetics and Cell Biology, IRCCS Ospedale San Raffaele, Milan, Italy
[2] Vita Salute University, Milan, Italy

(*Accepted for publication in Journal of Cellular and Molecular Medicine on 19 September 2014*)

ABSTRACT

Hemojuvelin (HJV), the coreceptor of the BMP-SMAD pathway that upregulates hepcidin transcription, is a Repulsive Guidance Molecule (RGMc) which undergoes a complex intracellular processing. Following autoproteolysis, it is exported to the cell surface both as a full-length and a heterodimeric protein. *In vitro* membrane HJV (m-HJV) is cleaved by the transmembrane serine-protease TMPRSS6 in order to attenuate signalling and inhibit hepcidin expression. In this study we investigated the number and position of HJV cleavage sites by mutagenizing arginine residues (R), potential TMPRSS6 targets, to alanine (A). We analysed translation and membrane expression of HJV R mutants and the pattern of fragments they release in the culture media in the presence of TMPRSS6. Abnormal fragments were observed for mutants at arginine 121, 176, 218, 288 and 326. Considering that all variants except HJV^{R121A} lack autoproteolytic activity and some (HJV^{R176A} and HJV^{R288A}) are expressed at reduced levels on cell surface, we identified the fragments originating from either full length or heterodimeric proteins and defined the residues 121 and 326 as the TMPRSS6 cleavage sites in both isoforms. Using the N-terminal FLAG-tagged HJV we showed that residue 121 is critical also in the rearrangement of the N-terminal heterodimeric HJV. Exploiting the recently reported RGMb crystallographic structure we generated a model of HJV that was used as input structure for all-atoms molecular dynamics simulation in explicit solvent. As assessed by *in silico* studies, we concluded that some arginines in the von Willebrand domain appear TMPRSS6 insensitive, likely because of partial protein structure destabilization.

1. INTRODUCTION

Hepcidin is the hepatic peptide hormone which controls iron absorption from the enterocytes and iron release from the stores by degrading the only known cellular iron exporter ferroportin [1]. Hemojuvelin (HJV) and TMPRSS6 play a crucial role in regulating hepcidin expression. In hepatocytes HJV on cell surface (m-HJV) acts as BMP-coreceptor, allowing BMP6 to signal through BMP-SMAD pathway to activate hepcidin transcription [2-5]. On the contrary, soluble HJV (s-HJV; Figure 1A) derived from furin cleavage at the RNRR motif ([6-8] acts as a decoy molecule, inhibiting hepcidin activation *in vitro* [9,10].

HJV belongs to the family of Repulsive Guidance Molecules (RGM) and is mutated in juvenile hemochromatosis [11]. The protein is characterized by a signal peptide, a RGD motif, a partial von Willebrand type D (vWD) domain and a glycosilphosphatidylinositol (GPI)-anchor domain [11] (Figure 1A). The protein undergoes partial autoproteolytic cleavage at the GDPH motif [12] to produce a heterodimer that is exposed on the cell surface. The latter is composed by a C-terminal fragment of about 33 kDa [13], joined by disulfide bonds [14] to a N-terminal fragment reported to be of about 15-20 kDa [12,13,15-17]. *In vitro*, HJV is present on the cell surface both as heterodimeric and full-length isoform [14,16]. Neogenin, BMPs and TMPRSS6 are HJV interactors. It has been reported that neogenin preferentially binds heterodimeric HJV, while BMP-2 interacts with single-chain HJV species [18]. However we have previously shown that only heterodimeric forms of HJV activates hepcidin *in vitro* [19].

The transmembrane serine protease TMPRSS6 is a major hepcidin inhibitor since its mutations are responsible of Iron Refractory Iron Deficiency Anemia (IRIDA), characterized by inappropriate hepcidin production [20]. Although a formal proof that *in vivo* HJV is the TMPRSS6 substrate is still lacking, *in vitro* the protease cleaves m-HJV into soluble fragments [21], a process that might abolish the signalling and repress hepcidin expression [22,23]. TMPRSS6 function is facilitated by the formation of a ternary complex with the transmembrane receptor neogenin on the cell surface [24]. The mechanism of TMPRSS6 cleavage and the cleavage sites of HJV are still undefined. One putative cleavage site has been suggested at arginine (R) 288 [25]. Since fragments originating from TMPRSS6 cleavage are multiple [21,26,27], we hypothesize that other sites are cleaved in HJV. In order to verify this hypothesis, we mutagenized HJV R residues to alanine (A) and analyzed the mutant proteins processing, their sensitivity to TMPRSS6 cleavage and their hepcidin activating ability. From the abnormal pattern of fragments released by the HJV variants, here we show that TMPRSS6 cleavage occurs at specific sites and that *in vitro* TMPRSS6 cleaves both the heterodimeric and the full-length m-HJV, originating different C-terminal and the same N-terminal fragments. We identified R residues in the vWD domain whose mutations indirectly cause cleavage-resistance, likely by destabilization of the HJV protein structure. Finally we better characterized the N-terminal fragments deriving from HJV autoproteolytic process.

2.MATERIALS AND METHODS

2.1 Cell culture and expressing vectors

Cell culture media and reagents were from Invitrogen (Carlsbad, CA) and Sigma-Aldrich (St. Louis, MO). HeLa cells were cultured in Dulbecco's modified Eagle's medium (DMEM) and Hep3B in Earle's minimal essential medium (EMEM), supplemented with 2mM L-glutamine, 200 U/ml penicillin, 1 mM sodium pyruvate and 10% heat-inactivated fetal bovine serum (FBS) at 37°C in 95% humidifier air and 5% CO2.

HJV mutants were generated from pcDNA3.1-HJV [19] using the QuickChange II XL mutagenesis (Agilent Technologies, La Jolla, CA), following manufacturer's instructions and using the oligonucleotides listed in Table S1.

TMPRSS6 wild type and TMPRSS6^{MASK}, lacking the serine protease domain, were obtained as previously described [21].

The FLAG-tag HJV expressing vector [2] (HJV^{FLAG}), kindly provided by Herbert Lin (Harvard, Boston, US), was mutagenized as described above.

2.2 Cell surface protein quantification by binding assay

HJV surface expression was quantified as previously described [13]. In brief, 10^4 HeLa cells were seeded in 48-well plates and transfected with 0.4 μg of plasmid DNA with 1 μl of Lipofectamine 2000 (Invitrogen). After 12 hrs the medium was replaced with DMEM supplemented with 2% FBS. After 36 hrs from transfection cells were fixed with 4% paraformaldehyde. Cells were permeabilized with Triton X-100 in PBS to assess whole HJV expression. Cells were

blocked with 5% non-fat milk in PBS, incubated with rabbit anti-HJV (1:1000) and then with the secondary HRP antibody. Peroxidase activity was measured with a HRP substrate (o-phenylenediamine dihydrochloride) (Sigma-Aldrich) according to the manufacturer's instructions. The amount of m-HJV was calculated as the ratio between the absorbance of unpermeabilized and permeabilized cells. Background absorbance was subtracted for each sample. Two-tail student's t test was used for statistical analysis.

2.3 Western blot analysis

HeLa cells were seeded in 100 mm diameter dishes at 70-80% of confluency and transiently transfected with 13 μg of plasmid DNA and 32,5 μl of liposomal transfection reagent Lipofectamine 2000 (Invitrogen) in 3 ml of Optimem (Invitrogen). After 18 hrs the medium was replaced with 4 ml of Optimem and 24 hrs later media were collected and concentrated using 5 kDa molecular weight (MW) cut-off ultrafiltration (Amicon Ultra; Millipore, Bilerica, MA). Cells were lysed, proteins were quantified and total lysates processed for Western Blot analysis as previously described [21] and as detailed in the Supplemental Methods.

2.4 Co-immunoprecipitation

HeLa cells were transfected with wild type or mutant HJV and TMPRSS6^{MASK} (20 μg of total plasmid DNA, ratio 1:1, in a 100 mm diameter dish). After 36 hrs cells were lysed in NET/Triton buffer; 500 μg of total lysates were pulled down using the anti-FLAG M2 agarose affinity gel (Sigma Aldrich) for 2 hrs at 4 °C, followed by three washing with NET/Triton buffer. Samples were eluted in

Laemmli sample buffer and subjected to SDS-PAGE on 10% acrylamide gel. Immunodetection was performed as described above using rabbit anti-HJV and rabbit anti-FLAG (Sigma-Aldrich) as primary antibodies.

2.5 Cell surface biotinylation assay

HeLa cells, seeded in 100 mm diameter dishes, were transiently transfected with 13 μg of plasmid DNA as described above. After 18 hrs the medium was changed with 4 ml of Optimem and 24 hrs later biotinylation of HeLa surface proteins was performed with EZ-Link NHS-SS-Biotin (Thermo Scientific) at 4 °C for 30 minutes, prior to lysis using NET/Triton buffer. Biotinylated proteins were pulled down using the Streptavidin Sepharose High performance beads (GE Helthcare, Buckinghamshire, UK) and equal amount of the resulting samples was loaded on a 10% SDS-PAGE. Immunodetection was performed as described above with anti-HJV and rabbit anti-Pan Cadherin (Abcam, Cambridge Science Park, UK) (for biotin and pull-down normalizations) as primary antibodies.

2.6 Hepcidin promoter based luciferase assay

A pGL2-basic reporter vector (Promega, Madison, WI, USA), harboring a 2.9 Kb fragment of human hepcidin promoter (Hep-Luc), was used to analyze the hepcidin promoter activity by luciferase assay in Hep3B cells cotransfected with wild type or mutant HJV expressing vectors, as already reported [19] and as detailed in the Supporting Information section. When indicated, transfected cells were incubated for 3 hours with 10 ng/ml of recombinant BMP6 (R&D System). Exogenous HJV levels were measured by qRT-PCR on transfected

Hep3B cells (see Supplementary Information). Experiments were performed in triplicate. Two-tail student's t test was used for statistical analysis.

2.7 Homology Modelling and Molecular Dynamics simulation

I-TASSER server [28] was used to predict the secondary and tertiary structure of HJV. The generated model (G163-L327) was based on the structural coordinates of the Repulsive Guidance Molecule b, RGMb (pdb id=4bq8, chain B and C) that shares a sequence identity of 48% with HJV (RGMc protein). All atoms Molecular Dynamics simulation in explicit solvent was performed using GROMACS4.6.5 software package [29]. Simulation details are in Supplementary Information.

3. RESULTS

3.1 Cell surface expression of the HJV variants

We mutagenized 24 (out of 29) HJV R residues to alanine (A). Their position in the protein is shown in Figure 1B. We did not mutagenize R residues located in the signal peptide (SP), since not present in the mature protein, and in the pro-protein convertase furin cleavage site (FCS), which is not involved in TMPRSS6 cleavage as previously described [21,25].

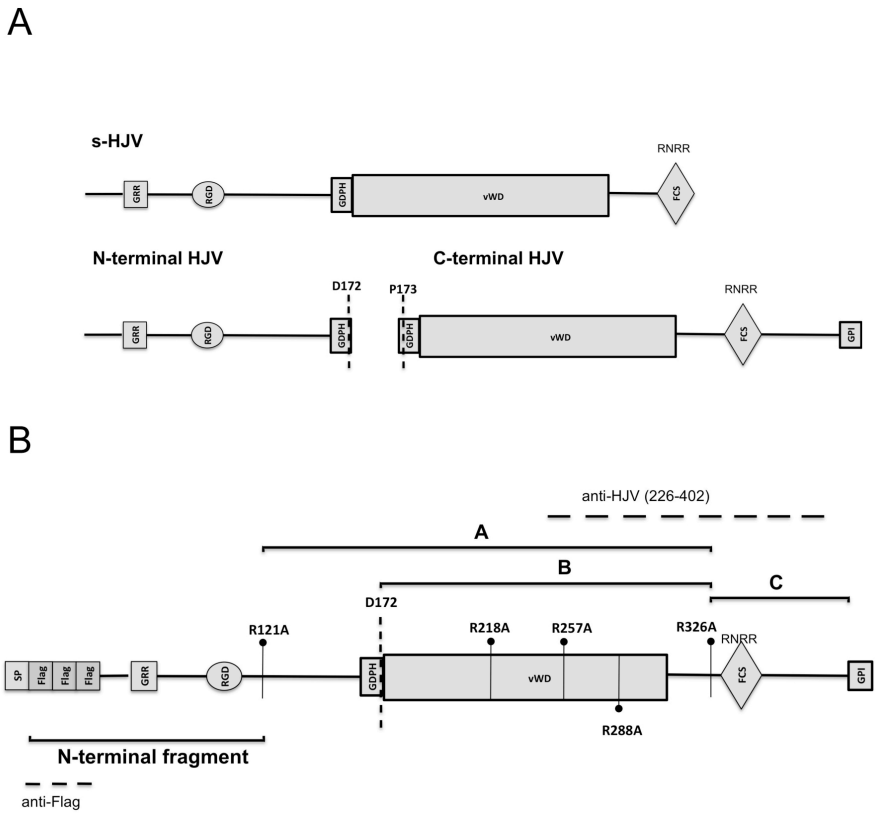

Figure 1. Schematic representation of the hemojuvelin protein
(A) Soluble HJV (s-HJV) [6-8], the C-terminal and the N-terminal portion of the heterodimeric HJV [15] are shown. (B) The Arginine (R) residues mutagenized to Alanine (A) are indicated. Dotted lines indicate the HJV sequence recognized by anti-HJV (raised against a peptide from amino acid 226 to 400) and by anti-FLAG antibodies. The size of fragments A, B and C, released after TMPRSS6 cleavage and recognized by the anti-HJV Ab (see also Figure 3 for comparison), and the HJV N-terminal fragment (from 33 to 121), recognized using the anti-FLAG antibody (see Figure 4 for comparison), are shown as solid line. SP: signal peptide; GRR: glycine rich domain; RGD (arginine-glycine-aspartic acid): integrin-binding domain; GDPH: autocatalytic cleavage site; vWD: partial von Willebrand domain type D; FCS: furin cleavage site; GPI: glycosylphosphatidylinositol anchor. The autoproteolysis motif is shown by a black dotted line.

We first assessed whether the HJV variants are correctly translated and reach the cell surface as the wild type protein. To this aim we used a previously developed binding assay that quantifies surface HJV in transfected cells [13]. Of the 24 available mutants, HJV^{R98A},

HJV^{R160A} and HJV^{R186A} are not efficiently translated. All the others reach the cell surface, except HJV^{R41A} (data not shown), HJV^{R176A} and HJV^{R288A} (Figure 2A) that are approximately 35% less expressed on the plasma membrane than wild type HJV. We then investigated the cellular processing of HJV mutants, including the presence of the 33 kDa band, an indicator of the proper autoproteolysis and plasma membrane localization. HJV^{R121A} behaves as the wild type protein and HJV^{R257A} maintains the ability to undergo autoproteolysis, although at reduced rate (Figure 2B). These variants are thus exported on the cell surface as both heterodimeric and full-length isoforms. HJV^{R176A}, HJV^{R218A}, HJV^{R288A} and HJV^{R326A} lack the 33 kDa band (Figure 2B and Figure S1), indicating that they do not undergo autoproteolysis and are expressed on the plasma membrane only as full-length isoforms.

All the mutants release s-HJV at the same degree as the wild type protein, pointing out that the R→A substitution does not affect the furin cleavage process (Figure 2B).

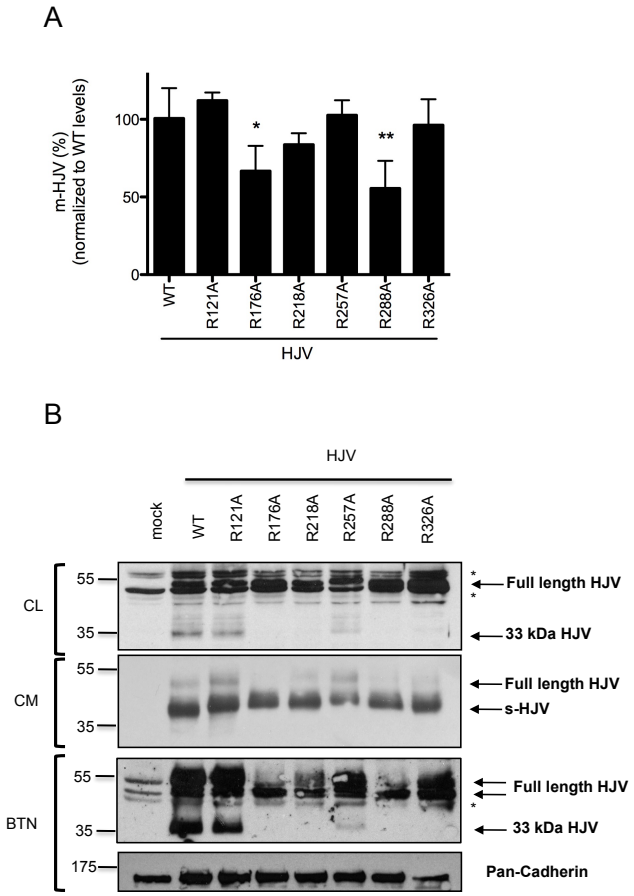

Figure 2. Cell surface expression of HJV variants

(A) HeLa cells, transiently transfected with 0.2 µg of wild type (wt) or mutant HJV expressing vectors were fixed, permeabilized (to assess whole HJV expression) and incubated with anti-HJV antibody. The amount of membrane-bound HJV was calculated as the ratio between the absorbance of unpermeabilized and permeabilized cells. Background absorbance was subtracted for each sample. HJV^{WT} levels are set to 100% and HJV variants surface expression was normalized to wild type levels. Statistical significance was calculated on three independent experiments, made in triplicate. Error bars indicate SD. * = P< .05., ** = P< .01 (B). HeLa cells were transfected with wild type (WT) or mutant HJV expressing vectors. Thirty-six hours later cell culture media were collected and concentrated (CM) and cell surface proteins were biotinylated. Cells were lysed and equal amounts of proteins were pulled down with streptavidin. Whole cell lysate (CL), cell media (CM) and biotinylated proteins (BTN) were loaded on a 10% SDS-PAGE and processed for western blot analysis. The anti-HJV antibody was used to detect HJV and anti-Pan Cadherin to normalize for cell surface expression. Experiments were performed three times. A representative Western blot is shown. The asterisks indicate unspecific bands. Numbers indicate size in kDa.

3.2 Identification of TMPRSS6 cleavage sites of HJV

TMPRSS6 releases in the conditioned medium discrete HJV fragments of approximately 30, 25 and 15 kDa, indicated as A, B and C, respectively (Figure 3 and [21]), as revealed by the anti-C terminal HJV antibody [13]. These fragments originate from the specific cleavage activity of the serine protease on HJV, since we have repeatedly shown that they are undetectable when a proteolytically inactive variant of TMPRSS6 is co-expressed with HJV [21,26,27].

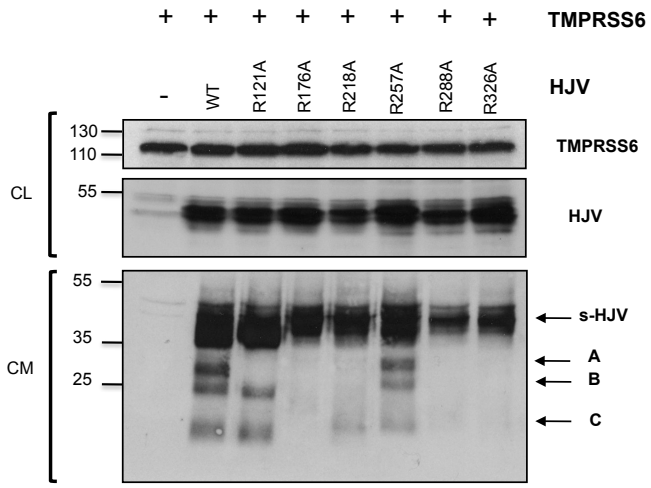

Figure 3. Analysis of TMPRSS6 mediated cleavage on C-terminal HJV
Cell culture media (CM) and total lysate (CL) of HeLa cells cotransfected with TMPRSS6 and WT or HJV variants were loaded onto a 10% SDS-PAGE and processed for western blot analysis. Fragments A, B and C originate from TMPRSS6 cleavage, while s-HJV is not affected by TMPRSS6 (see Figure 1B for fragments interpretation). The anti-HJV antibody was used to detect HJV and anti-FLAG to detect TMPRSS6. Experiments were performed three times. A representative Western blot is shown. Numbers indicate size in kDa.

The same pattern of fragments is expected to be modified or absent when R residues, targets of TMPRSS6 cleavage, are mutagenized. A previous study has examined the fragments resulting from TMPRSS6

cleavage using a different antibody [25], which reveals a single evident band of about 36 kDa, that could correspond to fragment A in our study. The use of different antibodies and molecular weight markers may explain the size discrepancies in the two studies.

In the presence of TMPRSS6, N-terminal mutants from R41A to R156A (Figure 1), except R121A (see below), behave as the wild type protein (representative N-terminal mutants are shown in Figure S2). Since the antibody recognizes the C-terminal region of HJV (Figure 1), we conclude that R mutagenesis at the N-terminal part of the protein does not perturb the TMPRSS6-mediated cleavage of the C-terminal portion of HJV.

We observe that HJV^{R121A}, when co-expressed with TMPRSS6, releases fragments B and C, but lacks fragment A (Figure 3). In addition, in a less exposed blot (Figure S3), a band is visible around 40 kDa, which could correspond to the abnormal fragment originated from the absence of the cleavage in R121. This clearly indicates that R121 is a TMPRSS6 target site and that its cleavage originates fragment A.

The HJV^{R218A} variant releases only the shortest size (C) fragment, whereas the HJV^{R257A} mutant behaves as the wild type protein (Figure 3 and Figure S4), although with lower efficiency, confirming previous finding [25]. R substitutions close to the GPI-anchor (positions 329, 344, 345 and 385) and outside the FCS result in normal fragments (data not shown). HJV^{R176A}, HJV^{R288A} and HJV^{R326A}, that show slightly reduced membrane localization (Figure 2A and B), do not release any fragment in the presence of TMPRSS6 (Figure 3). In theory each of these positions could be a TMPRSS6 cleavage site.

However, based on the fragment size, we favor the arginine at position 326 as cleavage site. Our interpretation takes into account that m-HJV in transfected cells may be either full-length or heterodimeric [13,16]. We observed that fragment B is present only in the two mutants (HJV^{R121A} and HJV^{R257A}) that undergo autoproteolysis and are exposed as heterodimeric forms (Figure 2B), and that R substitution at position 326 abrogates all fragments (Figure 3). We propose that fragment A originates from the cleavage at position 121 and 326 of the full length m-HJV and fragment B originates from the cleavage at position 326 of the heterodimeric isoform (from the GDPH motif to amino acid 326) (Figure 1B). Fragment C derives from cleavage at position 326 of the C-terminus of both m-HJV isoforms (from amino acid 326 to the GPI-anchor) (Figure 1B). Indeed its intensity is reduced in the HJV variants that do not undergo (HJV^{R218A}) or undergo only partial (HJV^{R257A}) autoproteolysis (Figure 3) and lack or show reduced heterodimeric m-HJV.

To investigate the cleavage products of the N-terminal portion of HJV, in the absence of specific antibodies we took advantage of the HJV^{FLAG} tag construct that in previous functional studies behaves as the wild type protein [2]. HeLa cells transfected with $HJV^{FLAG\ WT}$ alone release in the culture media the full length HJV (likely by endogenous PI-PLC cleavage of the GPI-anchor), s-HJV (that originates from furin cleavage) (Figure S5) and a smaller fragment of approximately 22 kDa (Figure 4).

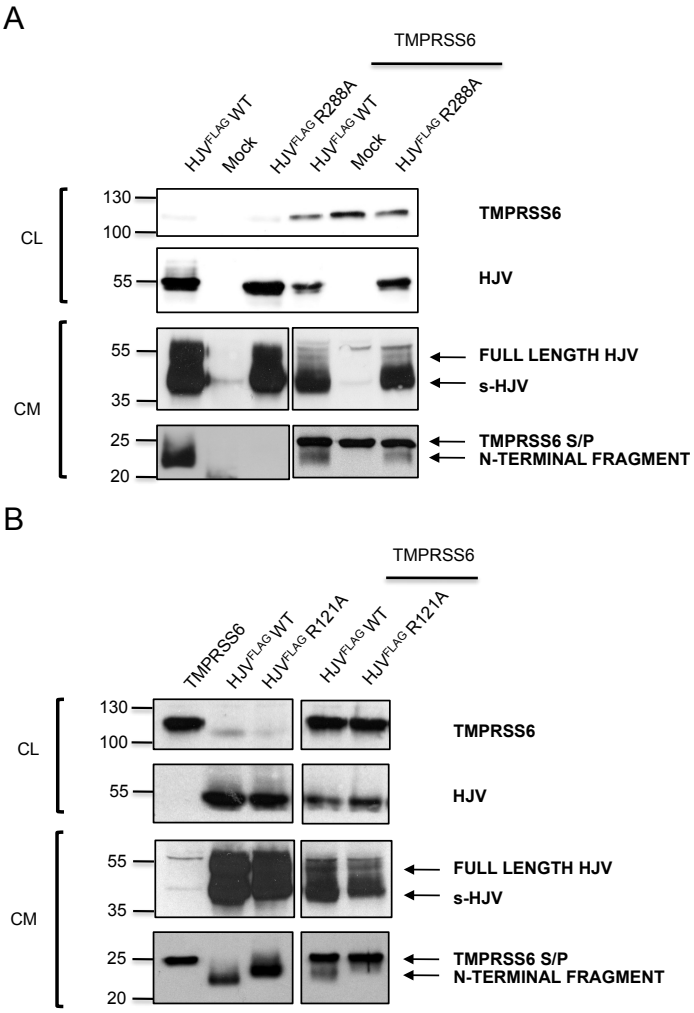

Figure 4. Analysis of TMPRSS6 mediated cleavage on N-terminal HJV
Cell culture media (CM) and lysates (CL) of HeLa cells cotransfected with empty vector (mock), $HJV^{FLAG\ WT}$, $HJV^{FLAG\ R288A}$ or $HJV^{FLAG\ R121A}$ alone or in combination with TMPRSS6 were loaded onto a 10% SDS-PAGE and processed for western blot analysis. The anti-FLAG antibody recognizes both TMPRSS6 (the serine protease domain released in the CM, S/P, and TMPRSS6 in CL) and 3 different HJV isoforms: full length HJV (CL and CM), s-HJV (CM) and N-terminal HJV fragments derived from autoproteolysis (CM). Experiments were performed three times. A representative Western blot is shown. Numbers indicate size in kDa.

Since the autoproteolytically inactive $HJV^{FLAG\ R288A}$ variant does not release the latter fragment (Figure 4A), we conclude that the 22 kDa

band represents the N-terminal region of the heterodimeric surface HJV, originating from the autoproteolytic activity (Figure 4). The size of this fragment is compatible with the reported size of ≈20 kDa [14,16,17], the difference being accounted by the three FLAG tags present in our expressing vector.

The same ≈22 kDa N-terminal fragment is visible when $HJV^{FLAG\ WT}$ is coexpressed with TMPRSS6 but is absent in $HJV^{FLAG\ R288A}$, lacking the autoproteolytic activity (Figure 4A). A band of ≈22 kDa appears when the latter mutant is expressed with TMPRSS6 (Figure 4A). This confirms that the fragment originates from full length HJV and that 121 is the most N-terminal cleavage site. Interestingly, the fragment generated by TMPRSS6 cleavage of full length HJV and that originating by autoproteolysis share the same molecular weight (from amino acid 33 to 121).

The $HJV^{FLAG\ R121A}$ mutant, that undergoes autoproteolysis, releases a larger fragments that migrates slower than those observed in the wild type protein (about 23-24 kDa) (Figure 4B). The different size is not due to the protein glycosylation status, since PNGase treatment does not abrogate the difference between wild type and $HJV^{FLAG\ R121A}$ fragments (Figure S6). Likely the GDPH cleavage is followed by additional cleavage occurring between amino acid 121 to 172 to generate the ≈23-24 kDa band.

3.3 All HJV mutants interact with TMPRSS6

To exclude that the altered pattern of fragments observed in some variants was due to impaired interaction with TMPRSS6, we investigated the ability of the studied mutants to interact with the

serine protease by co-immunoprecipitation. HeLa cells were cotransfected with HJV^{WT} or R variants in combination with $TMPRSS6^{MASK}$, a serine protease lacking the catalytic domain [22] that was used to prevent HJV degradation [21] and to improve the western blot sensitivity. All the HJV variants examined interact with the TMPRSS6 ectodomain (Figure S7), indicating that, in case HJV cleavage fragments were absent, this was not due to lack of interaction with TMPRSS6.

3.4 HJV Molecular Dynamics simulation

Since the crystallographic structure of RGMb protein (pdb id=4bq8C) [30] shares 48% sequence identity with HJV (RGMc), we used its coordinates to build a homology model of HJV (G163-L327). In order to investigate the cleavage accessibility of R176, R218, R257 and R288 and to rationalize the functional and structural effects of alanine mutations in these positions, we performed 100 ns of molecular dynamics simulation on HJV model and analyzed the dynamical behavior of these arginines during the trajectory. The position of R176, R218, R257 and R288 was mapped on the three-dimensional structure of HJV as shown in Figure 5A.

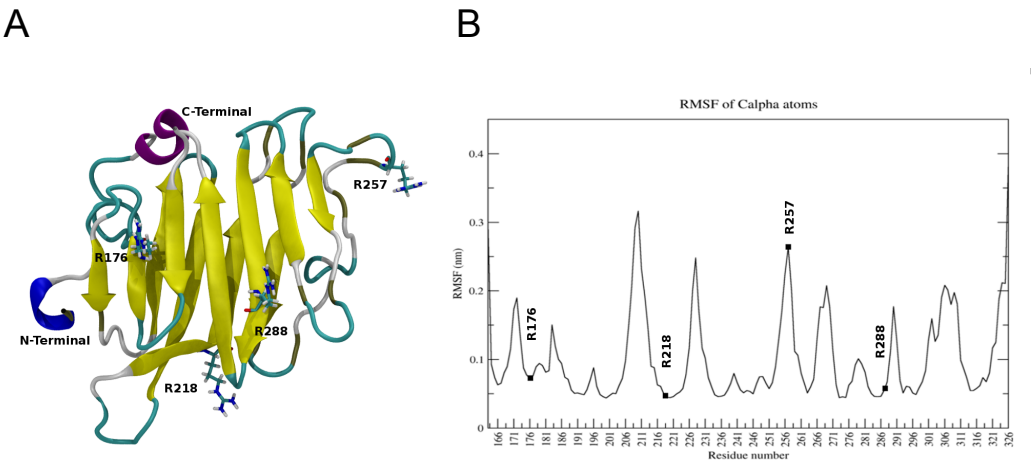

Figure 5: Structural characterization of HJV by means of Molecular Dynamics. (A) Representative HJV snapshot-structure extracted from molecular dynamics simulation shown as cartoon. The extended beta-sheet, the 3-10 helix, the alpha helix, the bridges, the turns and the coils regions are colored in yellow, blue, purple, tan, cyan and white, respectively. The side-chains of R176, R218, R257 and R288 are visualized in sticks. All molecular graphics were produced with VMD [32]. (B) The Root Mean Squared Fluctuations (RMSF) of HJV Cα atoms from their time-averaged positions. The RMSF were calculated over the last 80 ns of simulation. Cα atoms corresponding to R176, 218, R257 and R288 are visualized as black dots.

In particular we observed that the backbone atoms of R176, R218 and R288, that are within well defined secondary structure elements (three beta strands) appear quite rigid all along the simulation, as assessed by the low Root Mean Square Fluctuation (RMSF) of their Cα atoms (Figure 5B). Of note, the side-chain of the highly conserved R176 stably interacts with an aromatic cage formed by F182 and H180, creating stabilizing π-cation interactions with the aromatic ring and histidine-arginine pairing, respectively (Figure 6A and Figure S8).

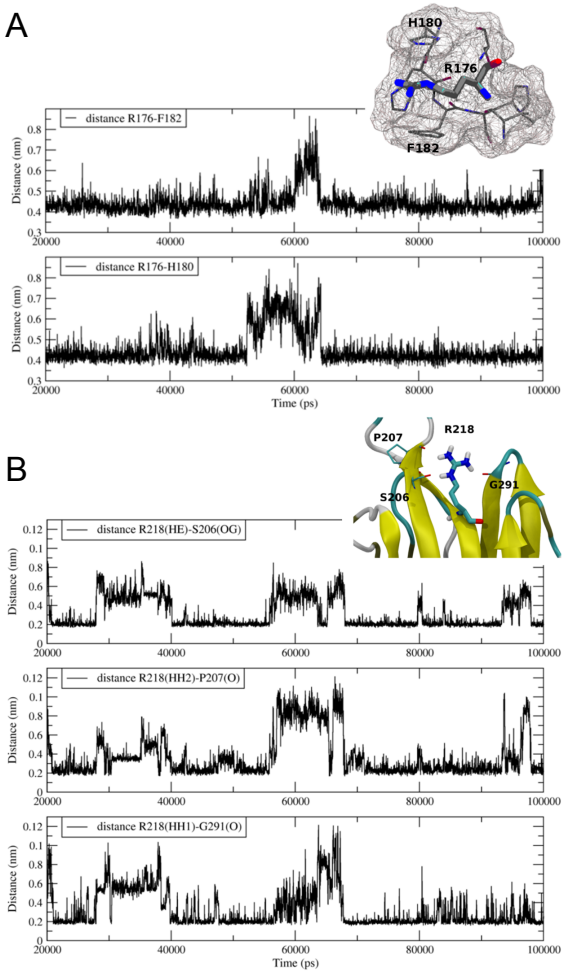

Figure 6. Aromatic cage around R176 and H-bonds network involving R218
(A) Representation of the distance between the centre of mass of R176 and F182 and of R176 and H180 side chains as a function of time. Distances were monitored during the last 80 ns of simulation. In the inset the surface of the cage-like structure is shown as wireframe. (B) Distances between R218 and S208, P207 and G291 are shown as a function of time. In particular distance between $R218_{HE}$-$S206_{OG}$, $R218_{HH2}$-$P207_{O}$ and $R218_{HH1}$-$G291_{O}$ were monitored during the last 80 ns of simulation.

Also the side-chain of R218 appears to make relevant stabilizing interactions with neighboring residues that are located on adjacent strands, as shown by an extended and persistent network of hydrogen bonds with S206, P207 and G291 (Figure 6B). Mutations of both

R218 and R176 into alanine are therefore expected to abolish the aforementioned stabilizing interactions, conceivably leading to a local destabilization of the HJV structure. At variance to R218 and R176, R288 does not create any stabilizing interactions, as its side-chain that protrudes out from the beta-sheet is totally exposed to the solvent. Most likely mutation R288A does not affect the structure stability, however the high conservation of this residues (Figure S9) and its involvement in the pathology when mutated into tryptophan [31] strongly suggests a functional role of this residue. Finally, R257 does not have any role in HJV structure, as it is part of a highly fluctuating solvent-exposed loop (Figure 5A), in agreement with its high RMSF value (Figure 5B). Conceivably, a mutation of this residue will not affect stability and might retain the wild-type functionalities.

3.5 Functional characterization of the HJV mutants

To investigate the ability of HJV R variants to act as BMP coreceptors, we analyzed basal hepcidin activation on Hep3B cells by using a hepcidin promoter luciferase based assay [19] in the presence of exogenous HJV. Equal transfection efficiency was verified by qRT-PCR (Figure S10).

HJV^{R121A} and HJV^{R257A} are able to activate hepcidin at the same rate of wild type HJV, confirming that maintenance of the correct processing and maturation is essential for the HJV-mediated hepcidin activating properties. HJV^{R176A} and HJV^{R288A} do not activate hepcidin, whereas HJV^{R218A} and HJV^{R326A} are only partially active (Figure 7A). To define whether HJV^{R121A} was responsive to BMPs, Hep3B cells, transfected with HJV^{WT}, HJV^{R121A} and HJV^{R288A}, were treated with

BMP6. HJV^{R121A} behaves as HJV^{WT}, whereas HJV^{R288A} is insensitive to BMP6 stimulation (Figure 7B and Table 1).

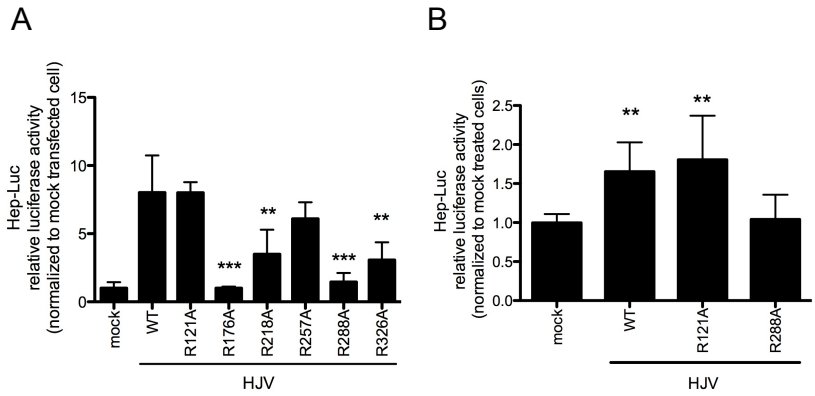

Figure 7. BMP-coreceptor activity of HJV variants
(A) Hep3B cells were cotransfected with a firefly luciferase reporter vector driven by a 2.9 kb proximal hepcidin promoter (Hamp) and pRL-TK (renilla luciferase vector) in combination with empty vector (mock) or wild type or mutant HJV expressing vectors. Experiments, made in triplicate, were performed three times. (B) Cells were transfected as indicated in A) and treated with 10 ng/ml BMP6 for 3 hours. Relative luciferase activity was calculated as the ratio between firefly (reporter) and renilla luciferase activity and expressed as a multiple of activity of cells transfected with the reporter alone. Mean values of mock transfected cells are set to 1 and the values of HJV^{WT} and HJV variants are normalized to mock transfected cells. Experiments, made in triplicate, were performed three times. A representative experiment is shown. Error bars indicate SD. Asterisks indicate the statistical difference between HJV variants and HJV^{WT}. **P< .01, ***P< .001.

Variants	Degradation fragments after TMPRSS6 cleavage	Cell surface expression	Autoproteolytic activity	BMP-coreceptor activity
HJV^{WT}	A-B-C	Yes	Yes	Yes
HJV^{R121A}	B-C	Yes	Yes	Yes
HJV^{R176}	None	35% reduction	No	No
HJV^{R218A}	C	Yes	No	Partial
HJV^{R257A}	A-B-C	Yes	Yes (reduced)	Yes
HJV^{R288A}	None	35% reduction	No	No
HJV^{R326A}	None	Yes	No	Partial

Table 1. Summary of the properties of the HJV variants studied in details

4. DISCUSSION

HJV is a coreceptor in the BMP-SMAD signalling pathway that upregulates hepcidin in response to increased iron [2], a pathway inhibited by the liver serine protease TMPRSS6. Although the substrate of TMPRSS6 in vivo is debated [17], the double KO mice $Tmprss6^{-/-}$ $Hjv^{-/-}$ is compatible with HJV being downstream TMPRSS6 [20]. *In vitro* the serine protease cleaves HJV, releasing multiple fragments in the culture media [21,25]. In order to better define the TMPRSS6-mediated HJV processing, we performed an

extensive R→A mutagenesis of potential cleavage sites, generating and characterizing 24 different HJV variants. As RGM proteins, HJV is present on the cell surface either as full length or as a heterodimer protein formed by a short N-terminal peptide (from amino acid 33 to 121; present paper) (Figure 1B) and a large C-terminal peptide (from the GDPH motif to amino acid 400) [15,16]. Combining the molecular mass of the fragments generated by TMPRSS6 on wild type HJV, and the lack of fragments in case of specific HJV R variants, we defined which fragments originate either from full length and/or from the heterodimer, and identified their corresponding cleavage sites. Among several variants which showed none or only abnormal fragments, HJV^{R121A} and HJV^{R326A} were especially informative. We showed that the largest fragment A is the result of the cleavage at position 121 and 326 of the full length HJV, fragment B derives from the heterodimeric protein encompassing the region from GDPH cleavage to position 326. The shortest fragment C originates from the C terminus (from 326 to the GPI anchor) of both full length and heterodimer isoforms (Figure 1B and Figure 3).

Previous work has indicated position 288 as a potential TMPRSS6 cleavage site [25]. Trying to reconcile our data with those previously reported, it is likely that fragment A corresponds to the 36 kDa fragment in [25], since the fragment is not released in mutant R288A in both studies. However, we observed that not only 288A, but also several substitutions within the vWD domain, except R257A, perturb the fragment pattern. We excluded that this occurs because of lack of interaction of these variants with TMPRSS6. Thus we investigated the vWD domain by an in silico approach to understand whether altering

the protein stability could indirectly affect TMPRSS6 cleavage. Taken together, the molecular dynamics simulation and the data regarding the altered HJV processing allowed us to define that the absence or the different pattern of fragments in the medium was likely due to local protein destabilization rather than to modification of the cleavage target residues. Indeed in silico simulations indicate that R176 and R218 mutagenesis would abrogate the stabilizing intramolecular interactions that might influence the cleavage processes. We confirmed that R257 does not have a structural role, as it is located on a flexible solvent exposed loop and thus its mutation is predicted to be irrelevant to the protein stability. We do not have clear explanation for the apparent TMPRSS6 cleavage-resistance of the 288 residue. However, we observed that R288 is a particularly conserved amino acid (Figure S9) and that missense change to tryptophan (R288W) causes a severe hemochromatosis disease [31], highlighting the relevance of this residue for HJV function. In addition we must consider that the R288A mutant is partially defective in membrane targeting. Unfortunately, we could not formulate any reliable prediction on the dynamic behavior of R121 and R326 since they are outside and at the very end of the modelled structure, respectively. Nevertheless, based on fragments size, cleavage at R288 seems unlikely and we favor positions 121 and 326 as TMPRSS6 cleavage sites (Figure 1B).

Since the available anti-HJV antibody recognizes only the C-terminal protein, to the aim of confirming our findings we generated selected variants (R121A and R288A) on a N-FLAG-tagged HJV. This allowed us to confirm that TMPRSS6 cleaves both m-HJV isoforms

and to define that there are no N-terminal cleavage sites beyond R121. Moreover, the use of the FLAG-tag construct allowed us to define that the N-terminal fragment derived from autoproteolysis at GDPH undergoes a subsequent more N-terminal rearrangement at R121, likely by other proteases, to generate the correct heterodimeric surface. Accordingly, fragments released by $HJV^{FLAG\ R121A}$ have higher molecular mass than those released by wild type HJV.

Interestingly HJV^{R121A} undergoes autoproteolysis and is correctly expressed on the cell surface. HJV^{R121A} has BMP-coreceptor activity (as HJV^{R257A}) in a hepcidin promoter assay both in basal conditions and after BMP6 stimulation. This is of interest, considering that the N-terminal segment of the HJV^{R121A} heterodimeric protein is anomalous and suggests that residues from 121 to 172 are not relevant to the heterodimeric protein function. Pathogenic mutants have been identified at position 168, 170 and 172 [31]; they do not undergo autoproteolysis and show defective hepcidin activation, thus strengthening the essential role of GDPH autocleavage for HJV functionality.

Autoproteolysis does not occur also in mutants of the vWD domain (HJV^{R176A}, HJV^{R218A} and HJV^{R288A}). Since this is a fundamental process for the correct membrane targeting of the heterodimeric protein [13,19] these variants loose their activity as BMP co-receptors. These results reinforce the idea that R176 and R218 are residues essential for the correct structure stabilization of mature HJV.

In conclusions we show that TMPRSS6 cleaves HJV at two specific sites both in full length and heterodimeric protein. Whether the HJV

fragments resulting from TMPRSS6 cleavage have a functional role still remains to be demonstrated.

5. SUPPLEMENTARY INFORMATIONS

5.1 MATERIALS AND METHODS

5.1.1 Western blot analysis

Transfected cells were lysed in NET/Triton buffer (150mM NaCl, 5mM EDTA, and 10mM Tris [pH 7.4] with 1% Triton X-100) and proteins were quantified by using the Bio-Rad Protein Assay (Bio-Rad, Hercules, CA); equal amount of total proteins (50 μg) were loaded on to 10% SDS-PAGE and transferred to Hybond C membrane (Amersham Bioscences Europe GmbH, Freiburg, Germany) by standard western blotting technique. Membranes were blocked with 2% ECL Advance Blocking Agent (Amersham Bioscences) or ECL Prime Blocking Agent (Amersham Bioscences) in TBS (0.5M Tris-Hcl [pH 7.4] and 0.15M NaCl) containing 0.1% Tween-20 (TBST), incubated 2 hrs with rabbit anti-HJV (1:1000) (Silvestri, Blood 2008) and rabbit anti-FLAG (1:1000) (Santa Cruz CA). After washing with TBST, blots were incubated 1 hr with goat HRP-conjugated secondary antirabbit and developed with a chemiluminescence detection kit (ECL, Amersham Bioscences). For deglycosylation, 100 μg of proteins from cell medium were incubated with PNGase F (New England Biolabs) according to manifacturer's instruction. Proteins were precipitated using cold acetone and then resuspended using Laemmli sample buffer. Proteins were then loaded on a 12% SDS-

Page. Immunodetection was performed as described above with anti-Flag.

5.1.2 Hepcidin promoter based luciferase assay

Hep3B cells, seeded at 70%-80% of confluency, were transiently transfected with the hepcidin promoter luciferase reporter construct (0.25 μg) combined with pRL-TK Renilla luciferase vector (Promega), to control for transfection efficiency, and with expressing vectors encoding wild type or mutant HJV (0.05 μg). Eighteen hours after transfection the medium was replaced with EMEM supplemented with 2% FBS. After 24 hours of serum starvation cells were lysed. When indicated, cells were treated with 10ng/ml of recombinant BMP6 (R&D system) for three hours and then processed. Luciferase activity was determined according to manifacture's instructions (Dual Luciferase Reporter Assay, Promega). Relative luciferase activity was calculated as the ratio between firefly (reporter) and Renilla luciferase activity, and expressed as multiple of the activity of cells transfected with the report alone. Experiments were performed in triplicate. The student's t test was used for statistical analysis.

5.1.3 Quantitative reverse transcriptase polymerase chain reaction

Total RNA was extracted from Hep3B cells transfected as described above in "Hepcidin promoter based luciferase assay". One μg of RNA, extracted with RNeasy mini kit (Quiagen), was used for first-strand synthesis of cDNA with the High Capacity cDNA Reverse

Transcription kit (Applied Biosystems, Warrington UK), according to the manufacturer's instructions. Gene expression levels were measured by quantitative real-time PCR using Sybr Green Master Mix (Applied Biosystem). Primers used for qRT-PCR are: HJV sense: 5'-TGACTTCCTCTTTGTCCAAGC-3'; HJV antisense: 5' TGCATGTTCTTAAATATGATGGTGA-3'; HPRT1 sense: 5'-GACCAGTCAACAGGGGACAT-3'; HPRT1 antisense: 5'-GTGTCAATTATATCTTCCACAATCAAG-3'.

5.1.4 Homology Modelling and Molecular Dynamics simulation

Protonation states were chosen to correspond to neutral pH. The system was solvated terminally capped in a 6x7x2 nm3 box containing 9.194 TIP3P [33] water molecules. The net charge of the proteins was neutralized with sodium ions. The Amber ff99SB-ILDN [34] force field was used to represent all systems. The system was initially subjected to energy minimization, followed by equilibration at 300K with 500 ps, during which water molecules and protein heavy atoms were position-restrained. In the second phase (1ns), both water molecules and protein atoms were unrestrained to allow system relaxation. All bonds involving hydrogen atoms were constrained with the SHAKE algorithm [35]. Equilibration was performed using the Nosé-Hoover thermostat [36] and a Berendsen barostat [37] to maintain a constant temperature (300K) and a constant pressure (1 atm). The unrestrained production runs were then simulated for 100 ns in a NPT ensemble, using the V-Rescale thermostat [38] and a Parrinello-Rahman barostat [39]with a relaxation time of 2 ps. A cutoff of 9 Å was used for the Lennard-Jones interaction and the

short-range electrostatic interactions. Verlet cutoff scheme was introduced [40]. The smooth particle mesh Ewald method [41] with a fourth-order interpolation scheme was used to compute the long-range electrostatic interactions. The pairlists were updated every 10 fs with a cutoff of 9 Å. A uniform integration step of 2 fs was used. Simulation was performed using 156 cores, adopting a Dynamic load balancing option. Trajectory obtained from the NPT run was used for subsequent data analysis. Simulations analysis was performed using the GROMACS package tools. Simulation stability was ascertained monitoring the Root Means Square Deviation (RMSD) along the simulation (Fig S8).

5.2 SUPPLEMENTARY TABLE AND FIGURES

Amino acid substitution	Sense	Antisense
R121A	CCAGCACAACTGCTCCGCTCAGGGCCCTACAGC	GCTGTAGGGCCCTGAGCGGAGCAGTTGTGCTGG
R176A	GGACCCCCATGTGGCTAGCTTCCACCATCACTTTC	GAAAGTGATGGTGGAAGCTAGCCACATGGGGGTCC
R218A	GGCCAACGCTACCGCCACCGCTAAGCTCACCATC	GATGGTGAGCTTAGCGGTGGCGGTAGCGTTGGCC
R257A	CTATCAATGGAGGTGACGCTCCTGGGGGGATCCAG	CTGGATCCCCCAGGAGCGTCACCTCCATTGATAG
R288A	GCACAACTATAATCATTGCTCAGACAGCTGGGCAG	CTGCCCAGCTGTCTGAGCAATGATTATAGTTGTGC
R326A	GCCCTCCAAGTCAGGCTCTCTCTCGATCAGAG	CTCTGATCGAGAGAGAGCCTGACTTGGAGGGC

Table S1. Oligonucleotides used to generate the HJV variants analyzed in details in this study

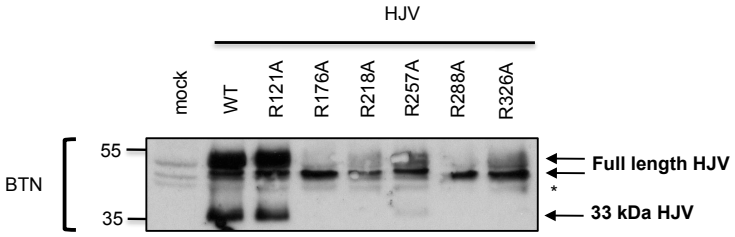

Figure S1. Cell membrane biotinylation of wild type and HJV arginine variants
Short exposure of blot of Figure 2B (BTN panel). Arrows indicate the full length and the 33 kDa HJV. Numbers indicate size in kDa.

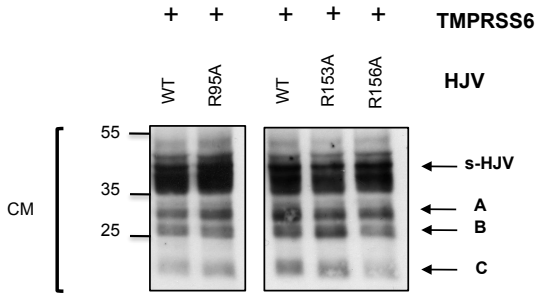

Figure S2. TMPRSS6 cleavage activity on representative N-terminal HJV arginine variants
Cell culture media (CM) of HeLa cells, cotransfected with TMPRSS6 and WT or HJV^{R95A}, HJV^{R153A} and HJV^{R156A} expressing vectors were loaded onto a 10% SDS-PAGE and processed for western blot analysis. Fragments A, B and C are derived from TMPRSS6-mediate m-HJV cleavage, while s-HJV is not affected (see **Figure 1** for fragments interpretation). Numbers indicate size in kDa.

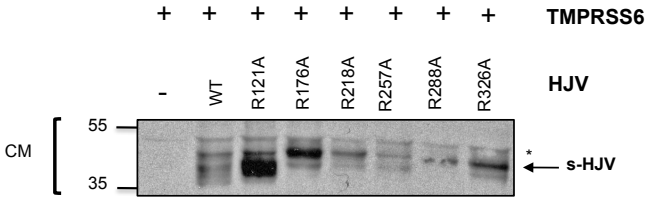

Figure S3. TMPRSS6 cleavage of HJV^{R121A} variant releases an extra band of approximately 40 kDa
Short exposure of blot of Figure 3 (CM). The band around 40 kDa in HJV^{R121A} lane probably originates from 33-326 amino acids. Asterisks indicate unspecific band. Numbers indicate size in kDa.

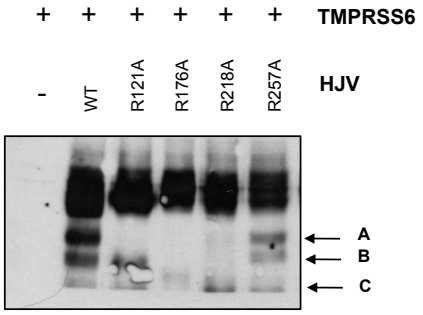

Figure S4. Cleavage of HJV^{R257A} by TMPRSS6
HeLa cells were transfected as indicated in Figure 3. Fragments A, B and C that originate from TMPRSS6 cleavage of HJV are indicated. Fragments originating from HJV^{R257A} migrate as those from HJV^{WT}. A representative Western blot is shown. Numbers indicate size in kDa.

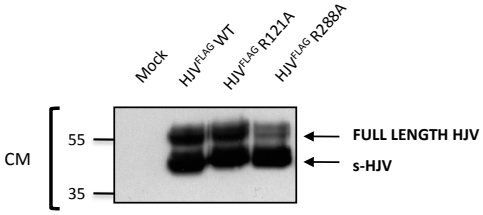

Figure S5. HJV^{FLAG} releases full length and s-HJV isoforms in the culture media of transfected cells.
Concentrated media of cells transfected with empty vector (mock) or HJV$^{FLAG\ WT}$, HJV$^{FLAG\ R121}$ and HJV$^{FLAG\ R288A}$ were loaded onto a 10% SDS-PAGE, processed for western blot analysis and incubated with anti-FLAG antibody. In the blot the two bands of full length HJV and s-HJV are distinguishable. Numbers indicate size in kDa.

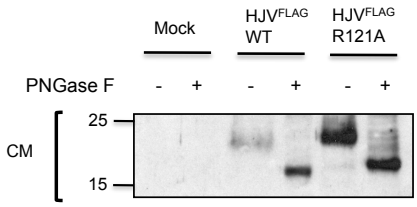

Figure S6. Glycosylation status of autoproteolytically-derived HJV N-terminal fragments
Hela cells were transfected with empty vector (mock), $HJV^{FLAG\ WT}$ or $HJV^{FLAG\ R121A}$. Cell culture media (CM) were collected and concentrated. Equal amount of protein was deglycosylated with PNGase F (+). Control samples were not deglycosylated (-). Proteins were precipitated using cold acetone, resuspended in Laemmli sample buffer and then loaded onto a 12% SDS-PAGE, blotted and incubated with anti-FLAG antibody. The detected band corresponds to the autoproteolytically-derived N-terminal fragment of HJV. Numbers indicate size in kDa.

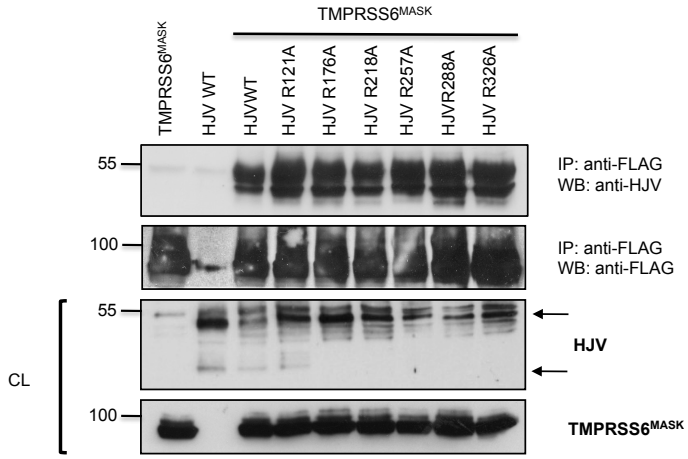

Figure S7. All HJV variants interact with TMPRSS6
HeLa cells were cotransfected with $TMPRSS6^{MASK}$ and HJV^{WT} or mutant HJV. Equal amount of total lysate was pulled down with anti-FLAG resin and then loaded onto a 10% SDS polyacrylamide gel electrophoresis, blotted and incubated with the anti-HJV antibody. Cell lysates (CL) were loaded onto a 10% SDS-PAGE, blotted and incubated with anti-HJV and anti-FLAG antibody. Arrows indicate full length HJV. Experiments were performed three times. A representative Western blot is shown. Numbers indicate size in kDa.

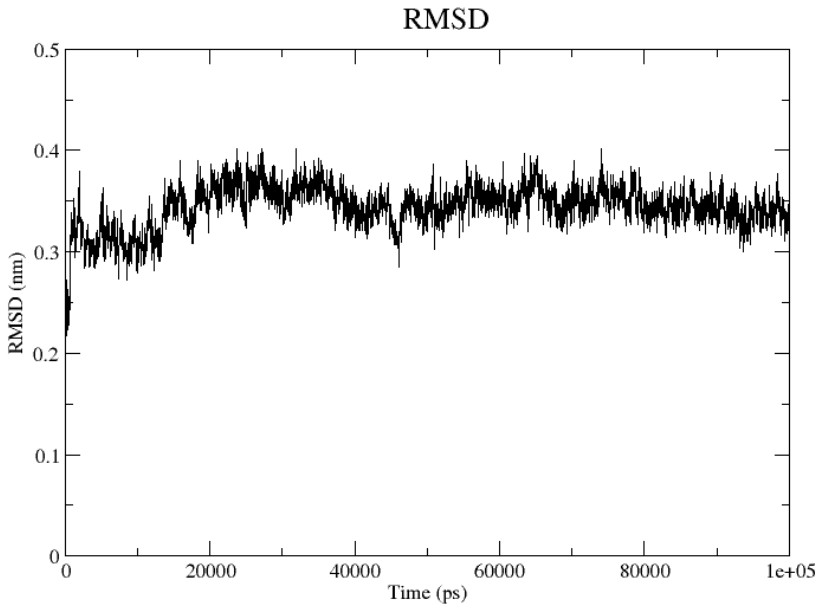

Figure S8. RMSD analysis of HJV backbone atoms.
Root Mean Square Deviation (RMSD) of HJV as function of time showing simulation stability. The RMSD was calculated on the backbone atoms after fitting on the backbone atoms and using the starting structure as reference.

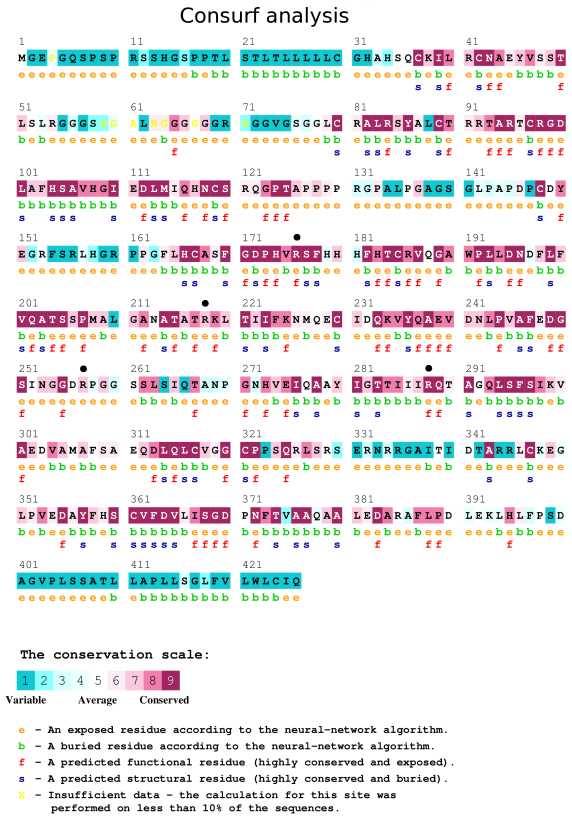

Figure S9. HJV sequence analysis. The Consurf server [42] was used to identify functionally and structurally important HJV residues. Multiple alignment was built using MAFFT and the homologues were collected from UNIREF90. The homologues were searched exploiting CS-BLAST with a maximal and minimal ID between sequence of 95 % and 35 % respectively. Calculation was performed on 119 unique sequences. R176, R218, R257 and R228 are highlighted as black dots.

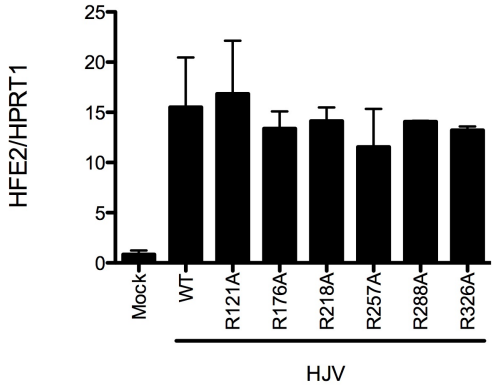

Figure S10. *HJV* expression levels in transfected Hep3B cells
Hep3B cells were transfected with empty vector or WT and HJV arginine variants (as described in Figure 7A) and RNA was isolated 36 hours post transfection. *HJV* mRNA expression was evaluated by qRT-PCR. mRNA expression ratio was normalized relative to housekeeping *HPRT1*. Error bars indicate SD. Experiments, made in triplicate, were performed three times.

ACKNOWLEDGMENTS

This work was partially supported by "Telethon Fondazione Onlus" Grant GGP12025, Ministero Sanità, MIUR-PRIN (Progetto di Rilevante Interesse Nazionale) 2010-2011 Ricerca Finalizzata RF-2010-2312048, to CC and Telethon grant TCP09935 to GM.

We wish to thank Herbert Lin (Harvard, Boston, US) for the gift of the N-terminal flag-tag HJV construct and Paolo Arosio (University of Brescia, Italy) for the gift of the anti-HJV antibody and for helpful discussion.

REFERENCES

1. **Nemeth E, Tuttle MS, Powelson J, *et al.*** Hepcidin regulates cellular iron efflux by binding to ferroportin and inducing its internalization. *Science*. 2004; 306: 2090-3.

2. **Babitt JL, Huang FW, Wrighting DM, *et al.*** Bone morphogenetic protein signaling by hemojuvelin regulates hepcidin expression. *Nat Genet*. 2006; 38: 531-9.
3. **Xia Y, Babitt JL, Sidis Y, *et al.*** Hemojuvelin regulates hepcidin expression via a selective subset of BMP ligands and receptors independently of neogenin. *Blood*. 2008; 111: 5195-204.
4. **Andriopoulos B Jr, Corradini E, Xia Y, *et al.*** BMP6 is a key endogenous regulator of hepcidin expression and iron metabolism. *Nat Genet*. 2009; 41: 482-7.
5. **Steinbicker AU, Bartnikas TB, Lohmeyer LK, *et al.*** Perturbation of hepcidin expression by BMP type I receptor deletion induces iron overload in mice. *Blood*. 2011; 118: 4224-30.
6. **Silvestri L, Pagani A, Camaschella C.** Furin-mediated release of soluble hemojuvelin: a new link between hypoxia and iron homeostasis. *Blood*. 2008; 111: 924-31.
7. **Kuninger D, Kuns-Hashimoto R, Nili M, Rotwein P.** Pro-protein convertases control the maturation and processing of the iron-regulatory protein, RGMc/hemojuvelin. *BMC Biochem*. 2008; 9: 9.
8. **Lin L, Nemeth E, Goodnough JB, *et al.*** Soluble hemojuvelin is released by proprotein convertase-mediated cleavage at a conserved polybasic RNRR site. *Blood Cells Mol Dis*. 2008; 40: 122-31.
9. **Lin L, Goldberg YP, Ganz T.** Competitive regulation of hepcidin mRNA by soluble and cell-associated hemojuvelin. *Blood*. 2005; 106: 2884-9.
10. **Nili M, Shinde U, Rotwein P.** Soluble repulsive guidance molecule c/hemojuvelin is a broad spectrum bone morphogenetic protein (BMP) antagonist and inhibits both BMP2- and BMP6-mediated signaling and gene expression. *J Biol Chem*. 2010; 285: 24783-92.
11. **Papanikolaou G, Samuels ME, Ludwig EH, *et al.*** Mutations in HFE2 cause iron overload in chromosome 1q-linked juvenile hemochromatosis. *Nat Genet*. 2004; 36: 77-82.
12. **Zhang AS, West AP Jr, Wyman AE, *et al.*** Interaction of hemojuvelin with neogenin results in iron accumulation in human embryonic kidney 293 cells. *J Biol Chem*. 2005; 280: 33885-94.
13. **Silvestri L, Pagani A, Fazi C, *et al.*** Defective targeting of hemojuvelin to plasma membrane is a common pathogenetic mechanism in juvenile hemochromatosis. *Blood*. 2007; 109: 4503-10.
14. **Nili M, David L, Elferich J, *et al.*** Proteomic analysis and molecular modelling characterize the iron-regulatory protein haemojuvelin/repulsive guidance molecule c. *Biochem J*. 2013; 452: 87-95.
15. **Zhang AS, Yang F, Meyer K, *et al.*** Neogenin-mediated hemojuvelin shedding occurs after hemojuvelin traffics to the plasma membrane. *J Biol Chem*. 2008; 283: 17494-502.
16. **Kuninger D, Kuns-Hashimoto R, Kuzmickas R, Rotwein P.** Complex biosynthesis of the muscle-enriched iron regulator RGMc. *J Cell Sci*. 2006; 119: 3273-83.
17. **Frydlova J, Fujikura Y, Vokurka M, *et al.*** Decreased hemojuvelin protein levels in mask mice lacking matriptase-2-dependent proteolytic activity. *Physiol Res*. 2013; 62: 405-11.

18. **Kuns-Hashimoto R, Kuninger D, Nili M, Rotwein P.** Selective binding of RGMc/hemojuvelin, a key protein in systemic iron metabolism, to BMP-2 and neogenin. *Am J Physiol Cell Physiol*. 2008; 294: C994-C1003.
19. **Pagani A, Silvestri L, Nai A, Camaschella C.** Hemojuvelin N-terminal mutants reach the plasma membrane but do not activate the hepcidin response. *Haematol*. 2008; 93: 1466-72.
20. **Finberg KE, Heeney MM, Campagna DR, *et al.*** Mutations in TMPRSS6 cause iron-refractory iron deficiency anemia (IRIDA). *Nat Genet*. 2008; 40: 569-71.
21. **Silvestri L, Pagani A, Nai A, *et al.*** The serine protease matriptase-2 (TMPRSS6) inhibits hepcidin activation by cleaving membrane hemojuvelin. *Cell Met*. 2008; 8: 502-11.
22. **Du X, She E, Gelbart T, *et al.*** The serine protease TMPRSS6 is required to sense iron deficiency. *Science*. 2008; 320: 1088-92.
23. **Folgueras AR, de Lara FM, Pendas AM, *et al.*** Membrane-bound serine protease matriptase-2 (Tmprss6) is an essential regulator of iron homeostasis. *Blood*. 2008; 112: 2539-45.
24. **Enns CA, Ahmed R, Zhang AS.** Neogenin interacts with matriptase-2 to facilitate hemojuvelin cleavage. *J Biol Chem*. 2012; 287: 35104-17.
25. **Maxson JE, Chen J, Enns CA, Zhang AS.** Matriptase-2- and proprotein convertase-cleaved forms of hemojuvelin have different roles in the down-regulation of hepcidin expression. *J Biol Chem*. 2010; 285: 39021-8.
26. **Silvestri L, Guillem F, Pagani A, *et al.*** Molecular mechanisms of the defective hepcidin inhibition in TMPRSS6 mutations associated with iron-refractory iron deficiency anemia. *Blood*. 2009; 113: 5605-8.
27. **Silvestri L, Rausa M, Pagani A, *et al.*** How to assess causality of TMPRSS6 mutations? *Hum mutat*. 2013; 34: 1043-5.
28. **Roy A, Kucukural A, Zhang Y.** I-TASSER: a unified platform for automated protein structure and function prediction. *Nat Protoc*. 2010; 5: 725-38.
29. **Hess B, Kutzner C, Van Der Spoel D, *et al.*** GROMACS 4: Algorithms for Highly Efficient, Load-Balanced, and Scalable Molecular Simulation. *J Chem Theory Comput*. 2008; 4
30. **Bell CH, Healey E, van Erp S, Lindahl E.** Structure of the repulsive guidance molecule (RGM)-neogenin signaling hub. *Science*. 2013; 341: 77-80.
31. **Lanzara C, Roetto A, Daraio F, *et al.*** Spectrum of hemojuvelin gene mutations in 1q-linked juvenile hemochromatosis. *Blood*. 2004; 103: 4317-21.
32. **Humpries W, Dalke A, Schulten. K** VMD: visual molecular dynamics. *J Mol Graph*. 1996; 14: 33-8.
33. **Jorgensen WL, Chandrasekhar J, Madura JD, *et al*.** Comparison of Simple Potential Functions for Simulating Liquid Water. *J Chem Phys*. 1983; 79: 926.
34. **Lindorff-Larsen K, Piana S, Palmo K, *et al*.** Improved side-chain torsion potentials for the Amber ff99SB protein force field. *Proteins*. 2010; 78: 1950-8.

35. **Ryckaert JP, Ciccotti G, Berendsen HJC**. Numerical integration of the cartesian equations of motion of a system with constraints: molecular dynamics of n-alkanes. *J Comput Phys*. 1977; 23: 327-41.
36. **Cheng A, Merz KMJ**. Application of the Nosé-Hoover Chain Algorithm to the Study of Protein Dynamics. *J Chem Phys*. 1996; 100: 1927-37.
37. **Berendsen HJC, Postma JPM, van Gunsteren WF, *et al***. Molecular-Dynamics with Coupling to an External Bath. *J Chem Phys* 1984; 81: 3684–90.
38. **Bussi G, Donadio D, Parrinello M.** Canonical sampling through velocity rescaling. *J Chem Phys*. 2007; 126: 014101.
39. **Parrinello M, Rahman A.** Polymorphic transitions in single crystals: A new molecular dynamics method. *J Appl Phys*. 1981; 52: 7182-90.
40. **Páll S, Hess B.** A flexible algorithm for calculating pair interactions on SIMD architectures. *Comput Phys Commun*. 2013; 184: 2641-50.
41. **Darden T, York D, Pedersen L.** Particle Mesh Ewald-an N.Log(N) method for Ewald sums in large systems. *J Chem Phys*. 1993; 98: 10089-92.
42. **Berezin C, Glaser F, Rosenberg J, *et al.*** ConSeq: the identification of functionally and structurally important residues in protein sequences. *Bioinformatics*. 2004; 20: 1322-4.

CHAPTER 3

Bmp6 expression in murine liver non parenchymal cells: a mechanism to control their high iron exporter activity and protect hepatocytes from iron overload?

Marco Rausa[1, 2], Alessia Pagani[1, 2], Antonella Nai[1, 2], Alessandro Campanella[1, 2], Clara Camaschella[1, 2] and Laura Silvestri[1, 2]

[1] Division of Genetics and Cell Biology, IRCCS San Raffaele Scientific Institute, Milan, Italy

[2] Vita Salute University, Milan, Italy

(Under revision)

ABSTRACT

Bmp6 is the main activator of hepcidin, the liver hormone that negatively regulates plasma iron influx by degrading the sole iron exporter ferroportin in enterocytes and macrophages. The *Bmp6* expression is modulated by iron but the molecular mechanisms are unknown. Although hepcidin is expressed almost exclusively by hepatocytes (HCs), *Bmp6* is produced also by non-parenchymal cells (NPCs), mainly sinusoidal endothelial cells (LSECs).

To investigate the regulation of *Bmp6* in HCs and NPCs, liver cells were isolated from adult wild type mice whose diet was modified in iron content in acute (1 day) or chronic (3 weeks) manner and in disease models of iron deficiency (*Tmprss6*$^{-/-}$ mouse) and overload (*Hjv*$^{-/-}$ mouse).

In wild type mice *Bmp6* expression is decreased in iron deficiency and increased in iron overload induced by chronic diet in all cell types. In 1-day diet only HCs and Kupffer cells modulate *Bmp6* following mild iron increase, while LSECs require a higher iron loading. When hepcidin expression is abnormal in disease models of iron overload (*Hjv*$^{-/-}$mice) and deficiency (*Tmprss6*$^{-/-}$ mice), *Bmp6* expression in NPCs, that are characterized by high ferroportin expression and high iron export activity, is not related to intracellular iron content, measured by *Tfr1* expression, suggesting that it reflects iron uptake.

We propose that NPCs, sensing liver iron influx, increase hepcidin through Bmp6 with a paracrine mechanism to control systemic iron homeostasis. Controlling hepcidin they regulate their own ferroportin, inducing iron retention and further Bmp6 production in an autocrine manner, a mechanism that contribute to protect HC from iron loading.

This protective mechanism is lost in disease models of hepcidin production.

1. INTRODUCTION

Hepcidin, the master regulator of iron metabolism, is a liver peptide hormone that negatively regulates dietary iron absorption and iron release from macrophages by binding and degrading of the sole cellular iron exporter ferroportin [1]. Although hepcidin activation is mediated by both circulating and liver iron content, how these two signals govern hepcidin changes is not fully clarified. The characterization of hemojuvelin (HJV), the protein mutated in type 2A hemochromatosis [2], as Bone Morphogenetic Protein (BMP)-coreceptor, functionally linked the BMP-Sons of Mothers Against Decapentaplegic (SMAD) pathway to hepcidin and iron regulation [3]. HJV selectively uses the BMP type II receptor ActRIIA [4], highly expressed in the liver, and the type I receptors ALK2 and ALK3 [5]. In the presence of the ligand, constitutively active type II receptor phosphorylates type I receptor, which phosphorylates SMAD1/5/8 proteins (R-SMADs) that in turn interact with SMAD4. The resulting multiprotein complex translocates to the nucleus to activate target genes [6]. Liver conditional inactivation of *Smad4* [7] or *Alk3* [5] causes severe iron overload due to downregulation of hepcidin, similar to the phenotype of $Hjv^{-/-}$ [8,9] and $Hamp^{-/-}$ [10] mice, whereas liver specific deletion of *Alk2* blunts the response of hepcidin to increased iron levels [5].

BMPs are members of the transforming growth factor beta (TGF-beta) superfamily [11]. *In vitro* several BMPs as BMP2, BMP4 and BMP6 activate hepcidin in the presence of HJV [12]. *In vivo*, Bmp6 is the sole BMP that regulates hepcidin expression in mice. *Bmp6* inactivation causes severe iron overload due to strong hepcidin downregulation and ferroportin stabilization, a phenotype comparable to that of *Hjv*$^{-/-}$ mice [9], suggesting that Bmp2 and Bmp4 do not compensate for the lack of Bmp6. Transcription of *Bmp6* is suppressed in iron deficiency and upregulated in iron overload [13]; this regulation is liver specific [14] and no other tissue modulates *Bmp6* in response to iron, in agreement with the central role of the liver in iron homeostasis.

The liver is composed by several cell types: parenchymal cells, essentially hepatocytes (HCs), and non-parenchymal cells (NPCs). Among the latter Kupffer cells are resident macrophages (constituting 80-90% of body tissue macrophages), sinusoidal endothelial cells (LSECs) have filter functions between blood and hepatocytes and high endocytic capacity for many ligands, hepatic stellate cells (HSc), or Ito cells, localize between the sinusoids and HCs, and are involved in liver fibrosis when activated [15]. Recently, NPCs (KCs, LSECs and HSc) were reported to express high levels of *Bmp6* compared to HCs [16,17], suggesting that they play a role in hepcidin regulation. Here we extend this observation analyzing *Bmp6* expression in isolated liver cell populations of wild type mice after changing the iron status by acute and chronic diets, and in disease models with opposite and pathological hepcidin levels: the iron loaded *Hjv*$^{-/-}$ mice which have low hepcidin, and the iron deficient *Tmprss6*$^{-/-}$ mice characterized by

high hepcidin levels. We demonstrate that *Bmp6* is highly expressed in NPCs and that chronic changes in iron status induced by diet modulate *Bmp6* in all cell types according to their intracellular iron content that is influenced by the hepcidin effect on their iron export capacity. However, in NPCs cells, characterized by high ferroportin activity, *Bmp6* expression is independent on cell iron content and more related to their iron uptake. We also show that *Bmp6* expression in LSECs is independent from HCs iron. In addition, in our *in vivo* models *Bmp6* increase both in parenchymal and NPCs does not induce *Tmprss6* transcription in HCs.

2. MATERIAL AND METHODS

2.1 Animal and diets

Wild type C57BL/6 male mice, obtained from Charles River, *Tmprss6* KO mice on a mixed 129/Ola X C57BL/6 background [18], and *Hjv* KO mice on an inbred 129S6/SvEvTac background [9] were housed under a standard 12-hour light/dark cycle with water and chow ad libitum in a pathogen-free animal facility of the San Raffaele Scientific Institute in accordance with the European Union guidelines. The study was approved by the Institutional Animal Care and Use Committee of the San Raffaele Scientific Institute (IACUC number: 514). Only male mice were analyzed when 7-8 week old. To induce stable changes of the iron status, 4 week-old C57BL/6 male mice were fed an iron-balanced (IB; carbonile iron 200 mg/kg; SAFE), an iron-loaded (IL; carbonile iron 8.3 g/kg; SAFE), or an iron-deficient diet

(ID), with virtually no iron (< 3 mg iron/kg; SAFE) for 3 weeks. To induce acute iron changes, C57BL/6 animals pretreated by 2 weeks ID diet to induce iron depletion, were administered 1 day an IB, ID or IL diet [19]. Anesthetized animals were sacrificed by cervical dislocation. All efforts were made to minimize suffering**.** Livers and spleens were snap-frozen for isolation of RNA or dried for tissue iron content analysis. Liver cell populations were separated as described below.

2.2 Analysis of hematological and iron parameters

Hemoglobin (Hb) levels were determined using a Sysmex KX-21 automated blood cell analyser (Sysmex America) from 0.2 mL of blood extracted by caudal puncture from anesthetized mice. Iron parameters were analyzed as previously described [20]. Briefly, transferrin saturation was calculated as the ratio of serum iron and total iron binding capacity levels, using The Total Iron Binding Capacity Kit (Randox Laboratories Ltd.), according to the manufacturer's instructions.

To measure liver (LIC) and spleen iron content (SIC) tissue samples were dried at 110°C overnight, weighed, and digested in 1 mL of 3M HCl, 0.6M trichloroacetic acid for 20 hours at 65°C. The cleared acid extract was added to 1 mL of working chromogen reagent (1 volume of 0.1% bathophenanthroline sulfate and 1% thioglycolic acid solution, 5 volumes of water, and 5 volumes of saturated sodium acetate). The solutions were then incubated for 30 minutes at room temperature until color development and the absorbance was measured at 535 nm. A standard curve was plotted using the acid

solution containing increasing amounts of iron diluted from a stock solution of Titrisol iron standard (Merck, Darmstadt, Germany) [20].

2.3 Liver cells separation

Liver cells were isolated according to Liu et al. [21] with some modifications. Briefly, mice were anesthetized and sacrificed by cervical dislocation. All efforts were made to minimize suffering**.** Livers were perfused in situ through the inferior vena cava with 0.16 mg/mL collagenase IV (Sigma-Aldrich) in an isosmotic saline solution after transection of the portal vein. After perfusion, livers were removed, teased with scalpels and incubated for 10 min at 37°C in a shaking water bath in a collagenase-solution containing DNase I. Cell suspensions were filtered through a 100-µm and a 70-µm cell strainer. Single cell suspension was then centrifuge at 50g for 3 min to pellet HCs. Cell pellet was washed three times with PBS containing 0.1% BSA and supernatants (containing NPCs) were collected. HCs were further purified by centrifugation on 10% Optiprep (1.06 g/mL) at 50 g for 10 min. NPCs were pelleted at 400 g for 10 min, resuspended in Optiprep 17.6% and stratified onto a 8.2% Optiprep. The cell fraction between the interface of the 8.2 and 17.6% Optiprep was enriched in KCs and LSECs. Middle layers were collected, cells were separated by centrifugation, and LSECs were isolated using MACS CD146 MicroBeads (Miltenyi Biotec). KCs were recovered from the flowthrough. Cell purity was validated by mRNA expression of specific genes: *Tmprss6* for HCs, *Cd146* for LSECs, and *Cd45* for KCs.

2.4 Spleen macrophages separation

Mice were anesthetized and sacrificed by cervical dislocation. All efforts were made to minimize suffering**.** Spleen was isolated and spleen capsule was punctured to send the spleen content out. Cells were resuspended in HBSS medium (Gibco Cell Colture, Portland, OR) and centrifuge at 370g for 10 min. Cell pellet was resuspended in HBSS and incubated on ice with 8 volumes of NH_4Cl for 10 min to lyse erythrocyte. After centrifugation at 370g for 10 min cell pellet was resuspended in HBSS, stratified onto FBS (Gibco Cell Colture, Portland, OR) and centrifuge at 370g for 10 min. Cell pellet was washed two times with PBS containing 0.5% BSA and 2mM EDTA. To isolate spleen macrophage population, cells were incubated with MACS anti-F4/80 biotin conjugated and pulled down with Streptavidin MicroBeads (Miltenyi Biotec). F4/80 negative cells were further incubated with MACS CD11 MicroBeads (Miltenyi Biotec).

2.5 qRT-PCR

RNAs from isolated HCs were extracted using the guanidinium thiocyanate–phenol–chloroform method (Trizol Reagent, Invitrogen), following the manufacturer's (Invitrogen) recommendations. RNAs from isolated KCs, LSECs and spleen-derived cells were extracted using the RNeasy mini kit (Qiagen), following manufacturer's instructions. Total RNA (200 ng for KCs and LSECs and 2 μg for HCs) was retro-transcribed to cDNA using the High Capacity cDNA Reverse Transcription Kit (Applied Biosystem), according to the manufacturer's instructions. Gene expression levels were measured by quantitative real-time PCR using TaqMan Gene Expression Master

Mix (Applied Biosystem). Primers used for qRT-PCR are listed in the Supplemental Table 1.

2.6 Western Blot analysis on liver cells

Liver cells were lysed in lysis buffer (200mM Tris-HCl [pH 8]; 1mM EDTA; 100mM NaCl; 10% glycerol; 0.5% NP-40) and proteins extracts were quantified using the Bio-Rad Protein Assay (Bio-Rad) according to the manufacturer's instructions. Fifty mg of protein extracts were re-suspended in Laemmli buffer, incubated 5 minutes at 95°C, loaded onto a 12% SDS-PAGE and then transferred to Hybond C membrane (Amersham Bioscience Europe GmbH) by standard Western blot technique. Membrane were stained with Ponceau staining for protein quantification and then blocked with 2% nonfat milk in TBS (0.5M Tris-HCl [pH 7.4] and 0.15M NaCl) containing 0.1% Tween 20 (TBST). Blocked membranes were then incubated overnight with anti-Tfr1 (1:2000; Zymed Laboratories. Inc., San Francisco). After washing with TBST, blots were incubated 1 hour with relevant HRP-conjugated antisera in TBST with 2% nonfat milk and developed using a chemoluminescence detection kit (ECL; Amersham Biosciences).

2.7 Electro mobility shift assay (EMSA)

EMSA was performed as already described [22]. Briefly, the ^{32}P-labeled IRE probe was generated by *in vitro* transcription of the plasmid pSPT-Fer. Cell extracts (2 μg of total proteins) were incubated with a molar excess of ^{32}P-labeled IRE probe (100.000 cpm) in the presence or absence of 2% β-mercaptoethanol. Proteins

were separated by non-denaturing polyacrylamide gel electrophoresis and dried gels were exposed to autoradiography. Band intensity of the exposed films was quantified by densitometry.

2.8 Statistical analysis

Data are presented as mean ± SE. Student's t-test was used to calculate significance ($P<0.05$).

3. RESULTS

3.1 *Bmp6* is expressed mainly in NPCs and correlates with intracellular iron content

To investigate *Bmp6* expression under basal conditions, HCs, KCs and liver sinusoidal LSECs were isolated from adult male mice as described in Material and Methods. HSc were not included in the analysis because of the low amount of cells we were able to purify from a single animal. The purity of the preparations was assessed by specific markers: *Tmprss6* for HCs, *Cd45* for KCs and *Cd146* for LSECs. HCs and LSECs expressed high levels of *Tmprss6* (Figure S1A) and *Cd146* (Figure S1B), respectively, whereas *Cd45* (Figure S1C) was predominantly expressed in KCs. *Hamp* was exclusively expressed in HCs (Figure 1A), whereas *Bmp6* was highly expressed in NPCs, mainly in LSECs (Figure 1B). To investigate whether *Bmp6* expression depends on cell iron content, we measured the Iron Regulatory Proteins (IRPs)/Iron Responsive Elements (IRE) binding activity that directly correlates to cell iron [23].

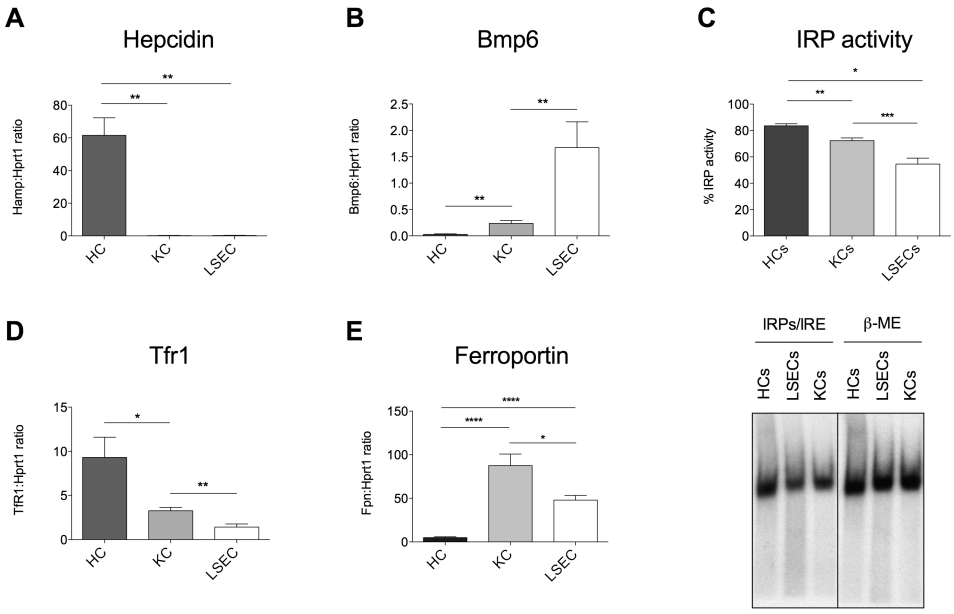

Figure 1. Isolated liver cells characterization.
Liver cells were isolated from 4-6 mice using the protocol reported in Experimental Procedures. Hepcidin (*Hamp*, A), Bone Morphogenetic Protein 6 (*Bmp6*, B), Transferrin Receptor 1 (*Tfr1,* D) and ferroportin (*Fpn*, E) mRNA expression was quantified by qRT-PCR relative to housekeeping *Hprt1* gene. (C) Upper panel: IRE/IRP-binding activity of HCs, KCs and LSECs, expressed as percentage of total activity. The plot refers to three independent experiments. Lower panel: IRE-IRPs electro mobility shift assay (EMSA). β-ME (beta-mercaptoethanol) was used to evaluate the total binding activity. A representative experiment was shown. Error bars indicate SE. *: P< .05; **: P< .01; ***: P< .001.

Alternatively we quantified *Tfr1* mRNA that is stabilized by IRPs in iron deficiency and degraded in iron overload and thus indirectly estimates intracellular iron content [23]. In all cell types, *Bmp6* levels inversely correlated with both IRPs binding activity (Figure 1C) and *Tfr1* expression (Figure 1D). Since *Tfr1* changes are easier to assess and more pronounced than changes of IRPs activity, we used *Tfr1* expression to investigate cells iron content in subsequent experiments. Notably, ferroportin (*Fpn*) expression was low in HCs and high in

NPCs, especially in KCs (Figure 1E). The latter finding, considering the lower levels of IRPs binding activity in NPCs as compared to HCs (Figure 1C), indicates that NPCs have a prevalent iron exporter functions.

3.2 Chronic dietary iron changes modulate *Bmp6* in all cell types

Liver and spleen are iron storage organs able to accumulate or release iron according to body needs. To investigate whether and how dietary iron changes modulate *Bmp6* expression in liver cells and in spleen macrophages, different cohorts of mice were fed an iron balanced (IB), iron deficient (ID) or iron loaded (IL) diet for 3 weeks. Iron parameters changed as expected: LIC (Figure S2A), SIC (Figure S2B) and transferrin saturation (TS, Figure S2C) were significantly increased and decreased in IL- and ID-treated mice, respectively. Also Hb was significantly increased in animals maintained an IL diet and decreased following an ID diet (Figure S2D). In HCs, *Hamp* (Figure S2E), Inhibitor of differentiation 1 [*Id1*, a target of the Bmp-Smad pathway] (Figure S2F) and *Bmp6* (Figure 2A) were transcriptionally modulated in the same direction of iron changes. Both KCs (Figure 2C) and LSECs (Figure 2E) upregulated *Bmp6* expression in dietary iron overload, while the opposite occurred in iron deficiency. In all cells (Figure 2B, 2D and 2F) *Tfr1* was stabilized in iron deficiency and downregulated in iron overload. We concluded that in wild type animals *Bmp6* is regulated in all liver cell types, according to their intracellular iron content, which reflects the difference between iron uptake and release. A similar regulation does not occur in the spleen: total spleen (Figure S3A), spleen-derived macrophages, as $F4/80^{+}$

(Figure S3B), Cd11b^{+} (Figure S3C) and F4/80^{-} Cd11b^{-} cells (Figure S3D), did not change *Bmp6* expression following systemic iron variations.

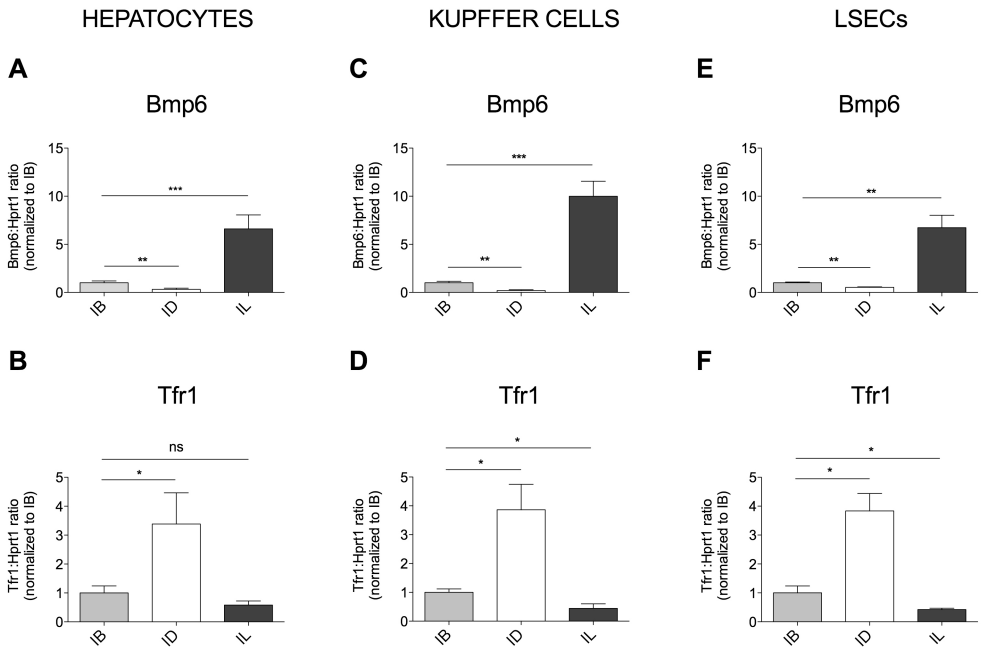

Figure 2. *Bmp6* and *Tfr1* expression in chronic dietary iron changes.
Bmp6 (A, C, E) and *Tfr1* (B, D, F) mRNA expression was evaluated by qRT-PCR in isolated HCs (A, B), KCs (C, D) and LSECs (E, F) from 4-12 mice/group. mRNA expression ratio was normalized relative to housekeeping *Hprt1*. Mean control value of IB-treated mice was set to 1. Error bars indicate SE. *: P< .05; **: P< .01; ***: P< .001; ns: not significant.

3.3 Changes in hepcidin expression do not require a change in LSECs Bmp6 expression in response to acute mild iron changes

To investigate the kinetic of *Bmp6* response after acute dietary iron variation, mice were iron-depleted by a low-iron diet for 2 weeks and maintained for 1 day the same diet (< 3 mg/kg iron, defined as ID in

Figure 3), or switched to a standard diet (200 mg/kg iron, defined as IB in Figure 3) or to a rich iron diet (8.3 mg/kg iron, defined as IL in Figure 3). 1 day ID, standard (IB) or IL diet, according to described protocols [19]. Results after IL diet were as expected: TS (Figure 3A), LIC (Figure 3B) and *Hamp* (Figure 3C) were all increased, *Bmp6* was increased and *Tfr1 mRNA* decreased in all cell types (Figure 3). In animals switched to a standard (IB) diet, the response of circulating and intracellular iron was uncoupled: TS was increased (Figure 3A), whereas LIC (Figure 3B) was unchanged and *Hamp* was only moderately increased compared with animals maintained an ID diet (Figure 3C). HCs and KCs *Bmp6* was concordant with *Hamp* and moderately increased in comparison with ID (Figure 3D and 3F). Remarkably, LSECs *Bmp6* remained low as in ID (Figure 3H).

Considering intracellular iron we observed a discrepancy between LIC and *Tfr1* mRNA: although LIC was similar in IB and ID (Figure 3B), HCs *Tfr1* was strongly induced only in ID (Figure 3E) and downregulated in IB as well as in IL mice, which had the highest LIC (Figure 3B). This observation suggests that a threshold of intracellular iron should likely be achieved to induce reduction of *Tfr1* expression and that *Tfr1* mRNA is a better sensor of iron decrease than increase.

KCs behaved as HCs: in IB *Bmp6* was slightly upregulated (Figure 3F) and *Tfr1* mRNA mildly decreased (Figure 3G) compared to ID mice. However, in LSECs both *Bmp6* (Figure 3H) and *Tfr1* expression (Figure 3I) were comparable between ID and IB mice, suggesting that, although iron absorption increases significantly when animals previously iron depleted are switched to 1 day IB diet [19], this is not

sufficient to activate *Bmp6* in LSECs, the activation requiring higher iron burden, as occurs in IL diet (Figure 3H).

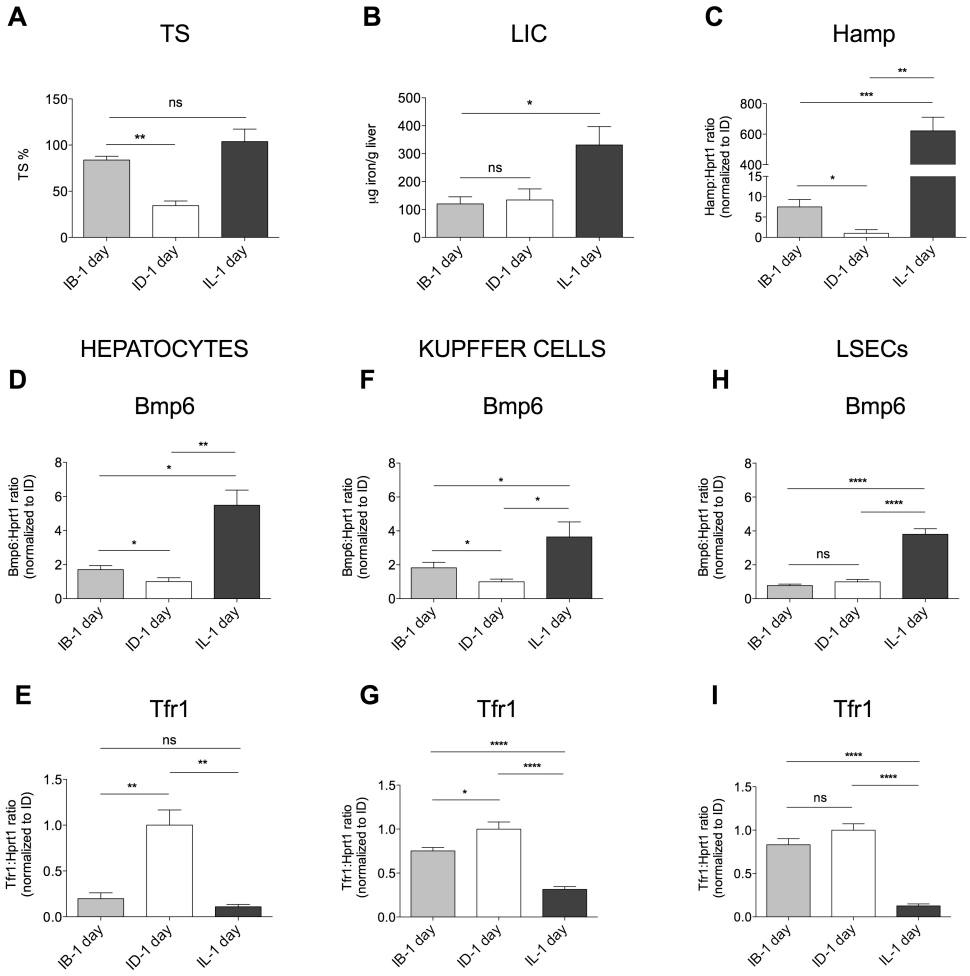

Figure 3. **Iron parameters and *Bmp6* expression levels in acute dietary iron changes.**
Transferrin saturation (TS, A) and non-heme liver (LIC, B) iron content were measured in mice (6-8/group) treated by an iron deficient diet for two weeks and then challenged with 1 day ID (ID-1day), iron balanced (IB-1day) and iron loaded (IL-1 day) diets. *Hamp* (C), *Bmp6* (D, F, H) and *Tfr1* (E, G, I) mRNA expression was evaluated by qRT-PCR in HCs (C, D, E), KCs (F, G) and LSECs (H, I) isolated from 4-7 mice/group. *Hprt1* was used as housekeeping gene. mRNA expression ratio was normalized to control (ID-1 day) mean value set to 1. Error bars indicate SE. *: P< .05; **: P< .01; ***: P< .001; ns: not significant.

3.4 *Bmp6 regulation* in the iron loaded *Hjv* KO mice

To investigate the regulation of *Bmp6* in pathological iron overload, we analyzed *Hjv* KO mice, characterized by severe iron overload with increased TS (Figure S4A) and LIC (Figure S4B and [8,9]), due to inactivation of the Bmp6-coreceptor *Hjv* that results in strong *Hamp* reduction (Figure S4C). Severe hepcidin insufficiency causes ferroportin stabilization and, although iron is increased in the circulation and in the liver, the spleen is iron poor (Figure S4D) [8,9].

In *Hjv* KO HCs *Bmp6* mRNA was increased (Figure 4A) and *TfR1* expression was suppressed (Figure 4B), compatible with high iron content, as demonstrated also by degradation of Tfr1 protein (Figure S5A). *Bmp6* was increased also in KCs and LSECs (Figure 4D and 4G). However, unlike HCs, *TfR1* was up-regulated in NPCs both at mRNA (Figure 4E and 4H) and protein levels (Figure S4B and S4C), suggesting low iron content. This is due to hepcidin suppression and high ferroportin export, and is in agreement with the low SIC (Figure S4D). In this model of iron overload with low hepcidin, *Bmp6* expression in NPCs is independent of the corresponding cell iron content, which is maintained low likely because of their elevated iron export ability, and possibly more related to their high iron uptake.

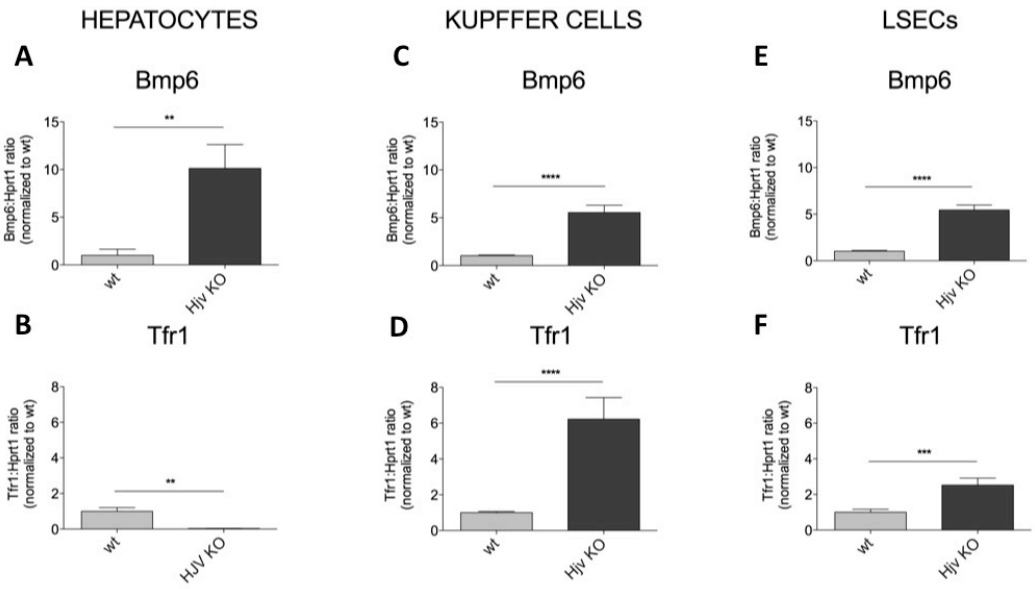

Figure 4. *Bmp6* and *Tfr1* expression in *Hjv* KO mice.
Bmp6 (A, C, E) and *Tfr1* (B, D, F) mRNA expression was evaluated in liver cells isolated from 6-10 mice by qRT-PCR, using *Hprt1* as the referred housekeeping gene. mRNA expression ratio was normalized to control wild type (wt) mean value set to 1. Error bars indicate SE. **: P< .01; ***: P< .001; ****: P< .0001.

3.5 Regulation of *Bmp6* in the iron deficient *Tmprss6* KO mice

The *Tmprss6* KO mouse model is characterized by iron deficient anemia, as assessed by low hemoglobin (data not shown), low LIC (Figure S6A), low TS (Figure S6B), due to hyperactivation of the BMP-SMAD pathway [24] and inappropriately high hepcidin levels (Figure S6C and [18]). Spleen iron of *Tmprss6* KO mice is comparable with that of wild type littermates (Figure S6D), thus inappropriate for its condition of iron deficiency.

In isolated HCs *Bmp6* expression was low (Figure 5A) and *TfR1* elevated (Figure 5B). However, *Tfr1* expression in KCs (Figure 5D) and LSECs (Figure 5F) was similar to wild type littermates, reflecting

spleen iron content (Figure S6D) and compatible with iron retention due to high hepcidin. *Bmp6* in KCs (Figure 5C) and LSECs (Figure 5E) was significantly lower than in wild type cells, as in HCs. In analogy with the *Hjv* KO model but in opposite direction, these results suggest that NPCs modulate *Bmp6* in a way independent on their iron content, in this case reflecting low iron uptake.

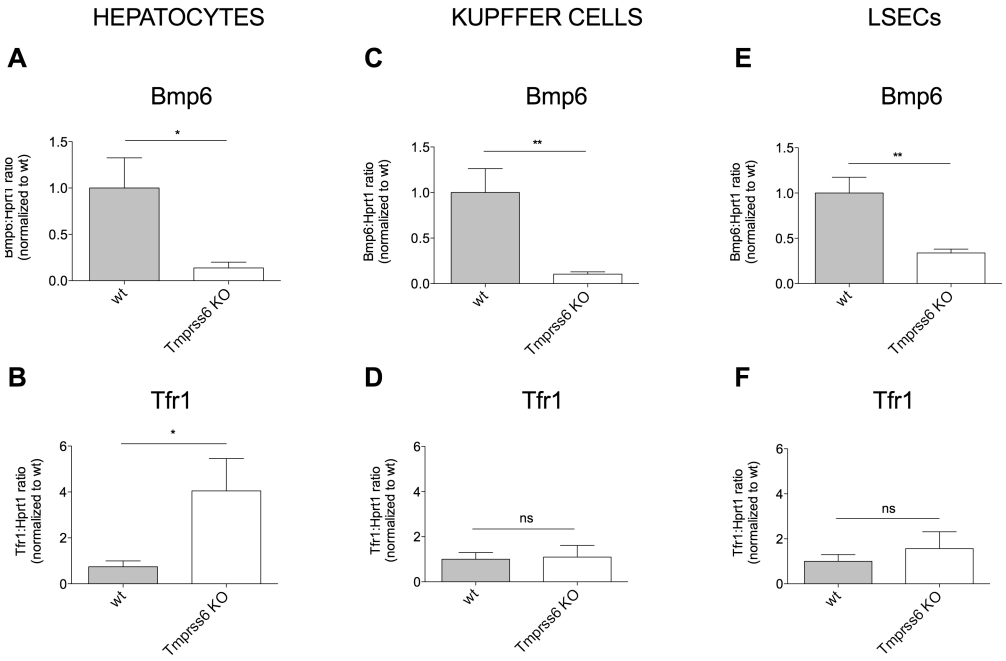

Figure 5. *Bmp6* and *Tfr1* expression in *Tmprss6* KO mice.

Bmp6 (A, C, E) and *Tfr1* (B, D, F) expression was measured in liver cells isolated from wild type (wt) and *Tmprss6* KO mice (4-6 mice/group) by qRT-PCR, using *Hprt1* as housekeeping gene. mRNA expression ratio was normalized to wt mean value set to 1. Error bars indicate SE. *: P< .05; **: P< .01; ns: not significant.

3.6 *Tmprss6* expression is independent of *Bmp6* expression

Recently *Bmp6* was shown to be a positive regulator of *Tmprss6* expression in mice treated with prolonged iron rich diet [25]. *Tmprss6* up-regulation was interpreted as a negative feedback mechanism to avoid excessive hepcidin production in response to iron increase [25]. We took advantage of the analyzed models to investigate whether *Bmp6* produced by HCs and/or NPCs could play a role in the regulation of *Tmprss6*. As shown in Figure S7, in our models we did not observe a transcriptional activation of *Tmprss6* in all high *Bmp6* conditions, including dietary both chronic (Figure S7A) and acute (Figure S7B) and disease-associated (Figure S7C) iron overload. Only a trend toward a slight increase was observed in chronic IL diet.

4. DISCUSSION

The liver hormone hepcidin controls systemic iron homeostasis in response to different stimuli, such as variations of total body iron, erythropoiesis expansion, hypoxia and inflammation. In response to iron increase, hepcidin is up-regulated by the BMP-SMAD signaling pathway, activated by BMP6 and inhibited by the serine protease TMPRSS6 [26]. At the same time iron regulates *BMP6* expression in a homeostatic manner [13]. The orchestration of iron metabolism by Bmp6 is a liver-specific function, since systemic iron changes do not modify *Bmp6* expression in other organs [14]. However, how *Bmp6*

expression is up-regulated by iron remains elusive and the specific contribution of the different liver cell types in *Bmp6* regulation in physiological and pathological conditions remains poorly understood.

In the present study we investigated the *Bmp6* expression in isolated liver cells, in response to physiological iron changes and in murine models of iron disorders. We also attempted to compare cell iron content and *Bmp6* expression in the different cell types. As a measure of iron content we used *Tfr1* mRNA, since in basal conditions its transcriptional regulation corresponds to the IRP1 activity (Figure 1F) in the different cell types. We also measured Tfr1 protein levels in *Hjv* KO model of iron overload.

We confirm that *Hamp* expression in basal conditions is high although HCs *Bmp6* is low, compatible with a paracrine hepcidin stimulation by the elevated NPCs *Bmp6*, as previously observed [27]. Interestingly, KCs and LSECs have lower IRP binding activity than HCs and express higher levels of ferroportin, findings compatible with an important function of iron exporters. At variance with published data [27] we observed that *Bmp6* changes are consensual to systemic and intracellular iron in all liver cells, including HCs, when variations of the iron status are stably induced by the chronic (3-weeks) diet. We propose that in steady state the equilibrium is reached between iron uptake and hepcidin-mediated iron export and that *Bmp6* expression reflects this equilibrium in all liver cells, including NPCs. We excluded that in the same chronic conditions spleen macrophages participate to *Bmp6* regulation, confirming the central role of liver *Bmp6* in hepcidin control.

Acute dietary iron changes in iron-depleted mice caused marked variations of *Hamp* and *Bmp6* in all liver cells only when animals were exposed to the iron-enriched (IL) diet. In IB-treated ones TS increased but *Bmp6* increase was mild in HCs and KCs and absent in LSECs, that remain relatively iron free likely because of their rapid iron release. In the interpretation of our results, the dynamics of iron uptake and release should be considered, the latter being more important in NPCs than in HCs, because of their higher ferroportin expression. It should also be noted that in the acute model of iron variation the effect of hepcidin on ferroportin is not as evident as in chronic models.

In the 1-day diet, despite HCs iron and *Bmp6* are both increased in IB-treated mice, LSECs do not up-regulate *Bmp6*. Thus LSECs do not respond to acute and likely modest and transient dietary iron changes.

A signal from HCs that drives *Bmp6* activation in NPCs has been previously proposed [27]. Our results suggest that *Bmp6* expression in LSECs increases only when circulating iron is stably high as in IL diet.

Disease models of iron overload (*Hjv* KO) and deficiency (*Tmprss6* KO) are especially informative to define Bmp6 regulation. Since characterized by abnormal hepcidin responses, that are opposite to the physiological ones, these models dissociate *Bmp6* expression from hepcidin response. *Hjv* KO mice have appropriately high *Bmp6,* as observed [19] but low hepcidin, and *Tmprss6* KO have the opposite phenotype with high hepcidin and low *Bmp6.* In our hands the direct correlation between iron (*Tfr1* mRNA and protein) and *Bmp6* is maintained in HCs, but not in NPCs whose iron content was as in

spleen macrophages. Although HCs have high (in case of *Hjv* KO) or low (in case of *Tmprss6* KO) iron content, KCs and LSECs appear iron poor in *Hjv* KO mice, and inappropriately iron replete in *Tmprss6* KO animals, reflecting the effect of hepcidin on ferroportin. The effect of abnormal hepcidin levels is quite evident in NPCs in these pathologic conditions. Nevertheless, *Bmp6* is upregulated in *Hjv* KO mice, and downregulated in *Tmprss6* KO animals in all liver cells examined. Since this occurs in NPCs that, opposite to HCs, have high ferroportin expression and considering the iron status of the models studied, is plausible to conclude that *Bmp6* expression in NPCs reflects their iron uptake (high in *Hjv* KO and low in *Tmprss6* KO).

It has been suggested that ferritin from HCs may act as a paracrine molecule to regulate *Bmp6* expression in LSECs [28]. Both HCs and NPCs regulate *Bmp6* expression apparently in response to changes of HCs iron, in chronic conditions. This has been proposed to require a signal/cytokine to transmit information on the iron state from HCs to NPCs [27]. We favor a different interpretation based on the following observations. First, a mild HCs iron increase in acute dietary iron treatment does not activate *Bmp6* in LSECs. Second, Fpn inactivation in HCs, that leads to liver iron overload and decreases serum iron and TS, does not increase, but even down-regulate, liver *Bmp6* expression [29].

We observe that NPCs *Bmp6* is discrepant with iron content measured as *Tfr1* mRNA (or protein) in several conditions. In the interpretation of the results, the higher ferroportin expression of NPCs in comparison with HCs should be considered. Our results are compatible with the possibility that NPCs regulate *Bmp6* expression

sensing the iron flux, especially the imported iron, while *Tfr1* reflects the labile iron pool resulting from the uptake/release balance, the latter being highly dependent on hepcidin itself and more evident when levels of hepcidin are stable in chronic conditions. This would explain why *Bmp6* is low in *Tmprss6* KO (where iron uptake is minimal, but the release is reduced by ferroportin degradation) and high in *Hjv* KO, where the uptake is massive but massive is also the export, due to the hepcidin deficiency. These disease models highlight the physiological crosstalk of liver cells, because of their altered hepcidin response.

In conclusion we have strengthened the crosstalk among the different liver cell types and showed a crucial role of NPCs in the modulation of *Bmp6* both in physiological and pathological conditions. Although HCs are able to increase *Bmp6* in iron overload, the major contribution is provided by the high *Bmp6*-expressing NPCs, especially LSECs, likely because they are in direct contact with the circulation and may behave as a liver iron sensor. Increasing hepcidin through Bmp6 (that is sensing a high iron influx), they contribute not only to systemic, but also to local iron regulation, withholding iron, as a possible protective mechanism of HCs (Figure 6). In *Hjv* KO model *Bmp6* production persists, but lack of hepcidin response abolishes the protective effect of LSECs and KCs on HCs iron loading. In *Tmprss6* KO mice *Bmp6* expression is low, irrespective of the relatively high iron content of NPCs, that is determined by the high hepcidin levels. This iron sequestration contributes to worsen systemic and HCs iron deficiency, as illustrated in Figure 6.

We have uncovered a previously unrecognized mechanism of controlled storage and release of iron by NPCs: the positive feedback

between *Bmp6* expression in these cells and ferroportin degradation by the induced hepcidin would allow these cells to accumulate iron for later needs and at the same time to protect HCs from iron overload.

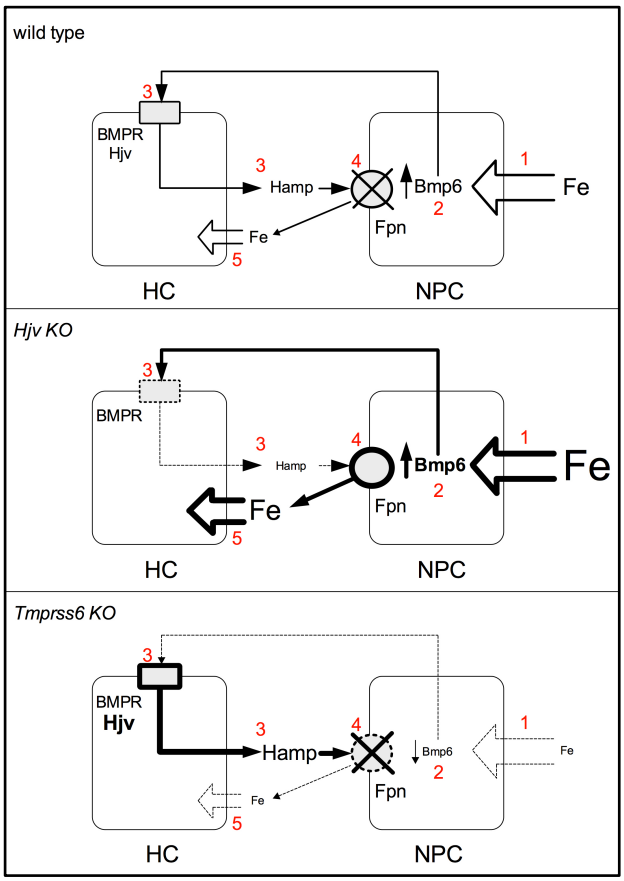

Figure 6. Proposed model of the crosstalk between *Bmp6*-producing NPCs and *hepcidin*-producing HCs in different conditions. (1) NPC iron entry; **(2)** Bmp6 production; **(3)** Bmp6-mediated activation of the BMPR-Hjv complex and hepcidin production; (**4**) hepcidin-mediated degradation of ferroportin; **(5)** HC iron entry. The thickness of solid lines and arrows is proportional to the amount of iron, Bmp6, ferroportin and hepcidin. The dotted line indicates inhibition of the pathway. HC: hepatocyte; NPCs: non parenchymal cells (Kupffer cells and sinusoidal endothelial cells); Hamp: hepcidin; BMPR: Bone Morphogenetic Protein Receptor; Hjv: hemojuvelin; Fpn: ferroportin.

5. SUPPLEMENTARY INFORMATIONS

5.1 TABLE AND FIGURES

Name	Id
Bmp6	Mm01332882_m1
Cd45	Mm01293575_m1
Cd146	Mm00522397-m1
Id1	Mm00775963_g1
Hamp	Mm00519025_m1
Hprt1	Mm01318743_m1
Slc40a1	Mm00489837_m1
Tfr1	Mm00441941_m1
Tmprss6	Mm0551119_m1

Supplemental Table 1. Oligonucleotides used for qRT-PCR.

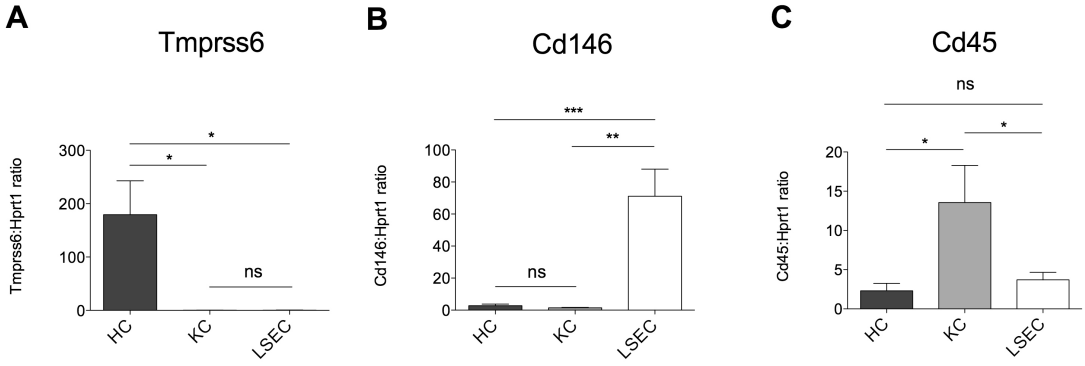

Figure S1. Isolated liver cells characterization.

Liver cells were isolated from 4 mice. *Tmprss6* (A), *Cd146* (B) and *Cd45* (C) mRNA expression was quantified by qRT-PCR relative to housekeeping *Hprt1* mRN*A* to evaluate the purity of HCs, KCs and LSECs, respectively. Error bars indicate SE. *: P< .05; **: P< .01; ***: P< .001.

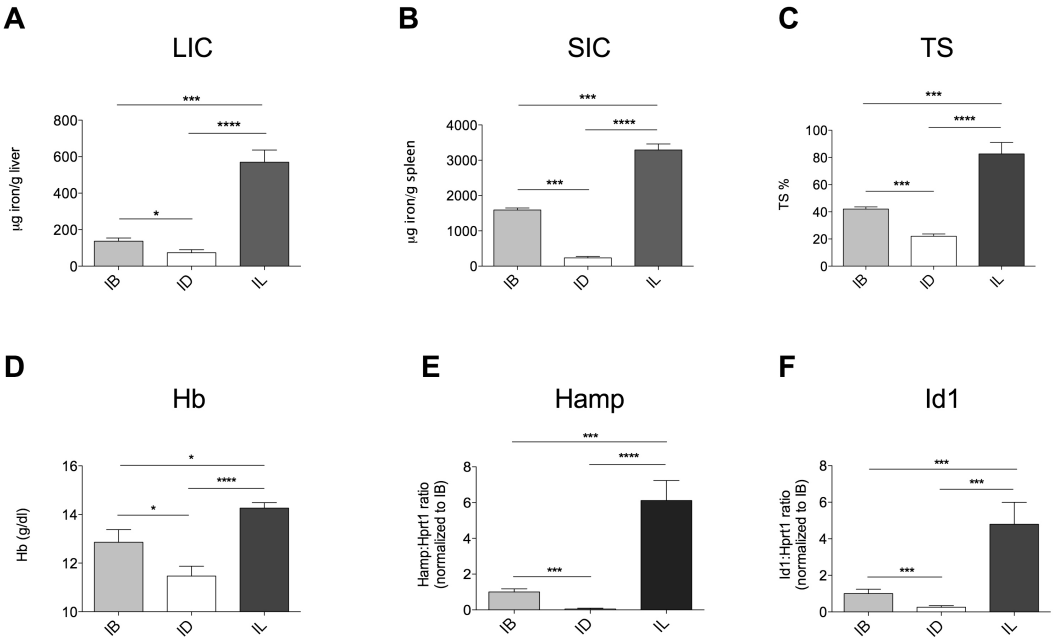

Figure S2. Iron parameters and hepatocyte iron-related genes in chronic dietary iron changes. Mice were fed an iron balanced (IB), iron deficient (ID) and iron loading (IL) diet for 3 weeks (6-8 mice/group). Non-heme liver (LIC, A), spleen (SIC, B) iron content, transferrin saturation (TS, C) and hemoglobin levels (Hb, D) are shown. In isolated hepatocytes hepcidin (*Hamp*) and *Id1* mRNA expression was quantified by qRT-PCR relative to housekeeping *Hprt1* gene. mRNA expression ratio was normalized setting control (IB) mean value to 1. Error bars indicate SE. *: P< .05; **: P< .01; ***: P< .001.

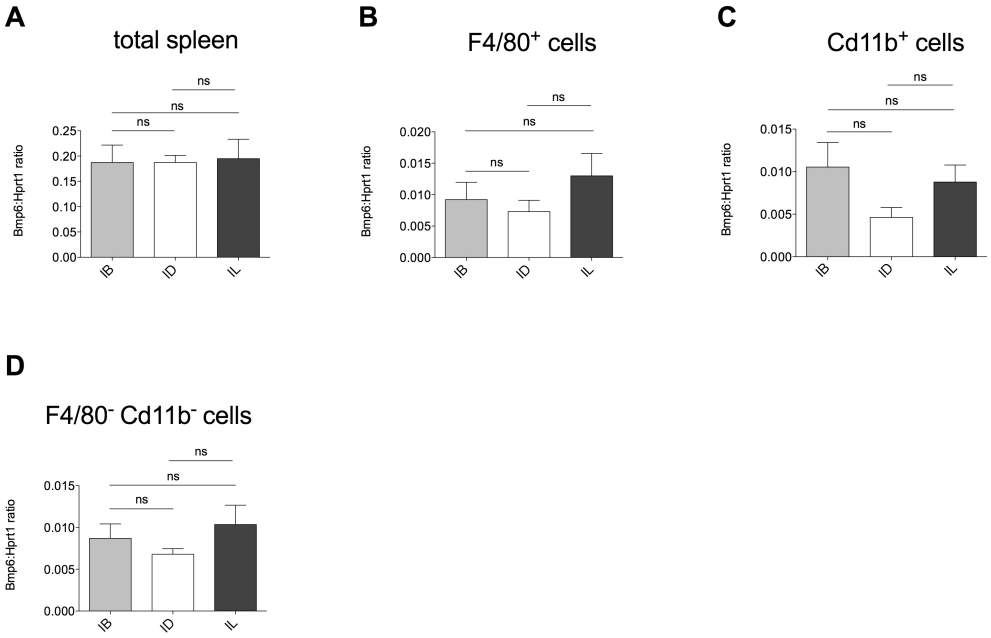

Figure S3. *Bmp6* expression in total spleen and spleen-derived cells. Spleen and spleen-derived cells were isolated from mice maintained an iron balanced (IB), iron deficient (ID) and iron loading (IL) diet for 3 weeks. *Bmp6* expression from total spleen (A, 3-4 mice), from F4/80^{+} cells (B, 6 mice), from Cd11b^{+} cells (C, 6 mice) and from negative fractions (D, 6 mice) was quantified by qRT-PCR relative to *Hprt1* as the housekeeping gene. Error bars indicate SE. ns: not significant.

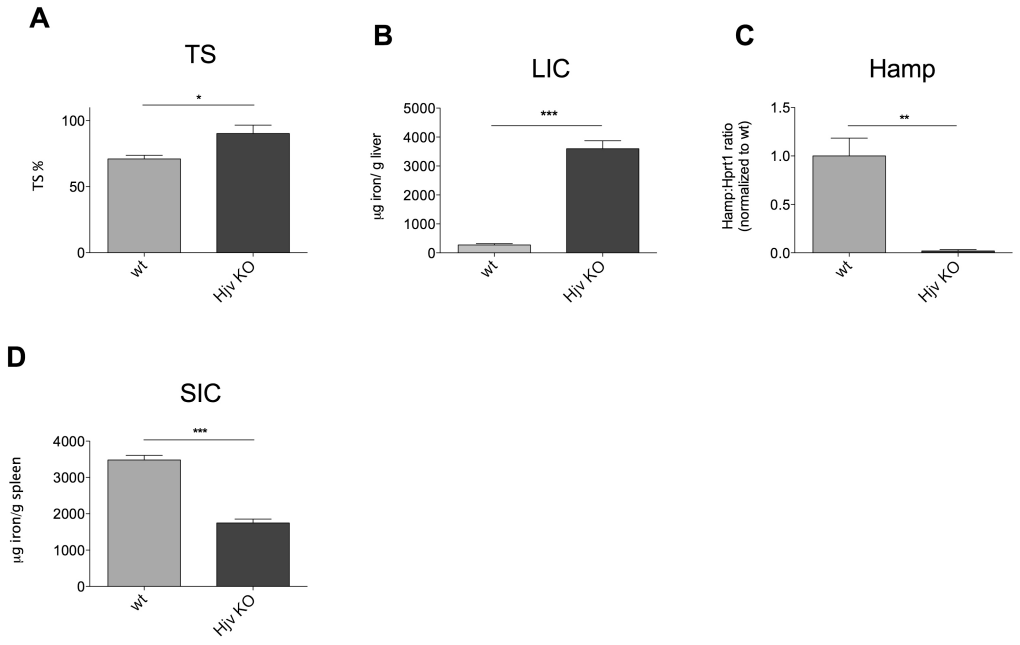

Figure S4. Iron parameters and hepcidin levels in *Hjv* KO mice. Transferrin saturation (TS, A), non-heme sliver iron content (LIC, B) and non-heme spleen iron content (SIC, D) were measured in wild type (wt) and *Hjv* KO animals (4 mice/group). In isolated HCs, hepcidin (*Hamp*, **C**) expression was measured by qRT-PCR, using *Hprt1* as housekeeping gene and mRNA expression ratio was normalized to control (wt) mean values set to 1. Error bars indicate SE. *: P< .05; **: P< .01; ***: P< .001.

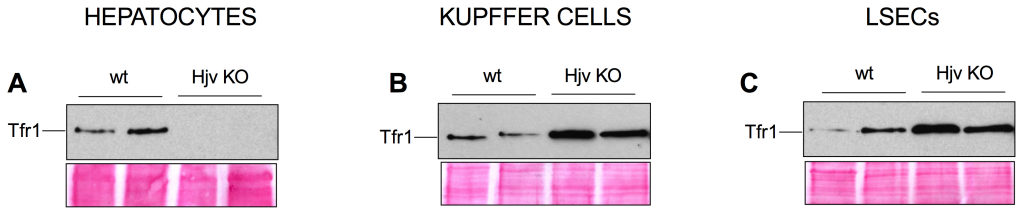

Figure S5. Tfr1 protein levels in cells isolated from Hjv KO mice.

HCs (A), KCs (B) and LSECs (C) were isolated from wild type (wt) and Hjv KO mice. Cells were lysed in Lysis Buffer as described in Material and Methods and protein extracts were loaded onto a 12% SDS PAGE and processed for Western Blot analysis. Anti-Tfr1 Ab was used to detect endogenous Tfr1. Equal protein transfer were verified by Ponceau staining.

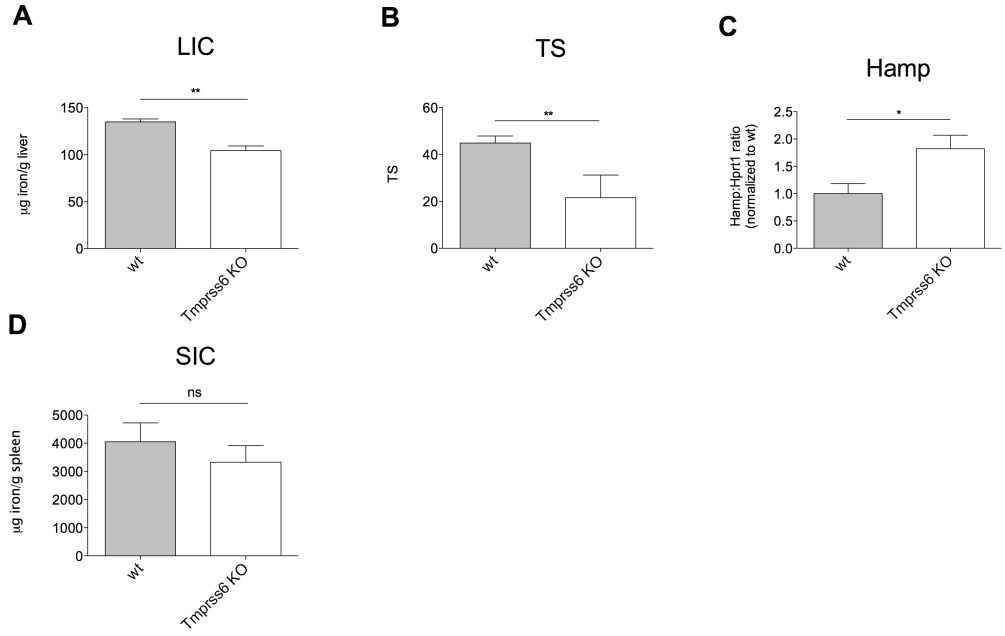

Figure S6. Iron parameters and hepcidin levels in *Tmprss6* KO mice. Non-heme liver (LIC, A) and spleen (SIC, D) iron content and transferrin saturation (TS, B) in wild type (wt) and *Tmprss6* KO mice (4-6 mice/group). Hepcidin mRNA expression (*Hamp*, C) was evaluated in isolated HCs by qRT-PCR relative to the housekeeping *Hprt1* gene. mRNA expression was normalized to control (wt) mean values set to 1. Error bars indicate SE. *: P< .05; **: P< .01; ns: not significant.

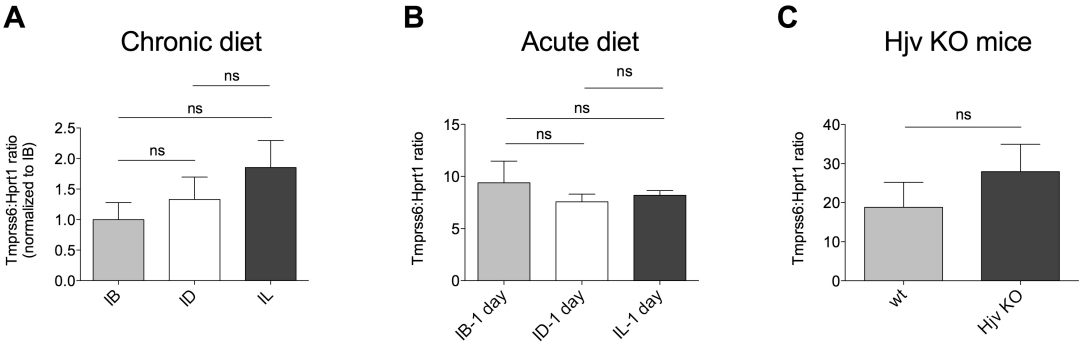

Figure S7. Hepatocytes *Tmprss6* expression in iron-loading and iron deficient conditions. *Tmprss6* expression was measured by qRT-PCR in HCs isolated from: A) mice maintained 3 weeks an iron balanced (IB), iron deficient (ID) and iron loading (IL) diet (6 mice/ group). mRNA expression ratio was normalized to a control (IB) mean values set to 1. B) mice maintained 2 weeks an ID diet and then treated with 1 day ID (ID-1 day), IB (IB-1 day), IL (IL-1 day) diet (4 mice/group). C) wild type (wt) and *Hjv* KO mice (4 mice/group). *Hprt1* was used as housekeeping gene for mRNA quantification. Error bars indicate SE. ns: not significant.

ACKNOWLEDGMENTS

We wish to thank Carlos Lopez-Otin (University of Oviedo, Oviedo, Spain) and Nancy Andrews (Duke University, Durham, NS) for the gift of *Tmprss6* KO and *Hjv* KO mice, respectively. This work was partially supported by "Telethon Fondazione Onlus" Grant GGP12025, Ministero Sanità, MIUR-PRIN (Progetto di Rilevante Interesse Nazionale) 2010-2011 and Ricerca Finalizzata RF-2010-2312048 to CC.

REFERENCES

1. Nemeth E, Tuttle MS, Powelson J, Vaughn MB, Donovan A, et al. (2004) Hepcidin regulates cellular iron efflux by binding to ferroportin and inducing its internalization. Science 306: 2090-2093.

2. Papanikolaou G, Samuels ME, Ludwig EH, MacDonald ML, Franchini PL, et al. (2004) Mutations in HFE2 cause iron overload in chromosome 1q-linked juvenile hemochromatosis. Nature genetics 36: 77-82.
3. Babitt JL, Huang FW, Wrighting DM, Xia Y, Sidis Y, et al. (2006) Bone morphogenetic protein signaling by hemojuvelin regulates hepcidin expression. Nature genetics 38: 531-539.
4. Xia Y, Yu PB, Sidis Y, Beppu H, Bloch KD, et al. (2007) Repulsive guidance molecule RGMa alters utilization of bone morphogenetic protein (BMP) type II receptors by BMP2 and BMP4. The Journal of biological chemistry 282: 18129-18140.
5. Steinbicker AU, Bartnikas TB, Lohmeyer LK, Leyton P, Mayeur C, et al. (2011) Perturbation of hepcidin expression by BMP type I receptor deletion induces iron overload in mice. Blood 118: 4224-4230.
6. Nohe A, Keating E, Knaus P, Petersen NO (2004) Signal transduction of bone morphogenetic protein receptors. Cellular signalling 16: 291-299.
7. Wang RH, Li C, Xu X, Zheng Y, Xiao C, et al. (2005) A role of SMAD4 in iron metabolism through the positive regulation of hepcidin expression. Cell metabolism 2: 399-409.
8. Niederkofler V, Salie R, Arber S (2005) Hemojuvelin is essential for dietary iron sensing, and its mutation leads to severe iron overload. The Journal of clinical investigation 115: 2180-2186.
9. Huang FW, Pinkus JL, Pinkus GS, Fleming MD, Andrews NC (2005) A mouse model of juvenile hemochromatosis. The Journal of clinical investigation 115: 2187-2191.
10. Nicolas G, Bennoun M, Devaux I, Beaumont C, Grandchamp B, et al. (2001) Lack of hepcidin gene expression and severe tissue iron overload in upstream stimulatory factor 2 (USF2) knockout mice. Proceedings of the National Academy of Sciences of the United States of America 98: 8780-8785.
11. Bragdon B, Moseychuk O, Saldanha S, King D, Julian J, et al. (2011) Bone morphogenetic proteins: a critical review. Cellular signalling 23: 609-620.
12. Xia Y, Babitt JL, Sidis Y, Chung RT, Lin HY (2008) Hemojuvelin regulates hepcidin expression via a selective subset of BMP ligands and receptors independently of neogenin. Blood 111: 5195-5204.
13. Kautz L, Meynard D, Monnier A, Darnaud V, Bouvet R, et al. (2008) Iron regulates phosphorylation of Smad1/5/8 and gene expression of Bmp6, Smad7, Id1, and Atoh8 in the mouse liver. Blood 112: 1503-1509.
14. Kautz L, Besson-Fournier C, Meynard D, Latour C, Roth MP, et al. (2011) Iron overload induces BMP6 expression in the liver but not in the duodenum. Haematologica 96: 199-203.
15. Yin C, Evason KJ, Asahina K, Stainier DY (2013) Hepatic stellate cells in liver development, regeneration, and cancer. The Journal of clinical investigation 123: 1902-1910.
16. Knittel T, Fellmer P, Muller L, Ramadori G (1997) Bone morphogenetic protein-6 is expressed in nonparenchymal liver cells and upregulated by transforming growth factor-beta 1. Experimental cell research 232: 263-269.
17. Zhang AS, Anderson SA, Wang J, Yang F, DeMaster K, et al. (2011) Suppression of hepatic hepcidin expression in response to acute iron

deprivation is associated with an increase of matriptase-2 protein. Blood 117: 1687-1699.
18. Folgueras AR, de Lara FM, Pendas AM, Garabaya C, Rodriguez F, et al. (2008) Membrane-bound serine protease matriptase-2 (Tmprss6) is an essential regulator of iron homeostasis. Blood 112: 2539-2545.
19. Ramos E, Kautz L, Rodriguez R, Hansen M, Gabayan V, et al. (2011) Evidence for distinct pathways of hepcidin regulation by acute and chronic iron loading in mice. Hepatology 53: 1333-1341.
20. Pagani A, Nai A, Corna G, Bosurgi L, Rovere-Querini P, et al. (2011) Low hepcidin accounts for the proinflammatory status associated with iron deficiency. Blood 118: 736-746.
21. Liu W, Hou Y, Chen H, Wei H, Lin W, et al. (2011) Sample preparation method for isolation of single-cell types from mouse liver for proteomic studies. Proteomics 11: 3556-3564.
22. Campanella A, Levi S, Cairo G, Biasiotto G, Arosio P (2004) Blotting analysis of native IRP1: a novel approach to distinguish the different forms of IRP1 in cells and tissues. Biochemistry 43: 195-204.
23. Rouault TA (2006) The role of iron regulatory proteins in mammalian iron homeostasis and disease. Nature chemical biology 2: 406-414.
24. Riba M, Rausa M, Sorosina M, Cittaro D, Garcia Manteiga JM, et al. (2013) A strong anti-inflammatory signature revealed by liver transcription profiling of Tmprss6-/- mice. PloS one 8: e69694.
25. Meynard D, Vaja V, Sun CC, Corradini E, Chen S, et al. (2011) Regulation of TMPRSS6 by BMP6 and iron in human cells and mice. Blood 118: 747-756.
26. Hentze MW, Muckenthaler MU, Galy B, Camaschella C (2010) Two to tango: regulation of Mammalian iron metabolism. Cell 142: 24-38.
27. Enns CA, Ahmed R, Wang J, Ueno A, Worthen C, et al. (2013) Increased iron loading induces Bmp6 expression in the non-parenchymal cells of the liver independent of the BMP-signaling pathway. PloS one 8: e60534.
28. Feng Q, Migas MC, Waheed A, Britton RS, Fleming RE (2012) Ferritin upregulates hepatic expression of bone morphogenetic protein 6 and hepcidin in mice. American journal of physiology Gastrointestinal and liver physiology 302: G1397-1404.
29. Zhang Z, Guo X, Herrera C, Tao Y, Wu Q, et al. (2014) Bmp6 expression can be regulated independently of liver iron in mice. PloS one 9: e84906.

CHAPTER 4

The erythroid function of Transferrin Receptor 2 revealed by *Tmprss6* inactivation in different models of Transferrin Receptor 2 knock out mice

Antonella Nai[1,*], Rosa Maria Pellegrino[2,*], Marco Rausa[1], Alessia Pagani[1], Martina Boero[2], Laura Silvestri[1], Giuseppe Saglio [2], Antonella Roetto[2] and Clara Camaschella[1]

[1]Vita Salute University and San Raffaele Scientific Institute, Division of Genetics and Cell Biology, Milan, Italy

[2] Department of Clinical and Biological Sciences, University of Torino, Torino, Italy

(*Haematologica. 2014 Jun; 99 (6): 1016-21)*

ABSTRACT

The transferrin receptor 2 (TFR2) is a transmembrane glycoprotein expressed in the liver and in the erythroid compartment, mutated in a form of hereditary hemochromatosis. Hepatic TFR2, together with HFE, activates the transcription of the iron-regulator hepcidin, while erythroid TFR2 is a member of the erythropoietin receptor complex. *TMPRSS6* gene, encoding the liver expressed serine protease matriptase-2, is the main inhibitor of hepcidin and inactivation of *TMPRSS6* leads to iron deficiency with high hepcidin levels. Here we evaluate the phenotype resulting from the genetic loss of *Tmprss6 in Tfr2* total (*Tfr2*$^{-/-}$) and liver-specific (*Tfr2*^{LCKO}) KO mice. *Tmprss6*$^{-/-}$ *Tfr2*$^{-/-}$ and *Tmprss6*$^{-/-}$*Tfr2*^{LCKO} have increased hepcidin levels and show iron-deficiency anemia as *Tmprss6*$^{-/-}$ mice. However, while *Tmprss6*$^{-/-}$ *Tfr2*^{LCKO} are phenotypically identical to *Tmprss6*$^{-/-}$ mice, *Tmprss6*$^{-/-}$ *Tfr2*$^{-/-}$ have increased red blood cell count and more severe microcytosis than *Tmprss6*$^{-/-}$ mice. In addition hepcidin expression in *Tmprss6*$^{-/-}$*Tfr2*$^{-/-}$ mice is higher than in wild-type, but lower than in *Tmprss6*$^{-/-}$ mice, suggesting a partial inhibition of the hepcidin activating pathway.

Our results prove that hepatic TFR2 acts upstream TMPRSS6. In addition *Tfr2* deletion causes a relative erythrocytosis in the iron deficient mice, that likely attenuates the over-expression of hepcidin of *Tmprss6*$^{-/-}$ mice. Since liver-specific deletion of *Tfr2* in *Tmprss6*$^{-/-}$ mice does not modify the erythrocyte count, we speculate that loss of Tfr2 in the erythroid compartment accounts for the hematological phenotype of *Tmprss6*$^{-/-}$*Tfr2*$^{-/-}$ mice. We propose that TFR2 is a

limiting factor for erythropoiesis particularly in conditions of iron-restriction.

1. INTRODUCTION

Transferrin receptor 2 (TFR2) is a transmembrane protein homologous to Transferrin receptor 1 (TFR1) that is mutated in hereditary hemochromatosis type 3[1,2]. TFR2 is expressed in the liver and, to a lower extent, in erythroid cells[3,4]. TFR2 protein is stabilized on cell surface by binding to its ligand diferric transferrin (holo-TF)[5] and, in a complex with the hemochromatosis protein HFE, is considered a sensor of circulating iron. In the current model in conditions of iron-deficiency HFE associates with TFR1; inversely, when TF saturation increases, competitive binding of holo-TF displaces HFE from TFR1 and the HFE-TFR2 complex activates *HAMP* transcription[6,7]. However, the phenotype of the HFE and TFR2-related disease is different[8] and the association between the two proteins has been recently questioned[9].

Hepcidin blocks dietary iron absorption and iron recycling from senescent erythrocytes by inducing the degradation of the iron exporter ferroportin on enterocytes and macrophages, respectively[10]. The mechanism of *HAMP* activation by the TFR2 and HFE is still unclear. Both proteins probably contributes to *HAMP* upregulation by Bone Morphogenetic Proteins (BMPs) in response to increased tissue iron[11,12]. BMP6, using Hemojuvelin (HJV) as a co-receptor, signals through Sons-of-Mother-Against-Decapenthaplegic 1/5/8

(SMAD1/5/8) proteins. In agreement HFE and TFR2 *in vitro* may form a multi-protein complex with HJV[13]. The role of hepatic TFR2 as a regulator of *HAMP* transcription is confirmed by the phenotype of the *Tfr2* total (*Tfr2*$^{-/-}$) and liver specific (*Tfr2*^{LCKO}) knock-out mouse models. Both mice are characterized by iron overload and low *Hamp* levels relative to their high iron stores, with *Tfr2*^{LCKO} having more severe liver iron accumulation than *Tfr2*$^{-/-}$ animals[14,15].

Recently TFR2 has been identified as a component of the erythropoietin receptor (EPOR) complex. *TFR2* and the *EPOR* are co-expressed during erythroid differentiation, TFR2 associates with EPOR in the endoplasmic reticulum and is required for the efficient transport of the EPOR to the cell surface. Moreover *TFR2* knockdown in vitro delays the terminal differentiation of erythroid precursors[16] indicating that TFR2 is required for efficient erythropoiesis.

The BMP6-HJV-HAMP pathway is inhibited by matriptase-2, a type II transmembrane serine protease encoded by the *TMPRSS6* gene. By cleaving HJV[17], TMPRSS6 strongly impairs the BMP-mediated *HAMP* activation in the liver. *TMPRSS6* mutations both in humans[18] and in mice[19,20] cause excessive *HAMP* production and iron-refractory iron deficiency anemia (IRIDA)[21]. The important role of TMPRSS6 in erythropoiesis is highlighted also by Genome Wide Association Studies: indeed, common *TMPRSS6* genetic variants associate with iron and erythrocyte traits in different populations[22-27]. By studying *Tmprss6* haploinsufficient mice[28] and hepcidin levels of normal individuals and the *TMPRSS6* common SNP (rs855791)[29] we demonstrated that even a partial inability to modulate hepcidin influences iron parameters and indirectly erythropoiesis.

The regulation of TMPRSS6 and its activity is incompletely understood: besides hypoxia[30], iron and BMP6, through the BMP-SMAD pathway, induce *TMPRSS6* expression likely as a negative feedback loop to limit excessive HAMP increase[31]. However, the *TMPRSS6* in vivo regulation according to the iron needs remains to be clarified. A possible role of Tmprss6 in iron overload was demonstrated by Finberg et al.[32] who showed that *Hfe*$^{-/-}$ mice with complete loss of *Tmprss6* revert the phenotype of iron overload to an iron-deficiency anemia with high *Hamp* levels. These findings suggest that HFE acts genetically upstream TMPRSS6 in the modulation of the BMP-SMAD pathway and of *HAMP* expression. In analogy with these results and given the role of TFR2 in erythropoiesis[16] we wondered whether TFR2 is involved in the regulation of TMPRSS6. To answer this question, we back-crossed *Tmprss6*$^{-/-}$ mice with animals with a complete deletion of *Tfr2* (*Tfr2*$^{-/-}$) and analyzed the hematological phenotype and the *Bmp-Smad-Hamp* pathway of the double mutant mice. Moreover, in order to discriminate between the hepatic and extra-hepatic functions of TFR2, we performed the same analysis in *Tmprss6*$^{-/-}$ mice lacking *Tfr2* specifically in the liver (*Tfr2*^{LCKO})[15].

2. MATERIALS AND METHODS

2.1 Mouse models

Mice were maintained in the animal facility of the Department of Clinical and Biological Sciences, University of Turin (Turin, Italy) in

accordance with the European Union guidelines. Each study was approved by the institutional animal care and use committee (IACUC) of the same institution.

Tmprss6$^{-/-}$ mouse model on a mixed C57BL/6-Sv129 background was kindly provided by Prof. C. Lopez-Otin (University of Oviedo, Oviedo, Spain) and maintained as brother-sister mating for more than 10 generations. *Tfr2*$^{-/-}$ and *Tfr2*^{LCKO} mice on a pure 129S2 background were generated as previously described[15]. For the experimental work described we bred *Tfr2*$^{-/-}$ or *Tfr2*^{LCKO} mice to *Tmprss6*$^{+/-}$ mice and then intercrossed the F1 progeny to generate various genotype combinations (F2: wt, *Tmprss6*$^{+/-}$, *Tmprss6*$^{-/-}$, *Tfr2*$^{-/-}$, *Tmprss6*$^{+/-}$*Tfr2*$^{-/-}$, *Tmprss6*$^{-/-}$*Tfr2*$^{-/-}$, *Tfr2*^{LCKO}, *Tmprss6*$^{+/-}$*Tfr2*^{LCKO}, *Tmprss6*$^{-/-}$*Tfr2*^{LCKO}). Mice were given a standard diet (480 mg iron/Kg) and only male mice were analyzed when 10-week-old. Blood was collected for hematological analyses, transferrin saturation and erythropoietin (Epo) levels. After sacrifice livers and spleens were weighed, dissected and snap-frozen immediately for RNA analysis or dried for tissue iron quantification.

2.2 Hematological analyses

Blood was obtained by retro-orbital puncture from anesthetized mice. Red blood cells (RBCs) and white blood cells (WBCs) counts, hemoglobin (Hb) concentration, hematocrit (Hct) and erythrocyte indexes (MCV, MCH) were measured using an ADVIA®120 Hematology System (Siemens Diagnostics).

Transferrin saturation was calculated as the ratio of serum iron and total iron binding capacity levels, using The Total Iron Binding

Capacity Kit (Randox Laboratories Ltd.), according to the manufacturer's instructions. Serum Epo levels were measured using mouse Epo quantikine set (R&D System), according to the manufacturer's instructions.

2.3 Tissue iron content

To measure iron concentration, tissue samples were dried at 110°C overnight, weighed, and digested in 1 mL of 3M HCl, 0.6M trichloroacetic acid for 20 hours at 65°C. The clear acid extract was added to 1 mL of working chromogen reagent (1 volume of 0.1% bathophenanthroline sulfate and 1% thioglycolic acid solution, 5 volumes of water, and 5 volumes of saturated sodium acetate). The solutions were then incubated for 30 minutes at room temperature until colour development and the absorbance measured at 535 nm. A standard curve was plotted using an acid solution containing increasing amounts of iron diluted from a stock solution of Titrisol iron standard (Merck, Darmstadt, Germany).

2.4 Quantitative RT-PCR

Total RNA was extracted from liver and spleen using the guanidinium thiocyanate–phenol–chloroform method (Trizol Reagent), following the manufacturer's (Invitrogen) recommendations. RNA (2 μg) was used for quantitative polymerase chain reaction (qPCR) analysis for first-strand synthesis of cDNA with the High Capacity cDNA Reverse Transcription kit (Applied Biosystems), according to the manufacturer's instructions.

For real-time PCR analysis, specific murine Assays-on-Demand products (20x) and TaqMan Master Mix (2x) from Applied Biosystems were used, and the reactions were run on 7900HT Fast Real-Time PCR System (Applied Biosystems) in a final volume of 20 μL. Each cDNA sample was amplified in triplicate and the RNA level was normalized to the corresponding level of Hprt1 mRNA. Primers used for qRT-PCR are in Supplemental Table 1.

2.5 Statistical analysis

Data are presented as mean ± SD. Unpaired 2-tailed Student's t-test was performed using GraphPad PRISM 5.0 and a $P<0.05$ was considered statistically significant.

3. RESULTS

3.1 *Tmprss6*$^{-/-}$*Tfr2*$^{-/-}$ mice are anemic and have increased red cells number

Ten-week-old *Tfr2*$^{-/-}$ mice have Hb levels higher than controls, while *Tfr2*^{LCKO} mice have levels comparable to wild type (wt) animals, as previously reported (15). Conversely *Tmprss6*$^{-/-}$ mice have the hematological phenotype of microcytic anemia with increased RBCs and reticulocyte counts accompanied by low levels of Hb, Hct, MCV and MCH. The heterozygous loss of *Tmprss6* in *Tfr2*$^{-/-}$ mice slightly reduces Hb levels although the difference versus *Tfr2*$^{-/-}$ mice is not statistically significant. On the contrary *Tmprss6*$^{+/-}$*Tfr2*^{LCKO} mice have Hb levels comparable to *Tfr2*^{LCKO} animals. Both *Tmprss6*$^{-/-}$*Tfr2*$^{-/-}$ and

Tmprss6$^{-/-}$*Tfr2*^{LCKO} mice are anemic and have Hb levels similar to *Tmprss6*$^{-/-}$ mice. However, the *Tmprss6*$^{-/-}$*Tfr2*$^{-/-}$ mice have higher number of RBCs than *Tmprss6*$^{-/-}$ animals, resulting in more severe microcytosis, while this is not the case for *Tmprss6*$^{-/-}$ mice with specific liver deletion of *Tfr2* (Table 1). In the absence of Tmprss6 reticulocytes were increased only in *Tfr2*$^{-/-}$ animals.

	WBC (*10^3cells/µL blood)	RBC (*10^6cells/µL blood)	Reticulocytes (*10^9cells/L blood)	Hb (g/dL)	Hct (%)	MCV (fL)	MCH (pg)
wt	7,2±2,6	8,6±0,7	302,8±149,9	13,1±0,4	43,3±2,7	50,8±1,5	15,1±1,4
***Tmprss6*$^{+/-}$**	5,6±1,4	9,3±0,8	243,7±28,8	13,2±0,8	45,3±3,3	48,5±0,8^{b}	14,1±0,5
***Tmprss6*$^{-/-}$**	5,9±4,1	11,0±1,4^{b}	771,1±265,5^{a}	8,0±0,9^{b}	32,3±2,2^{b}	29,5±2,5^{b}	7,3±0,7^{b}
***TfR2*$^{-/-}$**	10,4±2,9	9,5±0.8	324,8±116,7	15,1±1,4^{a}	48,9±4,8^{a}	51,7±0,9	16,0±0,6
***Tmprss6*$^{+/-}$ *TfR2*$^{-/-}$**	10,2±3,6	8,8±0,6	293,8±119,4	14,2±0,9^{a}	46,7±3,0	52,4±1,8	16,0±0,9
***Tmprss6*$^{-/-}$ *TfR2*$^{-/-}$**	8,1±5,8	13,9±2,0^{b,d,e}	2032,7±1063,7^{a,c,e}	8,3±0,9^{b,d}	35,6±4,6^{a,c}	25,7±2,5^{b,d,e}	6,0±0,3^{b,d,e}
***TfR2*^{LCKO}**	6,8±3,2	9,0±0,3	229,9±48,5	13,2±0,6	45,4±1,8	50,3±1,4	14,6±0,3
***Tmprss6*$^{+/}$ *TfR2*^{LCKO}**	8,1±2,8	9,5±0,6	264,0±68,0	13,9±0,9	47,7±1,9	50,1±1,3	14,7±0,4
***Tmprss6*$^{-/-}$ *TfR2*^{LCKO}**	10,4±3,5	10,7±1,5^{a,g,i}	1047,0±456,8^{a,h}	8,5±1,2^{b,h}	30,0±1,9^{b,h,i}	28,5±2,4^{b,h,i}	8,2±1,5^{b,h,i}

Table 1: Hematological data of all the genotype combinations analyzed
White Blood Cells (WBC), Red Blood Cells (RBC), Reticulocyte counts, Hemoglobin (Hb), Hematocrit (Hct), Mean Corpuscular Volume (MCV) and Mean Corpuscular Hemoglobin (MCH) are shown as means ± SDs of 4-7 male mice.
$^{a}p<0.05$, $^{b}p<0.005$ relative to wt (*Tmprss6*$^{+/+}$*Tfr2*$^{+/+}$) controls; $^{c}p<0.05$, $^{d}p<0.005$ relative to *Tfr2*$^{-/-}$; $^{e}p<0.05$, $^{f}p<0.005$ relative to *Tmprss6*$^{-/-}$; $^{g}p<0.05$, $^{h}p<0.005$ relative to *TfR2*^{LCKO}; $^{i}p<0.05$ relative to *Tmprss6*$^{-/-}$*Tfr2*$^{-/-}$. For complete statistical analysis see Supplemental Table 2.

3.2 Homozygous loss of *Tmprss6* reduces systemic and tissue iron levels of *Tfr2*$^{-/-}$ and *Tfr2*^{LCKO} mice

Transferrin saturation (TS) [Figure 1A] and Liver Iron Content (LIC) [Figure 1B] are significantly lower in the iron deficient *Tmprss6*$^{-/-}$ mice than in wt (defined as *Tmprss6*$^{+/+}$*Tfr2*$^{+/+}$ in Figure 1 and 2), while *Tfr2*$^{-/-}$ and *Tfr2*^{LCKO} animals show an important iron overload[15]. Deletion of *Tmprss6* gene in both *Tfr2*$^{-/-}$ and *Tfr2*^{LCKO} mice has a dose-dependent effect. The loss of a single allele slightly reduces TS and LIC in both models, although the differences are statistically significant only for the *Tfr2*$^{-/-}$ animals. The homozygous inactivation of *Tmprss6* lowers LIC of both *Tfr2*$^{-/-}$ and *Tfr2*^{LCKO} animals to the levels of *Tmprss6*$^{-/-}$ mice.

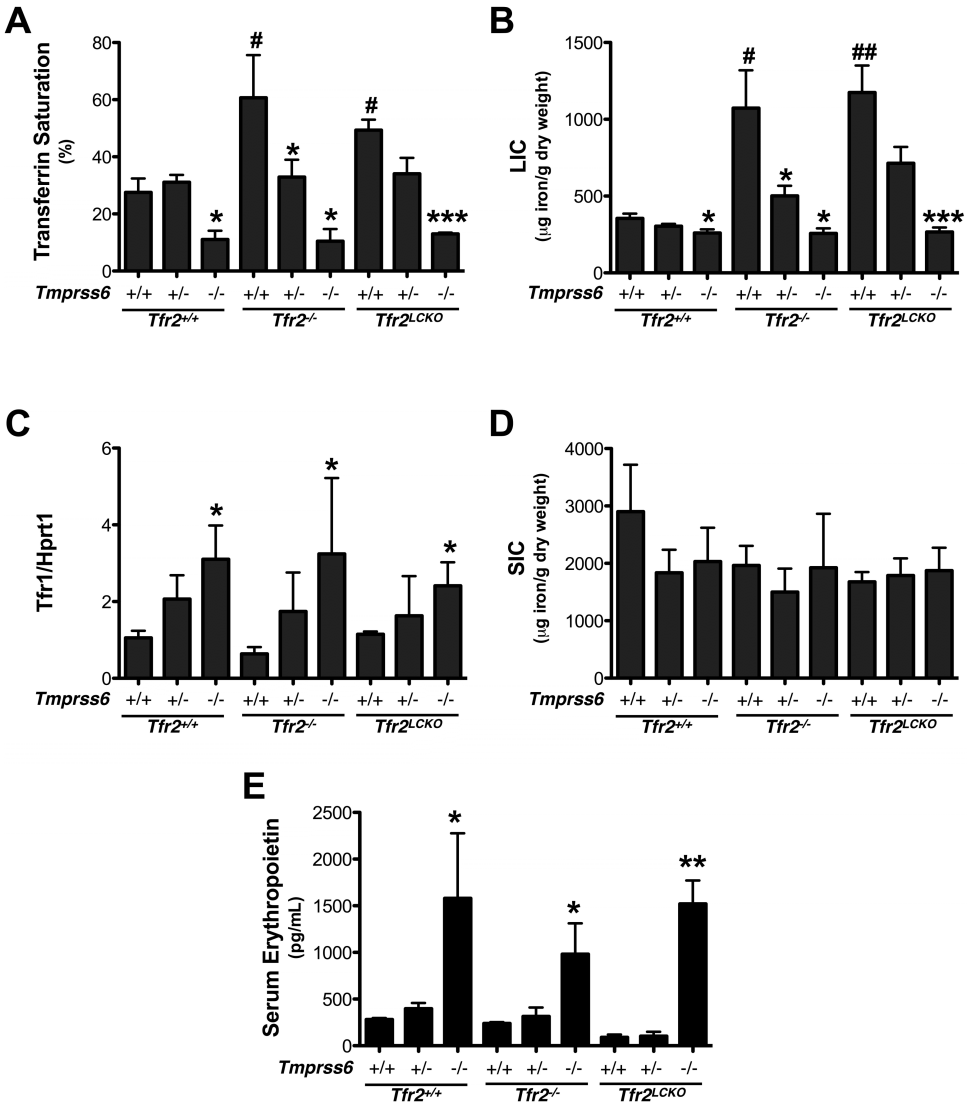

Figure 1: Effect of *Tmprss6* deletion on iron parameters and serum Epo levels of *Tfr2*$^{-/-}$ and *Tfr2*^{LCKO} mice

In the figure are graphed: transferrin saturation (A); hepatic non-heme iron content (LIC) (B); liver mRNA expression of Transferrin Receptor 1 (*Tfr1*)(C); splenic non-heme iron content (SIC)(D); serum erythropoietin (Epo) levels (E) in all genotype combination analyzed. Mean values of 3-6 animals for genotype are graphed and error bars indicate standard deviation. Symbols refer to a statistically significant difference: *P<0.05, **P<0.01 and ***P<0.005 respective to the relative *Tmprss6*$^{+/+}$ control of each *Tfr2* genotype; #P<0.05 and ##P<0.01 respective to wt (*Tmprss6*$^{+/+}$*Tfr2*$^{+/+}$) controls. For complete statistical analysis see Supplemental Table 2.

The LIC difference of the various genotypes is confirmed by the analysis of the *Tfr1* mRNA levels that are known to be inversely related to the cell iron content. *Tfr1* mRNA levels are high in *Tmprss6*$^{-/-}$, *Tmprss6*$^{-/-}$*Tfr2*$^{-/-}$ and *Tmprss6*$^{-/-}$*Tfr2*^{LCKO} animals and reduced according to gene-dosage of *Tmprss6* [Figure 1C].

We observed no differences in the spleen iron content (SIC) among all the genotypes analyzed [Figure 1D]. In addition spleen and liver size were similar between *Tmprss6*$^{-/-}$, *Tmprss6*$^{-/-}$*Tfr2*$^{-/-}$ and *Tmprss6*$^{-/-}$ *Tfr2*^{LCKO} animals (not shown).

Tfr2$^{-/-}$ and *Tfr2*^{LCKO} mice have serum erythropoietin (Epo) levels comparable to wt mice. As expected, anemic *Tmprss6*$^{-/-}$ mice have Epo levels higher than wt and comparable to *Tmprss6*$^{-/-}$*Tfr2*$^{-/-}$ and *Tmprss6*$^{-/-}$*Tfr2*^{LCKO} animals (Figure 1E).

3.3 *Tmprss6*$^{-/-}$*Tfr2*$^{-/-}$ mice have *Hamp* levels less inappropriately high than *Tmprss6*$^{-/-}$ mice

The expression of *Bmp6* reflects LIC in all the genotypes analyzed, being high in *Tfr2*$^{-/-}$ and *Tfr2*^{LCKO} animals and low in *Tmprss6*$^{-/-}$ as compared to wt controls, although in the latter case the difference is not statistically significant. *Bmp6* in *Tmprss6* haploinsufficient *Tfr2*^{LCKO} is indistinguishable from that of *Tfr2*^{LCKO} animals [Figure 2A]. The *Bmp6*/LIC ratio is comparable among all the genotypes analyzed proving that *Bmp6* expression is adequate to the hepatic iron content [Supplemental Figure 1].

As expected, *Hamp* [Figure 2B] is over-expressed in *Tmprss6*$^{-/-}$ mice while comparable to wt in both *Tfr2*$^{-/-}$ and *Tfr2*^{LCKO} mice. As a consequence the iron deficient *Tmprss6*$^{-/-}$ mice have a *Hamp*/LIC ratio

higher than wt animals, while both the iron-loaded *Tfr2* knock-out mice have a *Hamp*/LIC ratio lower than controls [Figure 2C].

In *Tmprss6*$^{-/-}$*Tfr2*$^{-/-}$ mice *Hamp* expression is higher than in wt mice, but lower than in *Tmprss6*$^{-/-}$ animals, while levels in *Tmprss6*$^{-/-}$ *Tfr2*^{LCKO} are comparable with those of *Tmprss6*$^{-/-}$ animals. This results in a *Hamp*/LIC ratio that in *Tmprss6*$^{-/-}$*Tfr2*$^{-/-}$ mice is higher than in controls, but lower than in *Tmprss6*$^{-/-}$, while the *Hamp*/LIC ratio of *Tmprss6*$^{-/-}$*Tfr2*^{LCKO} is comparable to that of *Tmprss6*$^{-/-}$ animals [Figure 2C]. The mRNA levels of Inhibitor of differentiation 1 (*Id1*), another target of the Bmp-Smad pathway, follow the same pattern of *Hamp* expression (Fig 2D), proving that in the double *Tmprss6*$^{-/-}$*Tfr2*$^{-/-}$ mice the Bmp-Smad pathway is more active than in wt mice, but less active than in *Tmprss6*$^{-/-}$ mice.

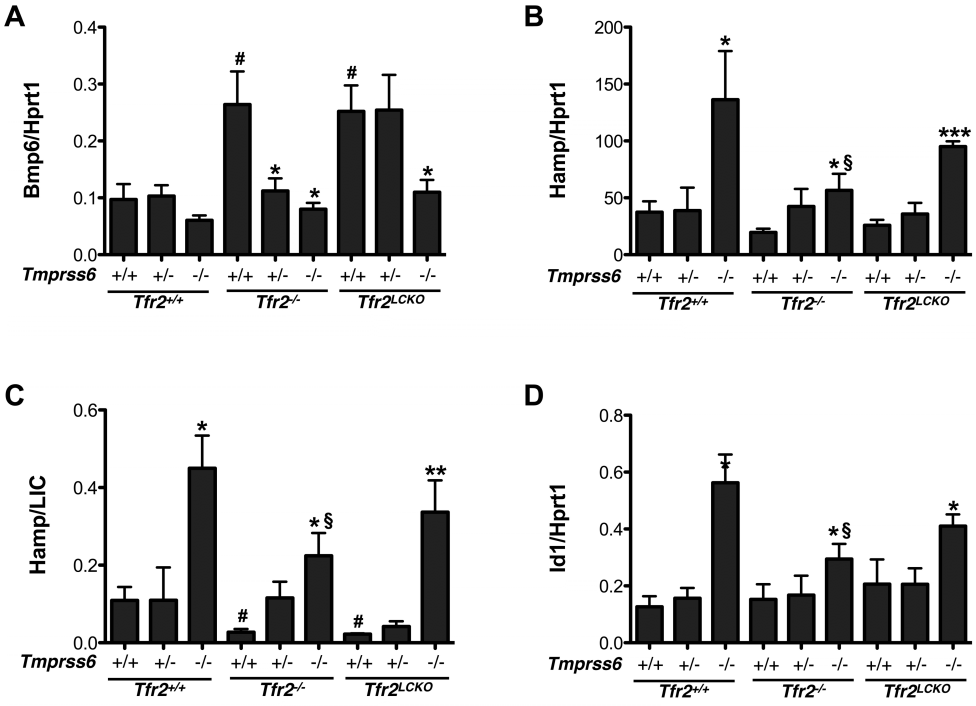

Figure 2: Effect of *Tmprss6* deletion on the Bmp-Smad pathway of *Tfr2*$^{-/-}$ and *Tfr2*^{LCKO} mice

In the figure are graphed liver mRNA expression of: Bone Morphogenetic Protein 6 (*Bmp6*; A); hepcidin (*Hamp*; B); *Hamp* normalized on LIC (*Hamp*/LIC; C) and inhibitor of DNA binding 1 (*Id1*; D) in all genotype combination analyzed. Mean values of 3-6 animals for genotype are graphed and error bars indicate standard deviation. Symbols refer to a statistically significant difference: *P<0.05, **P<0.01 and ***P<0.005 respective to the relative *Tmprss6*$^{+/+}$ control of each *Tfr2* genotype; # P<0.05 respective to wt (*Tmprss6*$^{+/+}$*Tfr2*$^{+/+}$) animals; § P<0.05 respective to *Tmprss6*$^{-/-}$ mice. For complete statistical analysis see Supplemental Table 2.

4. DISCUSSION

The analysis of animal models of *Tfr2*-hemochromatosis suggests that low hepcidin is due to an attenuated Bmp-Smad pathway. In theory TFR2 might promote BMP-SMAD signalling for hepcidin production by inhibiting the activity of TMPRSS6, as was hypothesized for

HFE[32], by up-regulating *BMP6* or through other unknown mechanisms. For this reason we analysed the effect of *Tmprss6* inactivation in mice with a total deletion of *Tfr2* (*Tfr2*$^{-/-}$) *versus* mice with specific ablation of *Tfr2* in the liver (*Tfr2*^{LCKO}). Since the latter maintain the Tfr2 function in other organs, the comparison of the phenotypes of the double KO animals may provide clues to the extra-hepatic functions of TFR2.

We found that in adult *Tfr2*$^{-/-}$ mice the heterozygous loss of *Tmprss6* slightly reduces the severity of hepatic iron overload and partially reverts the hematological phenotype, reducing the Hb levels. On the contrary *Tmprss6* haploinsufficiency does not correct the iron-overload phenotype of *Tfr2*^{LCKO} mice. This might be compatible with a more severe iron burden reported for the liver-specific KO[14,15], although in the present study, in which only males were examined, LIC was similar in *Tfr2*$^{-/-}$ and *Tfr2*^{LCKO}. Homozygous loss of *Tmprss6* led to systemic iron deficiency and severe anemia in both genotypes with low levels of Hb, TS and LIC and enhanced hepatic *Tfr1* expression, in analogy to what has been observed in *Hfe* KO mice with deletion of *Tmprss6*[32]. Similar results were also previously published in the *Tmprss6*$^{-/-}$*Tfr2*$^{-/-}$ mice[33], although differences of genetic backgrounds made the genotype comparison problematic.

The phenotype modification of *Tfr2*$^{-/-}$ and *Tfr2*^{LCKO} from iron overload to iron deficiency in the absence of *Tmprss6* demonstrates that TFR2 in the liver acts upstream the serine protease and might control its activity, thus raising the possibility that pharmacologic inhibition of TMPRSS6 is effective in limiting dietary iron absorption and

redistributing iron to macrophages in *TFR2*-Hemochromatosis, as shown for *HFE*-Hemochromatosis[34,35].

Loss of the protease activity of Tmprss6 led to increased expression of hepcidin in *Tfr2* iron loaded animals that explains reduced iron absorption and iron deficiency. However, in *Tmprss6*$^{-/-}$ mice with complete loss of *Tfr2* the hepatic mRNA levels of *Hamp* and *Id1*, although increased, do not reach the high levels observed in *Tmprss6*$^{-/-}$ mice. In contrast *Hamp* and *Id1* expression in *Tmprss6*$^{-/-}$*Tfr2*^{LCKO} are comparable to *Tmprss6*$^{-/-}$ mice. These differences are not mediated by an altered expression of *Bmp6* since *Bmp6* levels reflect the hepatic iron burden in all the genotypes analyzed. This appropriate regulation of *Bmp6* in *Tfr2*$^{-/-}$ animals indicates that Tfr2 is not required for adequate *Bmp6* response to increased tissue iron, a finding discordant from recent report of *Bmp6* being inappropriately low in *Tfr2*$^{-/-}$ mice[36]. Based on our results we speculate that in *Tmprss6*$^{-/-}$*Tfr2*$^{-/-}$ mice an inhibitory signal partially affects the efficiency of the Bmp-Smad pathway downstream Bmp6 leading to a lower than expected hepcidin activation.

Since inhibition of hepcidin is largely dependent on erythropoietic signals we analyzed the hematological phenotype of our models. The functional loss of both Tmprss6 and Tfr2 in the whole organism is associated with the same degree of iron deficiency of *Tmprss6*$^{-/-}$. However, as compared to mice lacking *Tmprss6* alone, *Tmprss6*$^{-/-}$*Tfr2*$^{-/-}$ mice showed a consistent increase of red cell number and hematocrit, that was not observed when *Tfr2* was specifically deleted in the liver. This observation strengthens that the hematologic

phenotype of *Tmprss6*$^{-/-}$*Tfr2*$^{-/-}$ is dependent on the lack of a still unknown extra-hepatic function of Tfr2.

We speculate that the loss of *Tfr2* in the erythroid compartment accounts for the increased red cells number observed in *Tmprss6*$^{-/-}$ *Tfr2*$^{-/-}$ mice and that erythropoiesis expansion is responsible for the partial inhibition of the Bmp-Smad pathway exclusively observed in these double mutant mice.

The iron-loaded *Tfr2*$^{-/-}$ mice are not characterized by increased RBCs count but have increased Hb ([15] and this paper) as compared with *Tfr2*^{LCKO}, indicating a deregulated erythropoiesis. Indeed, normal Hb in the iron-loaded *Tfr2*^{LCKO} mice points out that the high Hb levels observed in *Tfr2*$^{-/-}$ animals are not only due to their elevated iron burden, but to some other factors likely related to the absence of *Tfr2* in the erythroid compartment.

In the attempt to verify whether the high RBCs count of *Tmprss6*$^{-/-}$ *Tfr2*$^{-/-}$ mice was due to increased Epo levels, we measured serum Epo in all the models. Since *Tmprss6*$^{-/-}$, *Tmprss6*$^{-/-}$*Tfr2*$^{-/-}$ and *Tmprss6*$^{-/-}$ *Tfr2*^{LCKO} mice, which have the same degree of anemia, have comparable serum Epo levels we conclude that erythroid precursors lacking *Tfr2* might have an enhanced sensitivity to Epo stimulation. Our data seem discrepant with those reported by Foretnikova et al (16), who found increased serum Epo level in *Tfr2*$^{-/-}$ mice as compared with *Tfr2*^{LCKO}. However, the latter results were obtained in young animals (4 weeks of age), while our data refer to adult 10 week-old mice. It is of interest that the same Authors observed that *TFR2*-knockdown in human erythroid precursors led to a slight increase of total cell number after 12 days of cell culture.

In conclusion we propose that TFR2 is a modulator of erythropoiesis in keeping with its function as an EPOR partner. It is possible that TFR2, as an iron sensor, modulates the EPO sensitivity of the erythroid precursors. The increased red cell number might be the result of this function in iron-deficient *Tmprss6*$^{-/-}$*Tfr2*$^{-/-}$ animals. More specifically, since the iron-loaded *Tfr2*$^{-/-}$ mice are not characterized by an increased RBCs count, we propose that TFR2 is a limiting factor for erythropoiesis, that controls red cell number to avoid excessive production in conditions of iron-restriction. Further studies in mice with specific erythroid deletion of *Tfr2* will clarify this possibility.

5. SUPPLEMENTARY INFORMATIONS

5.1 SUPPLEMENTARY TABLE AND FIGURES

Name	Id
Hprt1	Mm01318743_m1
Hamp	Mm00519025_m1
Bmp6	Mm01332882_m1
Id1	Mm00775963_g1
Tfr1	Mm00441941_m1

Supplemental Table 1. Oligonucleotide primers (Applied Biosystem) used for qRT-PCR by TaqMan

	WBC	RBC	Ret	Hb	Hct	MCV	MCH	TS	LIC	Tfr1	SIC	EPO	Bmp6	Hamp	Hamp/LIC	Id1	Bmp6/LIC
Tmprss6$^{+/-}$ vs wt	ns	ns	ns	ns	ns	**	ns	ns	ns	ns	ns	ns	ns	ns	ns	ns	ns
Tmprss6$^{-/-}$ vs wt	ns	*	*	**	**	**	**	*	*	*	ns	*	ns	*	*	*	ns
Tfr2$^{-/-}$ vs wt	ns	ns	ns	*	*	ns	ns	*	*	ns	ns	ns	*	ns	*	ns	ns
Tmprss6$^{+/-}$*Tfr2*$^{-/-}$ vs wt	ns	ns	ns	*	ns	ns	ns	ns	ns	ns	ns	ns	ns	ns	ns	ns	ns
Tmprss6$^{-/-}$*Tfr2*$^{-/-}$ vs wt	ns	**	*	**	*	**	**	*	*	*	ns	*	ns	*	*	*	ns
Tfr2^{LCKO} vs wt	ns	ns	ns	ns	ns	ns	ns	*	*	ns	ns	ns	*	ns	*	ns	ns
Tmprss6$^{+/-}$*Tfr2*^{LCKO} vs wt	ns	ns	ns	*	ns	ns	ns	ns	*	ns	ns	ns	*	ns	*	ns	ns
Tmprss6$^{-/-}$*Tfr2*^{LCKO} vs wt	ns	*	*	**	**	**	**	**	*	*	ns	*	ns	**	*	*	ns
Tmprss6$^{-/-}$ vs *Tmprss6*$^{+/-}$	ns	*	**	**	**	**	**	*	*	ns	ns	*	ns	*	*	*	ns
Tfr2$^{-/-}$ vs *Tmprss6*$^{+/-}$	ns	ns	ns	*	ns	**	**	*	*	*	ns	ns	*	ns	*	ns	ns
Tmprss6$^{+/-}$*Tfr2*$^{-/-}$ vs *Tmprss6*$^{+/-}$	ns	ns	ns	*	ns	**	**	ns	*	ns	ns	ns	ns	ns	ns	ns	ns
Tmprss6$^{-/-}$*Tfr2*$^{-/-}$ vs *Tmprss6*$^{+/-}$	ns	**	**	**	*	**	**	*	*	*	ns	*	ns	ns	*	*	ns
Tfr2^{LCKO} vs *Tmprss6*$^{+/-}$	ns	ns	ns	ns	ns	ns	ns	*	*	ns	ns	ns	*	ns	*	ns	ns
Tmprss6$^{+/-}$*Tfr2*^{LCKO} vs *Tmprss6*$^{+/-}$	ns	ns	ns	*	ns	ns	ns	ns	*	ns	ns	ns	*	ns	*	ns	ns
Tmprss6$^{-/-}$*Tfr2*^{LCKO} vs *Tmprss6*$^{+/-}$	ns	*	*	**	**	**	**	**	*	ns	ns	*	ns	*	*	*	ns
Tfr2$^{-/-}$ vs *Tmprss6*$^{-/-}$	ns	*	*	**	**	**	**	**	**	*	ns	*	*	**	**	*	ns
Tmprss6+/-Tfr2-/- vs Tmprss6-/-	ns	*	*	**	**	**	**	*	*	ns	ns	*	ns	*	*	*	ns
Tmprss6-/-Tfr2-/- vs Tmprss6-/-	ns	*	*	ns	ns	*	*	ns	ns	ns	ns	ns	ns	*	*	*	ns
Tfr2LCKO vs Tmprss6-/-	ns	*	*	**	**	**	**	**	**	*	ns	**	*	**	**	*	ns
Tmprss6+/-Tfr2^{LCKO} *vs Tmprss6-/-*	ns	*	*	**	**	**	**	*	*	ns	ns	**	*	**	*	*	ns
Tmprss6-/-Tfr2^{LCKO} *vs Tmprss6-/-*	ns	ns	ns	ns	ns	ns	ns	ns	ns	ns	ns	ns	ns	ns	ns	ns	ns

	WBC	RBC	Ret	Hb	Hct	MCV	MCH	TS	LIC	Tfr1	SIC	EPO	Bmp6	Hamp	Hamp/LIC	Id1	Bmp6/LIC
Tmprss6$^{+/-}$*Tfr2*$^{-/-}$ vs *Tfr2*$^{-/-}$	ns	ns	ns	ns	ns	ns	ns	*	*	ns	ns	ns	*	ns	*	ns	ns
Tmprss6$^{-/-}$*Tfr2*$^{-/-}$ vs *Tfr2*$^{-/-}$	ns	**	*	**	*	**	**	*	*	*	ns	*	*	*	*	*	ns
Tfr2^{LCKO} vs *Tfr2*$^{-/-}$	ns	ns	ns	*	ns	ns	**	ns	ns	ns	ns	ns	ns	ns	ns	ns	ns
Tmprss6$^{+/-}$*Tfr2*^{LCKO} vs *Tfr2*$^{-/-}$	ns	ns	ns	ns	ns	ns	**	ns	ns	ns	ns	ns	ns	ns	ns	ns	ns
Tmprss6$^{-/-}$*Tfr2*^{LCKO} vs *Tfr2*$^{-/-}$	ns	*	*	**	**	**	**	**	**	*	ns	*	*	**	*	*	ns
Tmprss6$^{-/-}$*Tfr2*$^{-/-}$ vs *Tmprss6*$^{+/-}$*Tfr2*$^{-/-}$	ns	**	*	**	*	**	**	*	*	ns	ns	*	ns	ns	*	*	ns
Tfr2^{LCKO} vs *Tmprss6*$^{+/-}$ *Tfr2*$^{-/-}$	ns	ns	ns	*	ns	ns	*	ns	*	ns	ns	ns	*	ns	*	ns	ns
Tmprss6$^{+/-}$*Tfr2*^{LCKO} vs *Tmprss6*$^{+/-}$*Tfr2*$^{-/-}$	ns	ns	ns	ns	ns	ns	*	ns	*	ns	ns	ns	*	ns	*	ns	ns
Tmprss6$^{-/-}$*Tfr2*^{LCKO} vs *Tmprss6*$^{+/-}$*Tfr2*$^{-/-}$	ns	*	*	**	**	**	**	*	*	ns	ns	*	ns	*	*	*	ns
Tfr2^{LCKO} vs *Tmprss6*$^{-/-}$ *Tfr2*$^{-/-}$	ns	**	**	**	*	**	**	**	**	*	ns	*	*	*	*	*	ns
Tmprss6$^{+/-}$*Tfr2*^{LCKO} vs *Tmprss6*$^{-/-}$*Tfr2*$^{-/-}$	ns	**	**	**	*	**	**	**	*	ns	ns	*	*	ns	*	*	ns
Tmprss6$^{-/-}$*Tfr2*^{LCKO} vs *Tmprss6*$^{-/-}$*Tfr2*$^{-/-}$	ns	*	ns	ns	*	*	*	ns	ns	ns	ns	ns	ns	*	*	*	ns
Tmprss6$^{+/-}$*Tfr2*^{LCKO} vs *Tfr2*^{LCKO}	ns	ns	ns	*	ns	ns	ns	ns	ns	ns	ns	ns	ns	ns	ns	ns	ns
Tmprss6$^{-/-}$*Tfr2*^{LCKO} vs *Tfr2*^{LCKO}	ns	*	**	**	**	**	**	**	**	*	ns	*	*	**	*	*	ns
Tmprss6$^{-/-}$*Tfr2*^{LCKO} vs *Tmprss6*$^{+/-}$*Tfr2*^{LCKO}	ns	*	**	**	**	**	**	**	**	ns	ns	ns	*	**	*	*	ns

Supplemental Table 2. Evaluation of statistical significant differences through t-test analysis

Complete list of the P-values referred to Table 1 and Figure 1, 2 and supplemental Figure 1. Asterisks refer to a statistically significant difference. **P*<0.05; ***P*<0.005; ns= not significant. WBC= White Blood Cells; RBC= Red Blood Cells; Ret= reticulocytes; Hb= Hemoglobin; Hct= Hematocrit; MCV= Mean Corpuscolar Volume; MCH= Mean Corpuscolar Hemoglobin; TS= Transferrin Saturation; LIC=

Liver Iron Content; *Tfr1*= mRNA expression of Transferrin Receptor 1; SIC= Spleen Iron Content; EPO= erythropoietin; *Bmp6*= mRNA expression of Bone Morphogenetic Protein 6; *Hamp*= mRNA expression of Hepcidin; *Hamp*/LIC= Hepcidin/Liver Iron Content ratio; *Id1*= mRNA expression of Inhibitor of DNA binding 1; *Bmp6*/LIC= Bone Morphogenetic Protein 6/Liver Iron Content ratio.

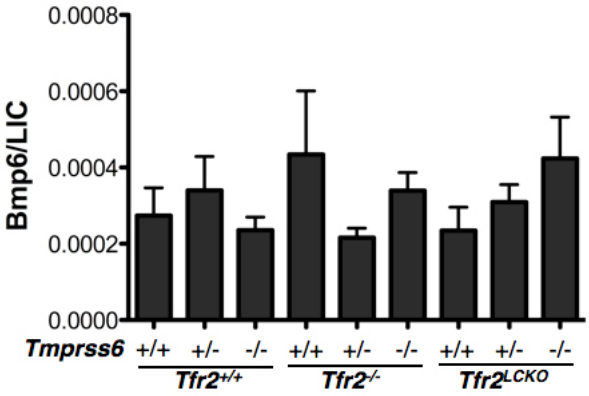

Figure S1. Normalization of *Bmp6* mRNA on the Liver Iron Content (LIC)
In the figure is graphed the hepatic expression of *Bmp6* normalized on the levels of Liver Iron Content (LIC). Mean Values of 3-6 animals for genotype are graphed and error bars indicate standard deviation.

ACKNOWLEDGMENTS

We acknowledge Prof. Carlos Lopez-Otin (Oviedo University, Spain) for releasing us *Tmprss6*$^{-/-}$ mouse.

REFERENCES

1. Camaschella C, Roetto A, Cali A, De Gobbi M, Garozzo G, Carella M, et al. The gene TFR2 is mutated in a new type of haemochromatosis mapping to 7q22. Nature genetics. 2000;25(1):14-5.
2. Roetto A, Totaro A, Piperno A, Piga A, Longo F, Garozzo G, et al. New mutations inactivating transferrin receptor 2 in hemochromatosis type 3. Blood. 2001;97(9):2555-60.
3. Kawabata H, Yang R, Hirama T, Vuong PT, Kawano S, Gombart AF, et al. Molecular cloning of transferrin receptor 2. A new member of the transferrin receptor-like family. The Journal of biological chemistry. 1999;274(30):20826-32.
4. Kawabata H, Germain RS, Ikezoe T, Tong X, Green EM, Gombart AF, et al. Regulation of expression of murine transferrin receptor 2. Blood. 2001;98(6):1949-54.

5. Johnson MB, Chen J, Murchison N, Green FA, Enns CA. Transferrin receptor 2: evidence for ligand-induced stabilization and redirection to a recycling pathway. Molecular biology of the cell. 2007;18(3):743-54.
6. Goswami T, Andrews NC. Hereditary hemochromatosis protein, HFE, interaction with transferrin receptor 2 suggests a molecular mechanism for mammalian iron sensing. The Journal of biological chemistry. 2006;281(39):28494-8.
7. Gao J, Chen J, Kramer M, Tsukamoto H, Zhang AS, Enns CA. Interaction of the hereditary hemochromatosis protein HFE with transferrin receptor 2 is required for transferrin-induced hepcidin expression. Cell metabolism. 2009;9(3):217-27.
8. Camaschella C. Understanding iron homeostasis through genetic analysis of hemochromatosis and related disorders. Blood. 2005;106(12):3710-7.
9. Rishi G, Crampton EM, Wallace DF, Subramaniam VN. In situ proximity ligation assays indicate that hemochromatosis proteins Hfe and transferrin receptor 2 (Tfr2) do not interact. PloS one. 2013;8(10):e77267.
10. Nemeth E, Tuttle MS, Powelson J, Vaughn MB, Donovan A, Ward DM, et al. Hepcidin regulates cellular iron efflux by binding to ferroportin and inducing its internalization. Science. 2004;306(5704):2090-3.
11. Meynard D, Kautz L, Darnaud V, Canonne-Hergaux F, Coppin H, Roth MP. Lack of the bone morphogenetic protein BMP6 induces massive iron overload. Nature genetics. 2009 Apr;41(4):478-81.
12. Andriopoulos B, Jr., Corradini E, Xia Y, Faasse SA, Chen S, Grgurevic L, et al. BMP6 is a key endogenous regulator of hepcidin expression and iron metabolism. Nature genetics. 2009;41(4):482-7.
13. D'Alessio F, Hentze MW, Muckenthaler MU. The hemochromatosis proteins HFE, TfR2, and HJV form a membrane-associated protein complex for hepcidin regulation. Journal of hepatology. 2012;57(5):1052-60.
14. Wallace DF, Summerville L, Subramaniam VN. Targeted disruption of the hepatic transferrin receptor 2 gene in mice leads to iron overload. Gastroenterology. 2007;132(1):301-10.
15. Roetto A, Di Cunto F, Pellegrino RM, Hirsch E, Azzolino O, Bondi A, et al. Comparison of 3 Tfr2-deficient murine models suggests distinct functions for Tfr2-alpha and Tfr2-beta isoforms in different tissues. Blood. 2010;115(16):3382-9.
16. Forejtnikova H, Vieillevoye M, Zermati Y, Lambert M, Pellegrino RM, Guihard S, et al. Transferrin receptor 2 is a component of the erythropoietin receptor complex and is required for efficient erythropoiesis. Blood. 2010;116(24):5357-67.
17. Silvestri L, Pagani A, Nai A, De Domenico I, Kaplan J, Camaschella C. The serine protease matriptase-2 (TMPRSS6) inhibits hepcidin activation by cleaving membrane hemojuvelin. Cell metabolism. 2008;8(6):502-11.
18. Finberg KE, Heeney MM, Campagna DR, Aydinok Y, Pearson HA, Hartman KR, et al. Mutations in TMPRSS6 cause iron-refractory iron deficiency anemia (IRIDA). Nature genetics. 2008;40(5):569-71.
19. Du X, She E, Gelbart T, Truksa J, Lee P, Xia Y, et al. The serine protease TMPRSS6 is required to sense iron deficiency. Science. 2008;320(5879):1088-92.
20. Folgueras AR, de Lara FM, Pendas AM, Garabaya C, Rodriguez F, Astudillo A, et al. Membrane-bound serine protease matriptase-2 (Tmprss6) is an essential regulator of iron homeostasis. Blood. 2008;112(6):2539-45.

21. Hershko C, Camaschella C. How I treat unexplained refractory iron deficiency anemia. Blood. 2014;123(3):326-33.
22. Benyamin B, Ferreira MA, Willemsen G, Gordon S, Middelberg RP, McEvoy BP, et al. Common variants in TMPRSS6 are associated with iron status and erythrocyte volume. Nat Genet. 2009;41(11):1173-5.
23. Ganesh SK, Zakai NA, van Rooij FJ, Soranzo N, Smith AV, Nalls MA, et al. Multiple loci influence erythrocyte phenotypes in the CHARGE Consortium. Nat Genet. 2009;41(11):1191-8.
24. Chambers JC, Zhang W, Li Y, Sehmi J, Wass MN, Zabaneh D, et al. Genome-wide association study identifies variants in TMPRSS6 associated with hemoglobin levels. Nat Genet. 2009;41(11):1170-2.
25. Soranzo N, Spector TD, Mangino M, Kuhnel B, Rendon A, Teumer A, et al. A genome-wide meta-analysis identifies 22 loci associated with eight hematological parameters in the HaemGen consortium. Nature genetics. 2009;41(11):1182-90.
26. Tanaka T, Roy CN, Yao W, Matteini A, Semba RD, Arking D, et al. A genome-wide association analysis of serum iron concentrations. Blood. 2010;115(1):94-6.
27. Traglia M, Girelli D, Biino G, Campostrini N, Corbella M, Sala C, et al. Association of HFE and TMPRSS6 genetic variants with iron and erythrocyte parameters is only in part dependent on serum hepcidin concentrations. J Med Genet. 2011;48(9):629-34.
28. Nai A, Pagani A, Silvestri L, Camaschella C. Increased susceptibility to iron deficiency of Tmprss6-haploinsufficient mice. Blood. 2010;116(5):851-2.
29. Nai A, Pagani A, Silvestri L, Campostrini N, Corbella M, Girelli D, et al. TMPRSS6 rs855791 modulates hepcidin transcription in vitro and serum hepcidin levels in normal individuals. Blood. 2011;118(16):4459-62.
30. Maurer E, Gutschow M, Stirnberg M. Matriptase-2 (TMPRSS6) is directly up-regulated by hypoxia inducible factor-1: identification of a hypoxia-responsive element in the TMPRSS6 promoter region. Biological chemistry. 2012;393(6):535-40.
31. Meynard D, Vaja V, Sun CC, Corradini E, Chen S, Lopez-Otin C, et al. Regulation of TMPRSS6 by BMP6 and iron in human cells and mice. Blood. 2011;118(3):747-56.
32. Finberg KE, Whittlesey RL, Andrews NC. Tmprss6 is a genetic modifier of the Hfe-hemochromatosis phenotype in mice. Blood. 2011;117(17):4590-9.
33. Lee P, Hsu MH, Welser-Alves J, Peng H. Severe microcytic anemia but increased erythropoiesis in mice lacking Hfe or Tfr2 and Tmprss6. Blood cells, molecules & diseases. 2012;48(3):173-8.
34. Schmidt PJ, Toudjarska I, Sendamarai AK, Racie T, Milstein S, Bettencourt BR, et al. An RNAi therapeutic targeting Tmprss6 decreases iron overload in Hfe(-/-) mice and ameliorates anemia and iron overload in murine beta-thalassemia intermedia. Blood. 2013;121(7):1200-8.
35. Guo S, Casu C, Gardenghi S, Booten S, Aghajan M, Peralta R, et al. Reducing TMPRSS6 ameliorates hemochromatosis and beta-thalassemia in mice. The Journal of clinical investigation. 2013;123(4):1531-41.

36. McDonald CJ, Wallace DF, Ostini L, Subramaniam VN. Parenteral vs oral iron: Influence on hepcidin signaling pathways though analysis of Hfe/Tfr2 null mice. American journal of physiology Gastrointestinal and liver physiology. 2014;306(2):G132-9.

CHAPTER 5

Summary, conclusions and future perspectives

During my PhD I focused my research on iron metabolism in mammals and in particular on the regulation of the liver hormone hepcidin, which has the fundamental role to control iron absorption and iron recycling. Hepcidin expression is finely tuned by different mechanisms of activation and inhibition. The project I developed in collaboration had the aim to better characterize the role and the activity of the hepcidin inhibitor, the serine protease TMPRSS6, in relation to other molecules involved in the hormone regulation. In particular we investigated the functional correlation between TMPRSS6 and HJV (the BMP coreceptor), BMP6 (the BMP involved in tissue iron-mediated hepcidin upregulation) and TFR2 (a

transmembrane protein involved in sensing circulating iron) by using *in vitro* and/or *in vivo* approaches.

Hepcidin is tightly regulated and alterations of its regulatory pathway may cause genetic iron overload or iron deficiency, interfering with either activation or inhibition, respectively. Genes inactivation causes disease through the imbalance between hepcidin up- and down-regulation.

In normal iron homeostasis the iron-dependent hepcidin activation in the liver responds to two signals. Increased iron stores activate the BMP-SMAD pathway through BMP6, whereas Tf-bound circulating iron activates hepcidin through the competitive interaction of Tf with TFR1 or TFR2, with the involvement of the hemochromatosis protein HFE [1]. The role of TMPRSS6 in iron deficiency is well established because its inactivation in mice and humans causes iron deficiency due to excessive hepcidin synthesis. However, the modalities of TMPRSS6 cleavage and its regulation and role in basal hepcidin activation remain poorly defined.

1. Analysis of the cleavage activity of TMPRSS6

The BMP-SMAD pathway is central also to hepcidin inhibition because it is the target of TMPRSS6. *In vitro* the serine protease cleaves HJV into distinct soluble fragments [2]. One HJV cleavage site was previously identified [3] as R288, but since the cotransfection of TMPRSS6 and HJV causes the release of 3 distinct fragments [2] (Chapter 2- Figure 1B and Figure 3), in this thesis it has been applied a systematic approach to identify other potential cleavage sites by extensive mutagenesis of HJV arginines. By comparing the size of the

fragments released by selected HJV mutants and appropriate antibodies, we demonstrate that TMPRSS6 cleaves HJV at two sites: R121 and R326 in the N- and the C-terminal part of the protein, respectively. We were able to define that the 3 fragments identified in the culture media [2,4] derive from both membrane-bound HJV: the full length isoform and the heterodimeric one. However, this is an *in vitro* observation and whether the same process occurs *in vivo* and which forms are prevalent remain to be understood. In the attempt to reconcile our data with those previously reported that identified R288 as cleavage site, we noticed that "A" fragment (Chapter 2- Figure 3) might corresponds to the 36 kDa fragment in the paper of Maxson et al. [3], because HJV^{R288A} does not release this fragment after TMPRSS6 activity in both studies. However, since we observed that substitutions other than 288A (i.e. 176A and 218A) (Chapter 2- Table 1) impair TMPRSS6 cleavage activity on HJV, we exploited an *in silico* approach to investigate whether the cleavage by TMPRSS6 could be indirectly affected by an altered HJV protein stabilization. The molecular dynamics simulation performed allowed us to define that the altered pattern or lack of fragments in the medium was likely due to HJV protein destabilization rather than to modification of the cleavage target residues at position 176 and 218. This is not true for the 288 residue; we observed that R288 is highly conserved among species and that missense mutation to tryptophan (R288W) causes a severe form of hemochromatosis [5]. In addition, it is also partially defective in membrane targeting (Chapter 2- Figure 2), highlighting the relevance of this residue for HJV processing and function.

Another issue that remains unsolved and should be further

investigated is whether or not the cleaved HJV fragments have functional relevance. Reasonably they should have some regulatory effect on hepcidin since at least one of them, the 30 kDa "A" fragment from residue 121 to 326, shares consistent sequence identity with s-HJV (amino acids 33-335). Released by furin cleavage [6], s-HJV has a documented effect on hepcidin transcription, acting as a decoy molecule by sequestering BMPs thus downregulating the BMP-SMAD signalling [7,8,9]. We speculate that "A" fragment might share a similar role to strengthen the signalling inhibition. In conclusion our hypothesis is that TMPRSS6, by cleaving m-HJV, has a dual effect: it reduces the GPI-anchored BMP coreceptor on the cell surface and at the same time it releases soluble fragments that would act as decoy molecules to further optimize and support the inhibitory activity.

HJV has been identified as a substrate of TMPRSS6 by *in vitro* studies. The formal proof that it is cleaved by TMPRSS6 *in vivo* is still lacking. In agreement with our *in vitro* results, inactivation of *Hjv* in *Tmprss6*$^{-/-}$ mice completely reverted the iron deficiency phenotype thus causing iron overload with low hepcidin, a phenotype indistinguishable from the *Hjv*$^{-/-}$ mice. This indicates that *Hjv* is genetically downstream *Tmprss6* and confirms that the cleavage activity of Tmprss6 needs a functional BMP-SMAD pathway [10]. In contrast with HJV being the TMPRSS6 substrate, it has been reported that Hjv protein levels are not increased and even reduced on the hepatocytes membrane of *Tmprss6*$^{-/-}$ mice, opposite to what is expected due to the absence of the serine protease [11,12]. Nevertheless, the activation of the BMP-SMAD pathway is strictly correlated to the endocytosis of BMP receptors from the cell

membrane [13,14] suggesting the possibility that the Hjv decrease in *Tmprss6*$^{-/-}$ hepatocytes could be due to an over-activation of the BMP-SMAD signalling. Whether TMPRSS6 has other substrates is a matter of investigation: *in vitro* its serine protease domain is able to hydrolyze different synthetic substrates, such as type I collagen, fibronectin and fibrinogen [15]. Recently, Fetuin A has been proposed as TMPRSS6 substrate because it is cleaved by the serine protease *in vitro* [16]. Fetuin A is a liver glycoprotein secreted in the serum with a modest activity on hepcidin both *in vitro* and *in viv*o. In the view of better clarifying whether HJV is actually the serine protease substrate our work is important. We have shown that R121 and R326 are cleavage sites, and that single HJV^{R121A} and HJV^{R326A} mutants are able to reach the cell surface as HJV^{WT} (Chapter 2- Figure 2) and both mutants partially retain the ability to activate hepcidin (Chapter 2- Figure 7). Therefore we should be able to generate a functional double HJV$^{R121A\text{-}R326A}$ mutant, unable to be cleaved by TMPRSS6. This variant should be used to generate transgenic mice expressing in the liver both the wild type and the mutant isoform of HJV. Since Tmprss6 activity is higher in conditions of iron deficiency and hypoxia [17,18], if HJV is the substrate of Tmprss6, the expression of hepcidin in mice injected with the TMPRSS6-HJV resistant variant will be higher compared to mice transgenic for the wild type form of HJV in conditions of iron deficiency/hypoxia.

2. *In vivo* studies of Bmp6 regulation: insights from the *Tmprss6* $^{-/-}$ model

We exploited the availability of *Tmprss6*$^{-/-}$ mice to better characterize the modalities of *Bmp6* expression in the liver. BMP6 is a member of the TGF-beta superfamily and it is mainly synthesised and released by the liver in response to iron [19]. The other BMPs do not have redundant activity, since *Bmp6* deficient mice are iron overloaded due to low BMP-SMAD dependent hepcidin activation [20] and the other BMPs can not compensate for the absence of Bmp6, thus pointing to Bmp6 as a key molecule in response to iron increase. However, how *Bmp6* is upregulated by iron and which liver cell subpopulations are involved in this process are still open questions. Liver non parenchymal cells (NPCs) were reported to express higher *Bmp6* than hepatocytes (HCs), suggesting they may have an important role in hepcidin regulation [17,21].

We show that in mice fed an iron rich or iron deficient diet for three weeks there is a direct correlation between iron content of HCs, liver sinusoidal endothelial cells (LSECs) and Kupffer cells (KCs) and their corresponding *Bmp6* expression (Chapter 3- Figure 2). Upregulation of *Bmp6* is inversely correlated with *Tfr1* mRNA levels that we used as an indirect measure of the iron status. The disease model of iron deficiency *Tmprss6*$^{-/-}$ was especially informative to clarify *Bmp6* regulation. Indeed *Tmprss6*$^{-/-}$ (like the opposite hemochromatosis model *Hjv*$^{-/-}$) dissociates *Bmp6* expression from hepcidin response. Homozygous *Tmprss6* loss causes inappropriately high hepcidin levels due to constitutively activation of hepcidin promoter and low *Bmp6* due to low liver iron concentration while homozygous *Hjv* loss

causes the opposite phenotype: low hepcidin with high *Bmp6* because of liver iron loading. The correlation between iron and *Bmp6* observed in animals whose iron status was modulated by chronic diets is maintained in hepatocytes of *Tmprss6* deficient mice but is lost in NPCs. These cells are expected to be iron poor because of the severe iron deficiency due to *Tmprss6* inactivation. Indeed *Bmp6* expression is low, but surprisingly, NPCs, at difference with HCs, appear iron replete (Chapter 3- Figure 5). This effect is probably due to the high hepcidin level that favours NPCs iron retention through ferroportin degradation. Iron sequestration does not occur in HCs, since their low surface ferroportin makes these cells less sensitive to the hepcidin effect. The opposite condition occurs in $Hjv^{-/-}$ model: HCs have high iron content whereas KCs and LSECs appear iron poor; nevertheless, *Bmp6* is upregulated in all the liver cell types from the $Hjv^{-/-}$ mice (Chapter 3- Figure 4). In this case low hepcidin levels cause iron efflux from NPCs.

The $Tmprss6^{-/-}$ and the $Hjv^{-/-}$ mice models helped to uncover a mechanisms of *Bmp6* crosstalk among liver cell populations suggesting that liver *Bmp6* upregulation is not directly mediated by increased iron stores. Although HCs may increase *Bmp6* in response to elevated iron concentrations, the first event involves the NPCs likely because they are in direct contact with the bloodstream. NPCs activate *Bmp6* in response to their iron influx and induce hepcidin by a paracrine mechanism. In a second step hepcidin controls the amount of iron retained within the NPCs. We have defined that hepcidin is regulated by a paracrine mechanism through NPCs *Bmp6*. This controls systemic iron homeostasis but also promote NPCs iron

retention/release as a protective mechanism towards HCs iron excess/deficiency. This mechanism is lost in disease models of hepcidin deregulation, in particular in *Tmprs6*$^{-/-}$ mice since HCs are iron deficient but NPCs retain iron, because of the high hepcidin levels.

3. *Tmprss6*$^{-/-}$, a useful model to define the hierarchy of molecule involved in hepcidin expression

Inactivation of *TMPRSS6* in humans [22] and mice [23,24] leads to inappropriately high hepcidin expression, lower plasma iron levels and causes a genetic disease defined "Iron refractory iron deficiency anemia" (IRIDA, OMIM #206200). Different murine models of iron overload have been crossed with *Tmprss6* deficient mice to obtain double knock out animals that have been important in order to clarify the hierarchy of the proteins involved in activation and inhibition of the hepcidin signalling pathway. *Tmprss6* is genetically upstream *Bmp6* and *Hjv* since double knockout mice for *Tmprss6* and *Bmp6* have the same iron overload phenotype of *Bmp6*$^{-/-}$ [25] and *Hjv-Tmprss6* deficient mice behave as the *Hjv* deficient animals [10]. These studies prove that the serine protease needs an active BMP-SMAD pathway to inhibit hepcidin. Indeed in the double mutant animals low hepcidin stabilizes ferroportin and increase iron release from the enterocytes and the stores, thus reverting the IRIDA phenotype. On the contrary double knockout mice for *Tmprss6* and *Hfe* have an IRIDA-like phenotype, excluding that HFE is a TMPRSS6 substrate and indicating that genetically it acts upstream of *TMPRSS6*. Moreover it also indicates that targeted inhibition of

TMPRSS6 can ameliorate the phenotype of HFE-hemochromatosis [26,27]. To evaluate whether Tmprss6 is implicated in the modulation of the Tfr2-dependent hepcidin expression, we generated two different double knock-out mice: the total *Tfr2*$^{-/-}$*Tmprss6*$^{-/-}$ and the liver-specific *Tfr2* knockout (*Tfr2*^{LCKO}) *Tmprss6*$^{-/-}$ mice. We show that the phenotype of *Tfr2*$^{-/-}$*Tmprss6*$^{-/-}$ mice is similar to that of the *Hfe*$^{-/-}$ *Tmprss6*$^{-/-}$ animals, since loss of *Tmprss6* results in systemic iron deficiency, characterized by low levels of hemoglobin, transferrin saturation and liver iron concentration, because of high hepcidin expression (Chapter 4- Figure 1-2).

Moreover the two models we generated are not identical since *Tfr2*$^{-/-}$ *Tmprss6*$^{-/-}$ animals have a consistent increase in red cell number and hematocrit, findings that are not observed in mice lacking *Tmprss6* alone or in combination with specific liver Tfr2 inactivation. Since TFR2 is expressed in liver and erythroid cells, these observations opened a new research line related to the erythroid role of Tfr2, to be further explored in a paper under evaluation.

4. Potential translational application: Tmprss6 as a potential therapeutic target for correction of iron diseases

There is increasing interest in manipulating the hepcidin pathway for therapy, both to increase hepcidin in disorders due to its inefficient production and to inhibit hepcidin expression in conditions of excessive synthesis as in inflammation. Inactivation of Tmprss6 in primary (*Hfe*$^{-/-}$ and *Tfr2*$^{-/-}$) or secondary (*Hbb*$^{th3/+}$) iron overload disorders provided the formal proof that modulation of Tmprss6 could be used to prevent or ameliorate iron overload through hepcidin

upregulation in pathological conditions characterized by inappropriately low hepcidin [26,27,28]. Inactivation of Tmprss6 by short interfering RNA [29] and anti-sense oligonucleotides [30] successfully increased hepcidin and improved anemia in *Hbb*$^{th3/+}$ mice. The same strategy has been shown to prevent iron overload in *Hfe*$^{-/-}$ mice, a model of type I hemochromatosis, even in adult animals. Our results on the *Tfr2*$^{-/-}$*Tmprss6*$^{-/-}$ mice indicate that this would be the case also in type III hemochromatosis due to inactivation of *Tfr2*. These studies have opened the possibility of developing new therapeutic strategy for primary and secondary iron overload in humans, in the latter cases leading also to a partial correction of anemia. It is conceivable that the therapeutic effect results from the increased hepcidin expression and not from the direct silencing of the serine protease [31].

To this aim it would be important to define whether the HJV fragments released by TMPRSS6 may have potential effect in decreasing the activation of the pathway, that could be exploited for therapy.

Hepcidin is upregulated during inflammation by IL6-IL6 receptor interaction and STAT3 signalling [32,33]: however this pathway requires the integrity of the BMP-SMAD pathway for a full hepcidin response [34]. In theory the activation of TMPRSS6 in inflammation might decrease the efficiency of the BMP-SMAD signalling, by inhibiting the antinflammatory response mediated by hepcidin increase. It has been shown that the *Tmprss6*$^{-/-}$ mice have a blunted inflammatory response after LPS injection, probably due to high

hepcidin levels [35]. Indeed *Tmprss6*$^{-/-}$ mice are characterized by the downregulation of pathway involved in the activation of macrophages and synthesis of proinflammatory cytokines and more in general signalling related to the inflammatory status [36]. Moreover inflammation is responsible for *Tmprss6* downregulation through inhibition of STAT5 phosphorylation [37]. These studies suggest a potential and novel therapeutic approach of modulation and enhancement of TMPRSS6 activity for treatment of the diseases in which hepcidin is upregulated as in the anemia of chronic disease. Tmprss6 upregulation would be able a different approach to improve erythropoiesis through hepcidin decrease.

References

1. Hentze MW, Muckenthaler MU, Galy B, Camaschella C (2010) Two to tango: regulation of Mammalian iron metabolism. Cell 142: 24-38.
2. Silvestri L, Pagani A, Nai A, De Domenico I, Kaplan J, et al. (2008) The serine protease matriptase-2 (TMPRSS6) inhibits hepcidin activation by cleaving membrane hemojuvelin. Cell metabolism 8: 502-511.
3. Maxson JE, Chen J, Enns CA, Zhang AS (2010) Matriptase-2- and proprotein convertase-cleaved forms of hemojuvelin have different roles in the down-regulation of hepcidin expression. The Journal of biological chemistry 285: 39021-39028.
4. Silvestri L, Rausa M, Pagani A, Nai A, Camaschella C (2013) How to assess causality of TMPRSS6 mutations? Human mutation 34: 1043-1045.
5. Lanzara C, Roetto A, Daraio F, Rivard S, Ficarella R, et al. (2004) Spectrum of hemojuvelin gene mutations in 1q-linked juvenile hemochromatosis. Blood 103: 4317-4321.
6. Silvestri L, Pagani A, Camaschella C (2008) Furin-medEated release of soluble hemojuvelin: a new link between hypoxia and iron homeostasis. Blood 111: 924-931.
7. Lin L, Valore EV, Nemeth E, Goodnough JB, Gabayan V, et al. (2007) Iron transferrin regulates hepcidin synthesis in primary hepatocyte culture through hemojuvelin and BMP2/4. Blood 110: 2182-2189.
8. Babitt JL, Huang FW, Xia Y, Sidis Y, Andrews NC, et al. (2007) Modulation of bone morphogenetic protein signaling in vivo regulates systemic iron balance. The Journal of clinical investigation 117: 1933-1939.

9. Nili M, Shinde U, Rotwein P (2010) Soluble repulsive guidance molecule c/hemojuvelin is a broad spectrum bone morphogenetic protein (BMP) antagonist and inhibits both BMP2- and BMP6-mediated signaling and gene expression. The Journal of biological chemistry 285: 24783-24792.
10. Finberg KE, Whittlesey RL, Fleming MD, Andrews NC (2010) Down-regulation of Bmp/Smad signaling by Tmprss6 is required for maintenance of systemic iron homeostasis. Blood 115: 3817-3826.
11. Krijt J, Fujikura Y, Ramsay AJ, Velasco G, Necas E (2011) Liver hemojuvelin protein levels in mice deficient in matriptase-2 (Tmprss6). Blood cells, molecules & diseases 47: 133-137.
12. Frydlova J, Fujikura Y, Vokurka M, Necas E, Krijt J (2013) Decreased hemojuvelin protein levels in mask mice lacking matriptase-2-dependent proteolytic activity. Physiological research / Academia Scientiarum Bohemoslovaca 62: 405-411.
13. Heining E, Bhushan R, Paarmann P, Henis YI, Knaus P (2011) Spatial segregation of BMP/Smad signaling affects osteoblast differentiation in C2C12 cells. PloS one 6: e25163.
14. Hartung A, Bitton-Worms K, Rechtman MM, Wenzel V, Boergermann JH, et al. (2006) Different routes of bone morphogenic protein (BMP) receptor endocytosis influence BMP signaling. Molecular and cellular biology 26: 7791-7805.
15. Velasco G, Cal S, Quesada V, Sanchez LM, Lopez-Otin C (2002) Matriptase-2, a membrane-bound mosaic serine proteinase predominantly expressed in human liver and showing degrading activity against extracellular matrix proteins. The Journal of biological chemistry 277: 37637-37646.
16. Stirnberg M, Maurer E, Arenz K, Babler A, Jahnen-Dechent W, et al. (2014) Cell surface serine protease matriptase-2 suppresses fetuin-A/AHSG-mediated induction of hepcidin. Biological chemistry.
17. Zhang AS, Anderson SA, Wang J, Yang F, DeMaster K, et al. (2011) Suppression of hepatic hepcidin expression in response to acute iron deprivation is associated with an increase of matriptase-2 protein. Blood 117: 1687-1699.
18. Lakhal S, Schodel J, Townsend AR, Pugh CW, Ratcliffe PJ, et al. (2011) Regulation of type II transmembrane serine proteinase TMPRSS6 by hypoxia-inducible factors: new link between hypoxia signaling and iron homeostasis. The Journal of biological chemistry 286: 4090-4097.
19. Kautz L, Besson-Fournier C, Meynard D, Latour C, Roth MP, et al. (2011) Iron overload induces BMP6 expression in the liver but not in the duodenum. Haematologica 96: 199-203.
20. Andriopoulos B, Jr., Corradini E, Xia Y, Faasse SA, Chen S, et al. (2009) BMP6 is a key endogenous regulator of hepcidin expression and iron metabolism. Nature genetics 41: 482-487.
21. Enns CA, Ahmed R, Wang J, Ueno A, Worthen C, et al. (2013) Increased iron loading induces Bmp6 expression in the non-parenchymal cells of the liver independent of the BMP-signaling pathway. PloS one 8: e60534.
22. Finberg KE, Heeney MM, Campagna DR, Aydinok Y, Pearson HA, et al. (2008) Mutations in TMPRSS6 cause iron-refractory iron deficiency anemia (IRIDA). Nature genetics 40: 569-571.

23. Du X, She E, Gelbart T, Truksa J, Lee P, et al. (2008) The serine protease TMPRSS6 is required to sense iron deficiency. Science 320: 1088-1092.
24. Folgueras AR, de Lara FM, Pendas AM, Garabaya C, Rodriguez F, et al. (2008) Membrane-bound serine protease matriptase-2 (Tmprss6) is an essential regulator of iron homeostasis. Blood 112: 2539-2545.
25. Lenoir A, Deschemin JC, Kautz L, Ramsay AJ, Roth MP, et al. (2011) Iron-deficiency anemia from matriptase-2 inactivation is dependent on the presence of functional Bmp6. Blood 117: 647-650.
26. Finberg KE, Whittlesey RL, Andrews NC (2011) Tmprss6 is a genetic modifier of the Hfe-hemochromatosis phenotype in mice. Blood 117: 4590-4599.
27. Lee P, Hsu MH, Welser-Alves J, Peng H (2012) Severe microcytic anemia but increased erythropoiesis in mice lacking Hfe or Tfr2 and Tmprss6. Blood cells, molecules & diseases 48: 173-178.
28. Nai A, Pagani A, Mandelli G, Lidonnici MR, Silvestri L, et al. (2012) Deletion of TMPRSS6 attenuates the phenotype in a mouse model of beta-thalassemia. Blood 119: 5021-5029.
29. Schmidt PJ, Toudjarska I, Sendamarai AK, Racie T, Milstein S, et al. (2013) An RNAi therapeutic targeting Tmprss6 decreases iron overload in Hfe(-/-) mice and ameliorates anemia and iron overload in murine beta-thalassemia intermedia. Blood 121: 1200-1208.
30. Guo S, Casu C, Gardenghi S, Booten S, Aghajan M, et al. (2013) Reducing TMPRSS6 ameliorates hemochromatosis and beta-thalassemia in mice. The Journal of clinical investigation 123: 1531-1541.
31. Camaschella C (2013) Treating iron overload. The New England journal of medicine 368: 2325-2327.
32. Wrighting DM, Andrews NC (2006) Interleukin-6 induces hepcidin expression through STAT3. Blood 108: 3204-3209.
33. Verga Falzacappa MV, Vujic Spasic M, Kessler R, Stolte J, Hentze MW, et al. (2007) STAT3 mediates hepatic hepcidin expression and its inflammatory stimulation. Blood 109: 353-358.
34. Casanovas G, Mleczko-Sanecka K, Altamura S, Hentze MW, Muckenthaler MU (2009) Bone morphogenetic protein (BMP)-responsive elements located in the proximal and distal hepcidin promoter are critical for its response to HJV/BMP/SMAD. Journal of molecular medicine 87: 471-480.
35. Pagani A, Nai A, Corna G, Bosurgi L, Rovere-Querini P, et al. (2011) Low hepcidin accounts for the proinflammatory status associated with iron deficiency. Blood 118: 736-746.
36. Riba M, Rausa M, Sorosina M, Cittaro D, Garcia Manteiga JM, et al. (2013) A strong anti-inflammatory signature revealed by liver transcription profiling of Tmprss6-/- mice. PloS one 8: e69694.
37. Meynard D, Sun CC, Wu Q, Chen W, Chen S, et al. (2013) Inflammation regulates TMPRSS6 expression via STAT5. PloS one 8: e82127.

Appendix

Publications 2011-2014

De Falco L, Silvestri L, Kannengiesser C, Morán E, Oudin C, **Rausa M**, Bruno M, Aranda J, Argiles B, Yenicesu I, Falcon-Rodriguez M, Yilmaz-Keskin E, Kocak U, Beaumont C, Camaschella C, Iolascon A, Grandchamp B, Sanchez M. Functional and clinical impact of novel tmprss6 variants in iron-refractory iron-deficiency anemia patients and genotype-phenotype studies. Human Mutation 2014 Nov;35(11):1321-9

Riba M., **Rausa M**., Sorosina M., Cittaro D., Martinelli Boneschi F., Nai A., Pagani A., Camaschella C. and Silvestri L. A strong anti-inflammatory signature revealed by liver transcription profiling of Tmprss6-/- mice, PloS One, July 2013; 8 (7).

Silvestri L., **Rausa M**., Pagani A., Nai A. and Camaschella C. How to Assess Causality of TMPRSS6 Mutations?, Human Mutation, April 2013; 34 (7).